

Do not Remove from Library

NASA TECHNICAL
MEMORANDUM

NASA TM X-64852



SKYLAB THRUSTER ATTITUDE CONTROL SYSTEM

Skylab Program Office

NASA

*George C. Marshall Space Flight Center
Marshall Space Flight Center, Alabama*

1. REPORT NO. NASA TM X-64852	2. GOVERNMENT ACCESSION NO.	3. RECIPIENT'S CATALOG NO.	
4. TITLE AND SUBTITLE SKYLAB THRUSTER ATTITUDE CONTROL SYSTEM		5. REPORT DATE July 1974	
		6. PERFORMING ORGANIZATION CODE	
7. AUTHOR(S) G. E. Wilmer, Jr.		8. PERFORMING ORGANIZATION REPORT #	
9. PERFORMING ORGANIZATION NAME AND ADDRESS George C. Marshall Space Flight Center Marshall Space Flight Center, Alabama 35812		10. WORK UNIT NO.	
		11. CONTRACT OR GRANT NO.	
12. SPONSORING AGENCY NAME AND ADDRESS National Aeronautics and Space Administration Washington, D. C. 20546		13. TYPE OF REPORT & PERIOD COVERED Technical Memorandum	
		14. SPONSORING AGENCY CODE	
15. SUPPLEMENTARY NOTES			
16. ABSTRACT <p>This report documents the preflight activities and the Skylab mission support effort for the Thruster Attitude Control System (TACS). The preflight activities include a description of problems and their solutions encountered in the development, qualification, and flight checkout test programs. The mission support effort is presented as it relates to system performance assessment, real-time problem solving, flight anomalies, and the daily system evaluation. Finally, the detailed flight evaluation is presented for each phase of the mission using system telemetry data.</p> <p>The report asserts that the TACS met or exceeded design requirements and fulfilled its assigned mission objectives.</p>			
17. KEY WORDS Blowdown Theoretical Performance Cold gas GN ₂ Propulsion System Flight Evaluation Development History		18. DISTRIBUTION STATEMENT Unclassified--Unlimited <i>James D. Ledbetter</i>	
19. SECURITY CLASSIF. (of this report) Unclassified	20. SECURITY CLASSIF. (of this page) Unclassified	21. NO. OF PAGES 119	22. PRICE NTIS

ACKNOWLEDGMENT

The author wishes to acknowledge the contributions to the preparation of this report made by Teledyne Brown Engineering, Huntsville, Alabama, and the McDonnell Douglas Astronautics Company, Huntington Beach, California.

TABLE OF CONTENTS

	Page
1. INTRODUCTION	3
2. THRUSTER ATTITUDE CONTROL SYSTEM DESCRIPTION AND PREMISSION ACTIVITY	5
2.1 SYSTEM DESCRIPTION	5
2.2 PREFLIGHT TEST AND CHECKOUT HISTORY	14
3. THRUSTER ATTITUDE CONTROL SYSTEM MISSION SUPPORT EFFORT . . .	23
3.1 THRUSTER ATTITUDE CONTROL SYSTEM PERFORMANCE PROGRAM	23
3.2 SPECIFIC IMPULSE PERFORMANCE VERIFICATION	24
3.3 SOLENOID VALVE COMPUTER MODEL	29
3.4 THERMAL ANALYSIS UPDATE	29
3.5 SOLENOID VALVE THERMAL TEST PROGRAM	30
3.6 ALTERNATIVES TO PRECLUDE SOLENOID VALVE THERMAL PROBLEMS	32
3.7 SUPPLEMENTAL SYSTEMS STUDIES	33
3.8 MISSION SUPPORT	36
3.9 PRESSURE TRANSDUCER NOISE	38
3.10 SPHERE TEMPERATURE ANOMALIES	38
3.11 INSTRUMENTATION ERROR ANALYSIS	39
3.12 THRUST LEVEL REQUIREMENTS	41
4. THRUSTER ATTITUDE CONTROL SYSTEM DETAILED MISSION EVALUATION	43
4.1 FIRST UNMANNED ORBITAL STORAGE PERIOD, SL-1	43
4.2 FIRST MANNED MISSION, SL-2 (28 DAYS)	55
4.3 SECOND UNMANNED ORBITAL STORAGE PERIOD	65
4.4 SECOND MANNED MISSION, SL-3 (59 DAYS)	68
4.5 THIRD UNMANNED ORBITAL STORAGE PERIOD	78
4.6 THIRD MANNED MISSION, SL-4 (84 DAYS)	81
APPENDIX A. THRUSTER ATTITUDE CONTROL SYSTEM COMPONENT OPERATING CHARACTERISTICS	91
APPENDIX B. THRUSTER ATTITUDE CONTROL SYSTEM IMPULSE USAGE	99

LIST OF TABLES

Table	Title	Page
1.	TACS Premission Minimum Thrust Level Requirements . . .	42
2.	TACS Minimum Thrust Level Requirements Analysis	42

LIST OF ILLUSTRATIONS

Figure	Title	Page
1.	Thruster Attitude Control System (TACS) Schematic	6
2.	Skylab Cluster Configuration	7
3.	Storage Sphere Installation	8
4.	Thruster Module Installation	9
5.	Thruster Solenoid Control Valve	10
6.	Thruster Nozzle	11
7.	GN ₂ Storage Sphere	11
8.	Fill and Drain Disconnect	12
9.	Typical Brazed Connection	13
10.	Bimetallic Joint Installation	13
11.	Flexible Metal Tubing	15
12.	GN ₂ Filter	15
13.	Pressure Transducer	16
14.	Temperature Transducer	16
15.	Thruster Pressure Switch	16
16.	Temperature Transducer Stainless Steel "Clamshell" Doubler	20
17.	Total Impulse Variation With Mass and Temperature	25
18.	Thrust Coefficient Variation With Chamber Pressure and Temperature	26
19.	Specific Impulse, 70% Two-Phase Efficiency	27
20.	Specific Impulse, 50% Two-Phase Efficiency	28
21.	Position Plane I Thruster Module Inlet Temperature . . .	31
22.	Scientific Airlock Thruster System Schematic	35
23.	Average GN ₂ Bulk Gas Temperature	40
24.	Average System Pressure	40
25.	Thruster Attitude Control System GN ₂ Fill Envelope . . .	44
26.	Usable Total Impulse Remaining, SL-1	46
27.	GN ₂ Pressure, SL-1	47
28.	GN ₂ Mass, SL-1	48

LIST OF ILLUSTRATIONS (Continued)

Figure	Title	Page
29.	Thrust, SL-1	49
30.	Nominal Minimum Impulse Bit, SL-1	50
31.	Accumulated Minimum Impulse Bit Firings, SL-1	51
32.	Accumulated Full-On Firings, SL-1	52
33.	Average GN ₂ Bulk Gas Temperature, SL-1	53
34.	Beta Angle, SL-1	53
35.	Module Inlet Temperatures, SL-1	54
36.	Usable Total Impulse Remaining, SL-2	56
37.	GN ₂ Pressure, SL-2	57
38.	GN ₂ Mass, SL-2	58
39.	Thrust, SL-2	59
40.	Nominal Minimum Impulse Bit, SL-2	60
41.	Accumulated Minimum Impulse Bit Firings, SL-2	61
42.	Accumulated Full-On Firings, SL-2	62
43.	Average GN ₂ Bulk Gas Temperature, SL-2	63
44.	Beta Angle, SL-2	63
45.	Module Inlet Temperatures, SL-2	64
46.	System GN ₂ Pressure, Second Unmanned Phase	65
47.	Average GN ₂ Bulk Gas Temperature, Second Unmanned Phase	66
48.	Beta Angle, Second Unmanned Phase	66
49.	Module Inlet Temperatures, Second Unmanned Phase	67
50.	Usable Total Impulse Remaining, SL-3	69
51.	GN ₂ Pressure, SL-3	70
52.	GN ₂ Mass, SL-3	71
53.	Thrust, SL-3	72
54.	Nominal Minimum Impulse Bit, SL-3	73
55.	Accumulated Minimum Impulse Bit Firings, SL-3	74
56.	Accumulated Full-On Firings, SL-3	75
57.	Average GN ₂ Bulk Gas Temperature, SL-3	76
58.	Beta Angle, SL-3	76
59.	Module Inlet Temperatures, SL-3	77

LIST OF ILLUSTRATIONS (Concluded)

Figure	Title	Page
60.	GN ₂ Pressure, Third Unmanned Phase	78
61.	Average GN ₂ Bulk Gas Temperature, Third Unmanned Phase	79
62.	Beta Angle, Third Unmanned Phase	79
63.	Module Inlet Temperatures, Third Unmanned Phase	80
64.	Usable Total Impulse Remaining, SL-4	82
65.	GN ₂ Pressure, SL-4	83
66.	GN ₂ Mass, SL-4	84
67.	Thrust, SL-4	85
68.	Nominal Minimum Impulse Bit, SL-4	86
69.	Accumulated Minimum Impulse Bit Firings, SL-4	87
70.	Accumulated Full-On Firings, SL-4	88
71.	Average GN ₂ Bulk Gas Temperature, SL-4	89
72.	Beta Angle, SL-4	89
73.	Module Inlet Temperatures, SL-4	90

LIST OF ABBREVIATIONS

ADDT	All Digital Data Tape
AM	Airlock Module
APCS	Attitude and Pointing Control System
ATMDC	Apollo Telescope Mount Digital Computer
CMG	Control Moment Gyroscope
CSM	Command and Service Module
DOY	Day of Year
EREP	Earth Resources Experiment Package
EVA	Extravehicular Activity
FOF	Full-On Firings
HOSC	Huntsville Operations Support Center
IMD	Inhibit Momentum Dump
IU	Instrument Unit
JOP 13D	Night Sky Objects
JOP 18D	Comet Kohoutek--attitude hold offset pointing--elongation greater than 0.089 rad
JSC	Johnson Space Center
K	Comet Kohoutek
KSC	Kennedy Space Center
LENP	Lower-Body Negative Pressure (Experiment M092)
LVDC	Launch Vehicle Digital Computer
MDAC	McDonnell Douglas Astronautics Company
MIB	minimum impulse bit
MOPS	Mission Operations Planning System
MSFC	Marshall Space Flight Center

LIST OF ABBREVIATIONS (Concluded)

NBS	National Bureau of Standards
NUZ	Navigation parameter equivalent to the negative of the beta angle
OWS	Orbital Workshop
ΔP	Delta-Pressure
S019	Ultraviolet Stellar Astronomy
S063K	Ultraviolet Airglow Horizon Photography
S183K	Ultraviolet Panorama
S210K	Far Ultraviolet Electronographic Camera
S232	Barium Cloud Observation
SAL	Scientific Airlock
SAS	Solar Array System
SI	Solar Inertial
S-IVB	Third Stage of the Saturn-V Vehicle
SL-1	First Unmanned Orbital Storage Period
SL-2	Skylab First Manned Mission
SL-3	Skylab Second Manned Mission
SL-4	Skylab Third Manned Mission
TACS	Thruster Attitude Control System
ZLV	Z-axis Along the Local Vertical Attitude

SUMMARY

The Thruster Attitude Control System (TACS) had a usable total impulse capability at propellant loading of 376,996 N-sec (84,752 lbf-sec). During the Skylab mission, 340,311 N-sec (76,505 lbf-sec) were expended or approximately 133,447 N-sec (30,000 lbf-sec) more than the "worst case" premission prediction. The abnormally heavy impulse demands required of the TACS were primarily attributable to problems encountered during the early phases of the mission with the meteoroid shield, later problems with the rate gyroscopes, the Control Moment Gyroscope (CMG) number one failure, and finally with increased maneuvering requirements resulting from the Comet Kohoutek experiments.

The performance of the TACS met or exceeded flight design requirements. There was no indication of a propellant leak, and no hardware anomalies were detected throughout the 9-month flight.

1. INTRODUCTION

The Thruster Attitude Control System (TACS) is a cold gas (N_2) propulsion system designed to provide attitude control of the Skylab Cluster during launch vehicle separation, Command and Service Module (CSM) docking, and for maneuvering the vehicle during certain experiments such as the Earth Resources Experiment Package (EREP) and Comet Kohoutek viewing periods. The system operates in a blowdown mode with the thrust varying from 444.8 N (100 lbf) to 44.5 N (10 lbf) over the operating pressure range.

This report details the preflight activities and the mission support effort. The mission support and evaluation efforts are given the primary emphasis. Section 2. contains a description of the TACS and documents the problem areas and their solutions during the development test program, qualification test program, and flight checkout testing. The mission support effort is documented in Section 3. Section 4. contains the detailed flight evaluation of the TACS utilizing real-time flight data.

2. THRUSTER ATTITUDE CONTROL SYSTEM DESCRIPTION AND PREMISSION ACTIVITY

A description of the TACS with detailed information on each component is presented in this section. This description is designed to acquaint the reader with the capabilities and operational characteristics of the system. The preflight test and checkout history is presented for the TACS development, qualification, and checkout test programs.

2.1 SYSTEM DESCRIPTION

A schematic representation of the TACS is presented in Figure 1. The location of the system on the Skylab spacecraft and the mounting of key components are shown in Figures 2, 3, and 4. The detailed operating characteristics of each component described below are presented in Appendix A.









There are 24 propellant control valves (Figure 5) in the system, four per thruster manifolded together to provide series-parallel redundancy. The solenoid actuated, pneumatically-operated valve contains a small pilot poppet integral and coaxial with the main poppet. The pilot poppet controls pressure forces that open the main poppet. The pilot poppet and main poppet are linked mechanically so that energizing the solenoid coil opens the valve against the springs at low supply pressures. When the solenoid is deenergized, both poppets are pressure-unbalanced closed to ensure leak-tight sealing.

The six thruster nozzles (Figure 6) have 50:1 expansion ratios and bell-shaped expansion contours. These features were selected to maximize specific impulse while confining the exhaust plume to minimize impingement on the vehicle aft skirt. An impingement shield is provided to eliminate unbalanced forces on the vehicle caused by plume impingement on aft skirt structural elements.

The 22 N₂ supply storage spheres (Figure 7) in the system are of the same design as those used in the S-IVB ambient He repressurization system. They are constructed of welded titanium hemispheres, and are qualified for operating pressures up to 2.206×10^7 N/m² (3200 psig). The storage spheres are loaded through a self-sealing disconnect (Figure 8) mounted at the vehicle skin. The disconnect was hard-capped prior to launch to provide redundant sealing protection against gas leakage.

The propellant supply and distribution system is induction brazed at all tubing connect points (Figure 9) to minimize leakage. Fluxless induction brazing provided a lightweight leakproof joint. A modification to the inlet fitting of each sphere and the addition of a bimetal joint (Figure 10) provide the capability of "in-place" brazing of the supply feed line to the distribution manifold and the sphere temperature

Legend

-  Thruster
-  Solenoid Valve
-  Filter
-  Fill Disconnect
-  Storage Sphere GN₂
-  P_s Pressure Transducer
-  P_c Pressure Switch
-  Temperature Transducer

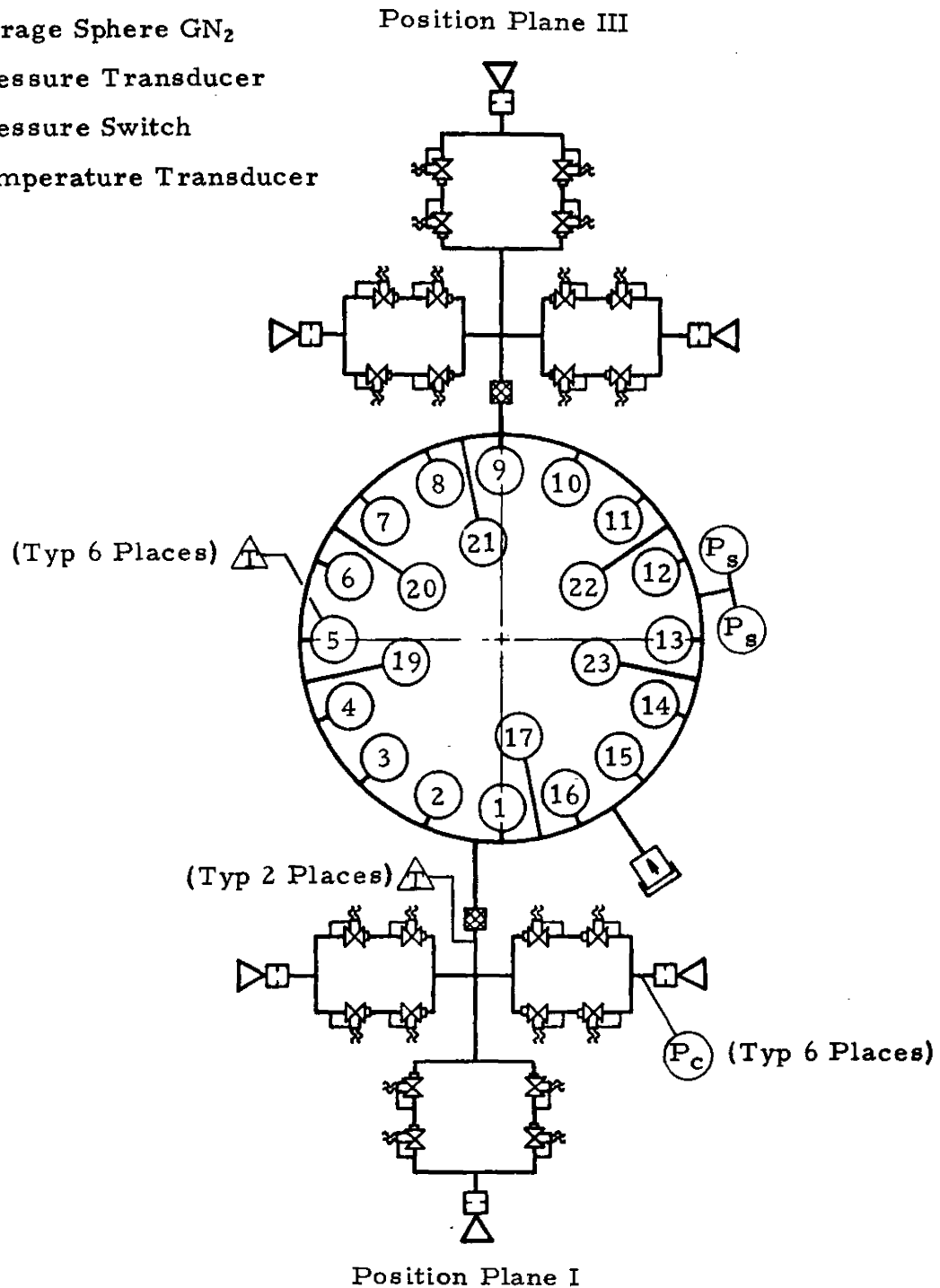


Figure 1.- Thruster Attitude Control System (TACS) Schematic

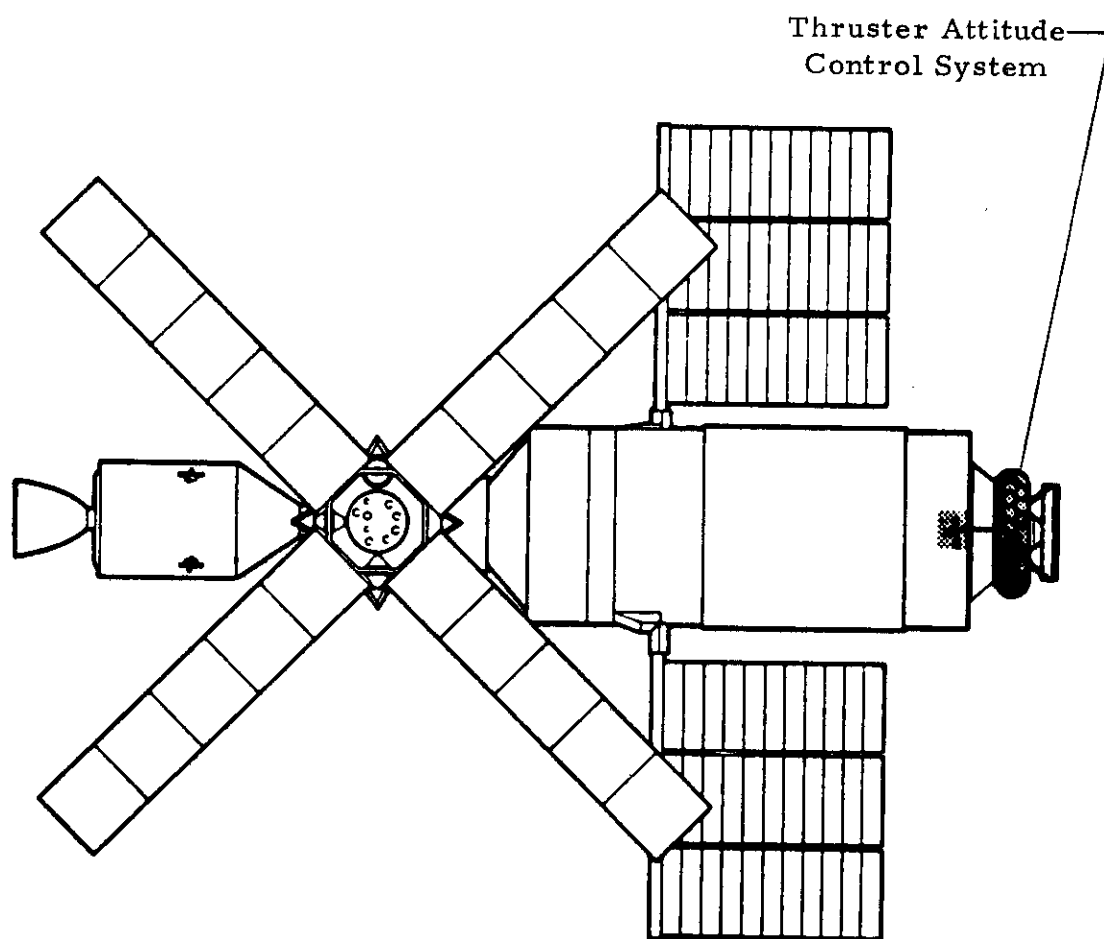


Figure 2.- Skylab Cluster Configuration

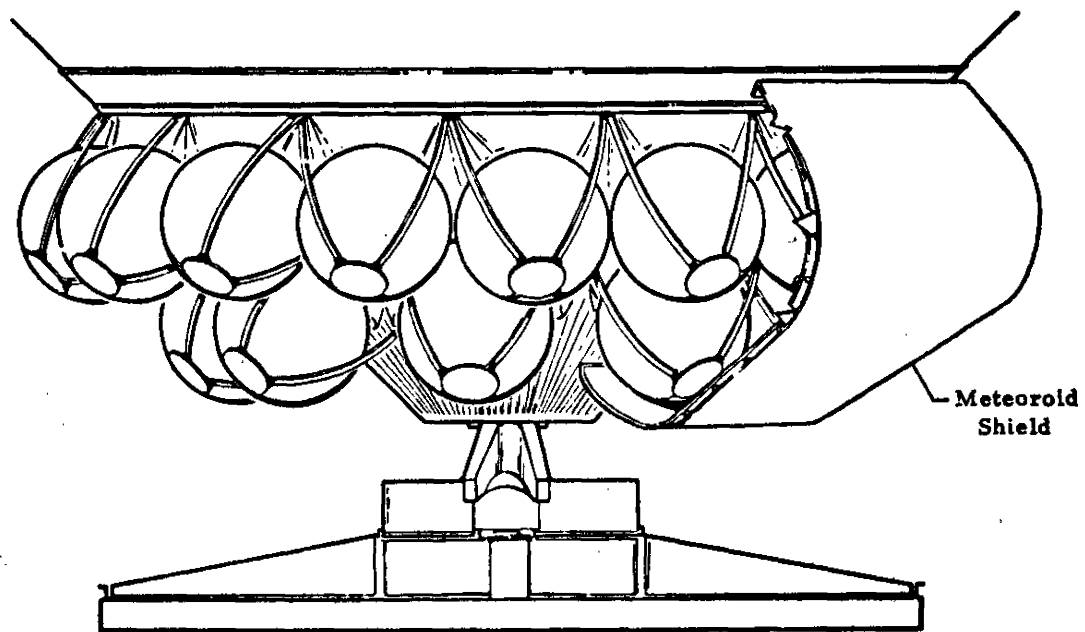


Figure 3.- Storage Sphere Installation

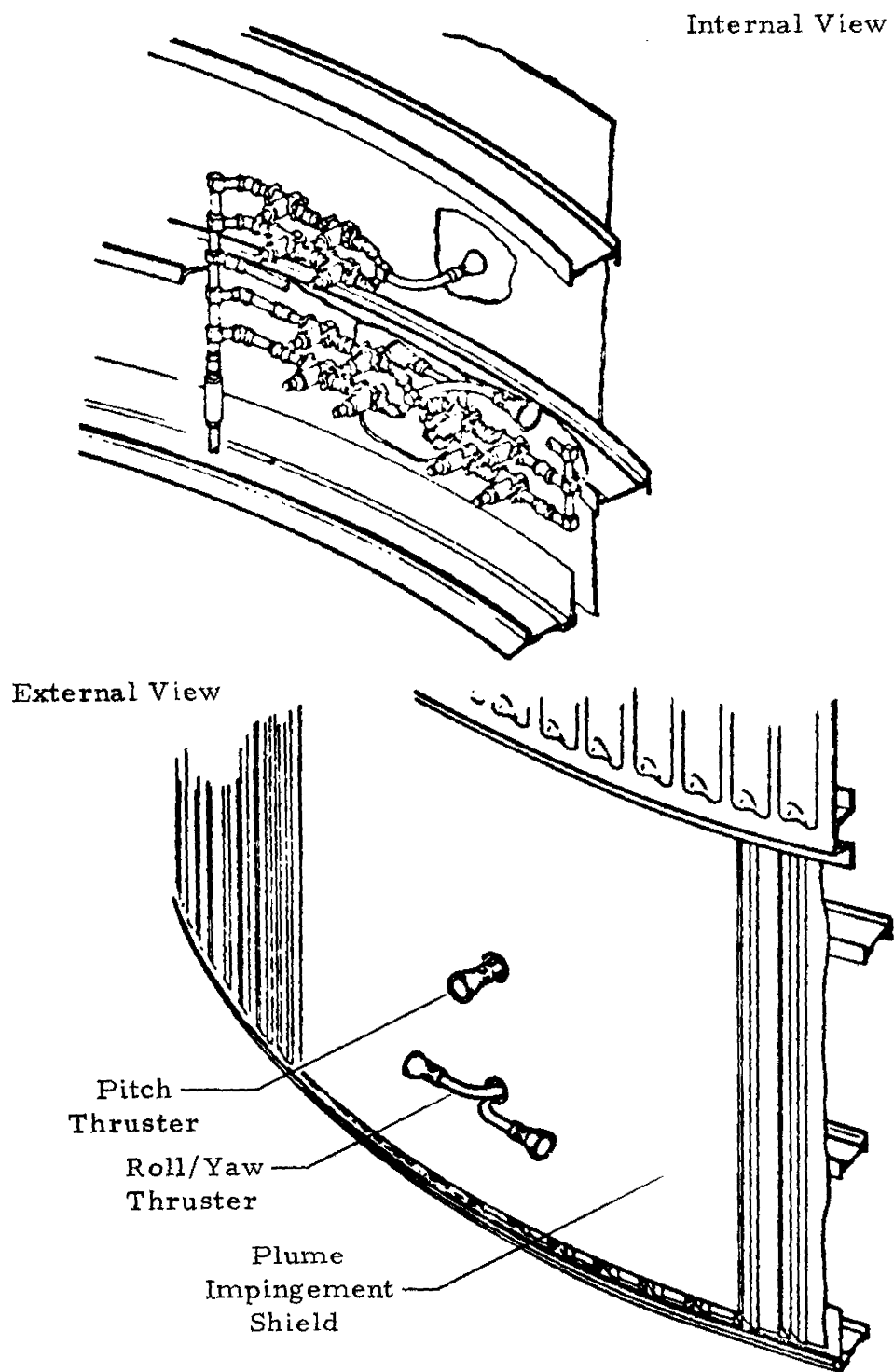


Figure 4.- Thruster Module Installation

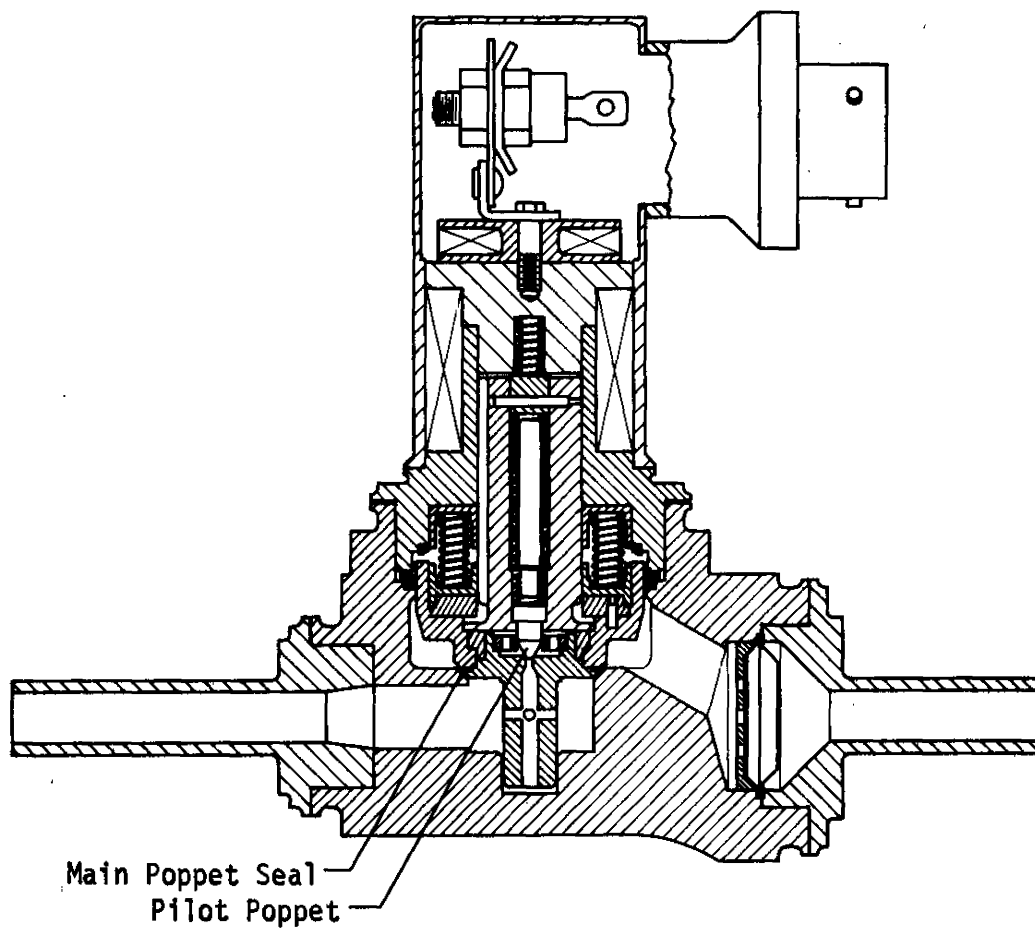


Figure 5.- Thruster Solenoid Control Valve

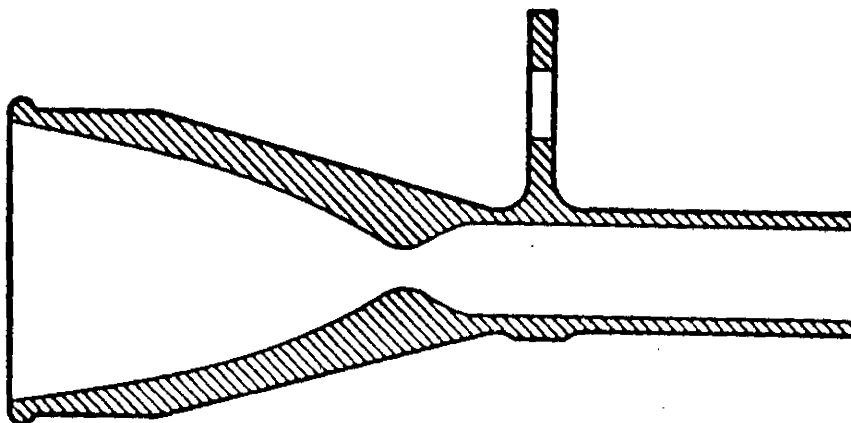


Figure 6.- Thruster Nozzle

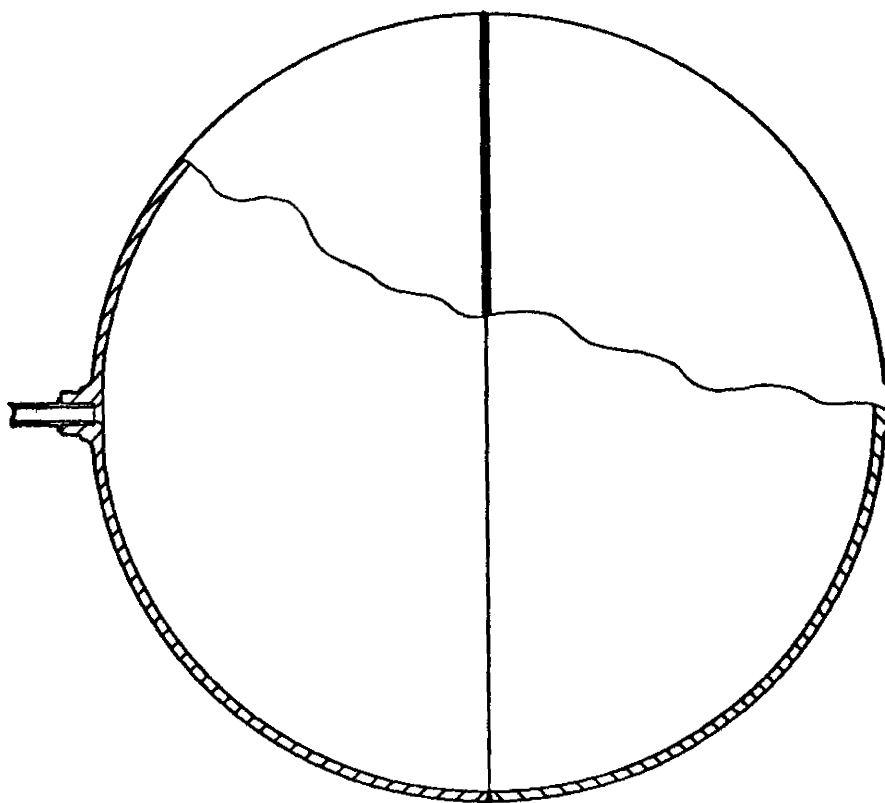
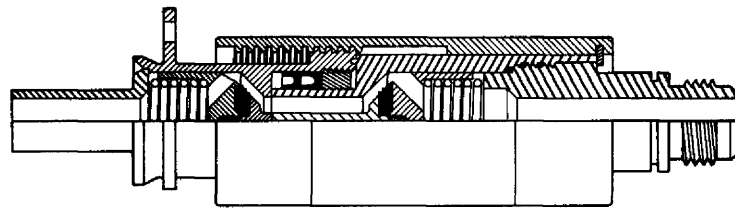
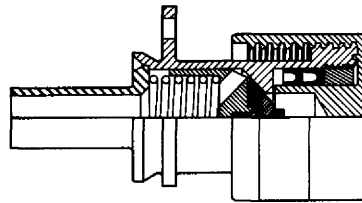


Figure 7.- GN_2 Storage Sphere



Ground Loading Configuration



Flight Configuration

Figure 8.- Fill and Drain Disconnect

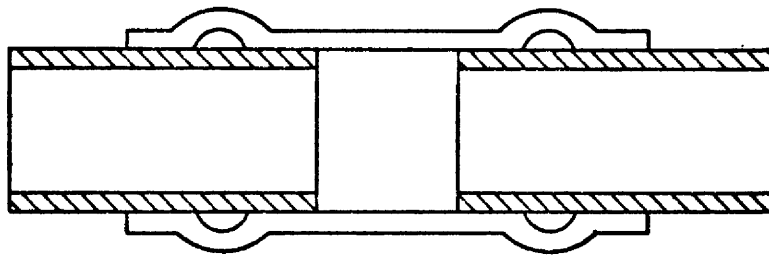


Figure 9.- Typical Brazed Connection

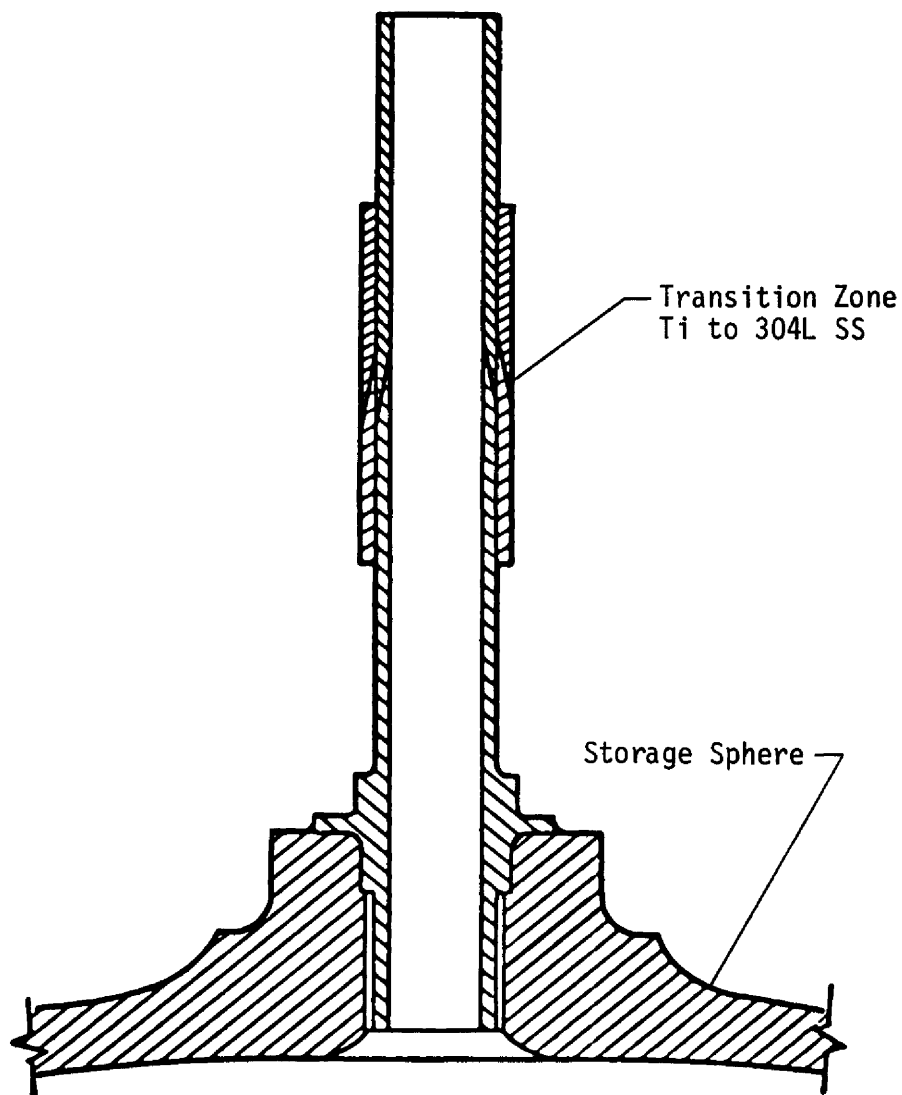


Figure 10.- Bimetallic Joint Installation

instrumentation. The propellant distribution system includes 24 flexible metal tubing sections (Figure 11) to provide for relative motion between the "shock" mounted thruster module panels and the hard mounted distribution manifold. The two supply line filters (Figure 12) located at the inlet to each cluster of three modules utilize a multilayer etched-disk construction to provide a 10-micron, nominal filtering capability.

Instrumentation was provided for system loading, checkout, and flight monitoring. Two pressure transducers (Figure 13) located on the distribution manifold were provided to monitor system pressure. A third pressure transducer was provided for ground monitoring but not used during the flight. Six temperature transducers (Figure 14) located in six storage spheres equally spaced on the aft vehicle support structure were provided to determine the average bulk gas temperature. A temperature transducer was located at the inlet to each cluster of three modules at position planes I and III. Six pressure switches (Figure 15), one for each thruster, provided a positive indication of thruster firings.

2.2 PREFLIGHT TEST AND CHECKOUT HISTORY

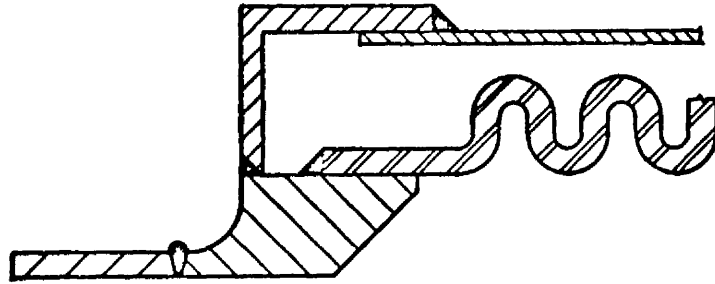
The TACS was certified for flight after successful completion of development, qualification, and checkout test programs. This effort included development and qualification tests of the solenoid control valve, the in-line gas filter, the fill-drain disconnect, the storage sphere, the bimetal joint, the manifolding, the temperature transducer, the pressure transducer, and the pressure switch. The primary test objectives, major problem areas, and solutions are summarized in this section.

2.2.1 Thruster Module Assembly Development and Qualification Test Programs

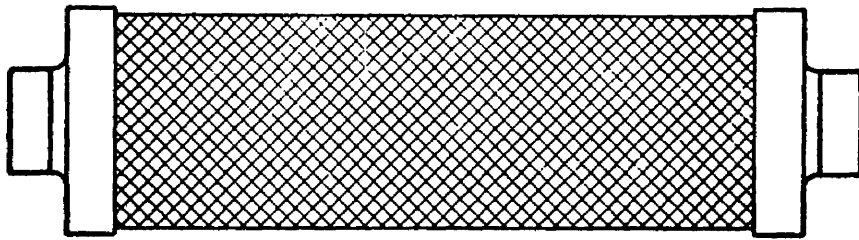
Development test program.- The purpose of the development test program for the thruster module assembly was to evaluate and establish a production configuration for the TACS solenoid valve. The development valves were tested at the valve, dual valve, and module levels to evaluate the valves' functional, performance, and dynamic characteristics at various environmental and system operating conditions.

Several different main poppet seal materials and configurations were evaluated in the initial phase of testing. The configuration that demonstrated minimum leakage rates over the operating pressure range was a conical poppet with a conical sealing surface using DuPont's "Vespel" as the seal material. Also, the preload on the main poppet springs was increased and all machined parts were chemically deburred to further enhance the leakage characteristics.

Testing of this configuration revealed that the upstream valves did not seal effectively with a high inlet pressure and low ΔP across the valve. All valves exhibited sufficient sealing characteristics at moderate



Internal Cross Section View



External View

Figure 11.- Flexible Metal Tubing

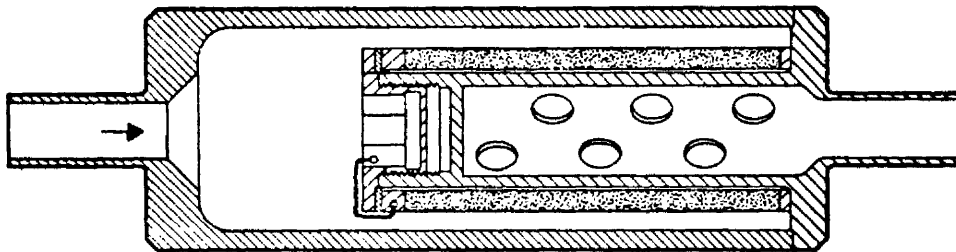


Figure 12.- GN₂ Filter

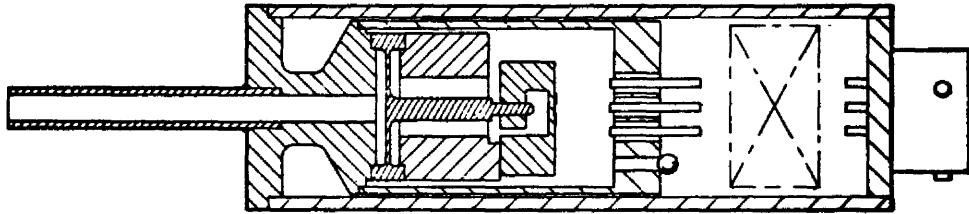


Figure 13.- Pressure Transducer

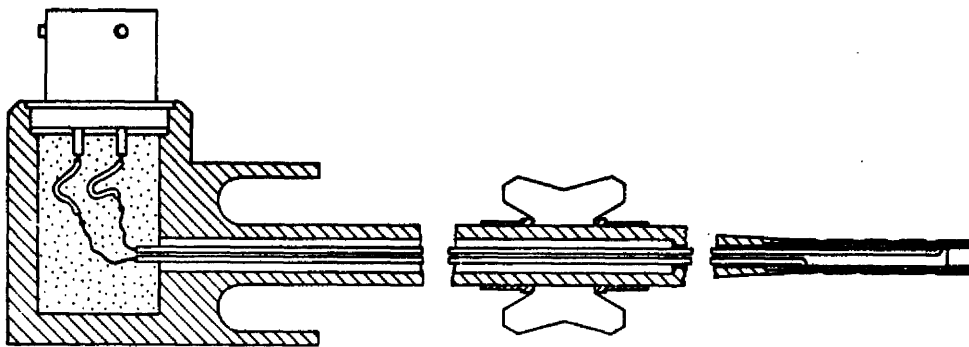


Figure 14.- Temperature Transducer

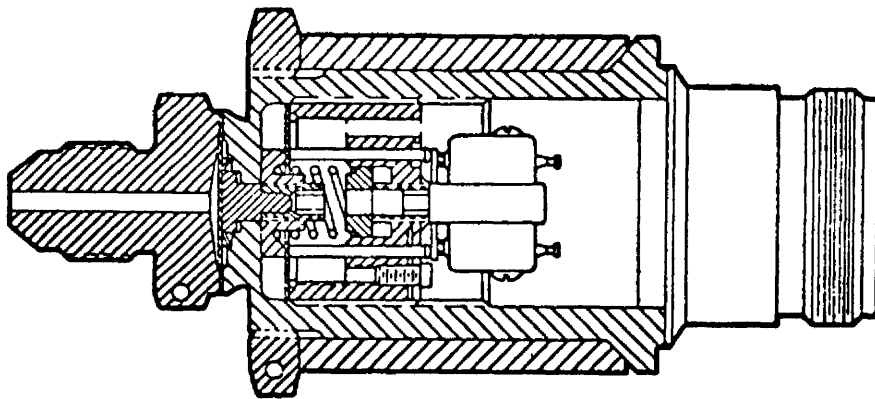


Figure 15.- Thruster Pressure Switch

or high ΔP with gas trapped downstream of the valves and were leak tight at all inlet pressures with ambient downstream pressure. The problem was solved by maintaining the proper ΔP across each upstream valve during operation. This was accomplished by removal of the Zener diode in the valve's voltage suppression circuit which increased the closing time of the downstream valve, thus lowering the trapped pressure between the valves.

During high temperature testing, electrical shorts developed in the magnum solenoid coil wire. This was corrected by changing the coil wire to constantan and changing the insulation from teflon to polyimide. Also, this wire was wrapped on an aluminum spool, and the entire assembly was potted to provide greater heat dissipation.

A problem with bent plunger flanges was identified in the downstream valves. Analysis revealed that pressure surges from the upstream valves caused the plunger flange to impact the orifice plate, thus yielding the plunger flange. This resulted in slow pneumatic response within the valve. A main poppet stop was incorporated in all production valves which precluded impact of the plunger flange with the orifice plate.

Testing also revealed the existence of a leak path behind the lip seal retainer which tended to slow the valve's opening response. The cause of the problem was associated with gas leakage into the solenoid chamber. A "Vespel" static seal was added behind the lip seal retainer. Also, the plunger vent holes were increased from two to four, and microlube lubricant was applied to the lip seal to further enhance the response characteristics of the valve.

Loss of voltage suppression was encountered during testing which was associated with failure of the diodes in the voltage suppression circuit. This was solved by changing to high reliability diodes from a new supplier.

During vibration tests of a module assembly it was determined that the valve main poppets were experiencing high dynamic loads and were actually unseating (chattering) at a frequency which might cause damage to the poppet seals and seats. To reduce the loads on the valve poppets during vibration, "shock" mounts were installed between the thruster valve panels and the vehicle aft skirt. Because the "shock" mounting introduced more degrees of freedom of movement between the valve panels and the distribution manifold, additional flexible metal tubing sections were required.

Qualification test program.- The purpose of the qualification test program for the thruster module assembly was to establish the flight worthiness of the solenoid valve, module, and cluster (three modules). The pressure switches, temperature transducer, filter, flexible metal tubes, and manifold were included in the test specimen.

During prequalification production acceptance tests at the module level, an upstream valve developed a blowing leakage. Subsequent disassembly revealed that the main poppet seal was fragmented with large segments missing. Extensive tests at simulated production acceptance test conditions revealed that the valve failure was due to an incorrect test setup. The inlet manifold was improperly sized causing a high reverse ΔP condition to exist across the upstream valve, thus failing the seal under severe backflow conditions. This sensitivity to backflow was recognized, and all subsequent test and operating procedures were reviewed and rewritten as required to ensure that no valve was subjected to possible reverse flow conditions.

During vibration testing of the inlet manifold installation, consisting of the filter and one flexible tube assembly mounted on a section of the aft skirt, the clamp that mounted the filter to the skirt yielded. The clamps were redesigned and the tests repeated. The specimen successfully met the qualification requirements with an additional tube clamp between the fill line and thruster manifold and the addition of doublers to the filter support bracket. Post-vibration tests revealed that the filter would not meet imposed cleanliness requirements. The cleanliness requirements were waived and no further action was taken because the flight filters had been installed, and each valve contained an integral filter capable of providing protection from the amount of contaminants that would be released by the filter.

Qualification testing of the thruster module assembly (three modules) consisted of proof, leakage, functional, vibration, ordnance shock, duty cycling, continuous duty, thermal vacuum environment, electrical, and nozzle cover blow-off tests. At the beginning of the test program, mishandling caused the module inlet temperature transducer to become inoperative, thus necessitating the qualification of this component under a separate test program. All pressure switches used in the test specimen failed at various times in the program. The cause of failure was determined to be diaphragm fatigue in all cases. Further qualification testing occurred in a separate test program. During high temperature functional testing and prior to vibration tests, a downstream valve developed a blowing leak. The cause of the severe leakage was determined to be a fragmented seal with similar characteristics to the earlier failure in the module production acceptance tests. Extensive testing and analytical investigation did not reveal the exact cause of failure. The most probable cause of the failure was attributed to a reduction in impact and fatigue resistance of the seal material, resulting from the assembly stress condition which varies randomly with material strength properties, manufacturing tolerances, and flow forces. The valve was replaced and all testing was successfully completed.

Concurrent with the thruster module assembly qualification tests, additional test programs were performed to investigate lip seal installation on valve operating characteristics, to evaluate and identify environmental and operational conditions which might contribute to or cause the seal to fail, to establish confidence in the production seal configuration, and to develop and evaluate backup seal configurations for use if the production seal configuration had been assessed unsatisfactory for flight.

The extensive seal failure testing did not identify any specific factors which caused the seals to fail. Increased confidence was gained in the production seal configuration for flight from this test program. A backup seal was developed and tested but was not implemented into the production valve program because it did not offer any known advantage over the production configuration seal.

Because of the difficulties experienced with qualifying the pressure switch and temperature transducer in the thruster module assembly qualification test program, these items were qualified at the component level in a separate test program. Both components were subjected to proof, leakage, functional, vibration, shock, burst, and cycle testing.

Prior to the qualification of the temperature transducer at the component level during checkout of the flight TACS, one of the module inlet temperature transducers was found to have an out of specification leak from a weld joint. The magnitude of the leak did not warrant removal of the transducer; however, a stainless steel "clamshell" doubler (Figure 16) was epoxy bonded over the body of all the transducers to preclude further leakage of this type. The temperature transducer with the "clamshell" doubler attached to it completed all qualification testing with no anomalies or deviations from the requirements.

In the qualification test program the pressure switch failed to actuate during the post-vibration cycle life test. The cause of failure was determined to be a fatigue rupture of the stainless steel diaphragm. An evaluation test program was performed using pressure switches with Kapton diaphragms and production flight pressure switches with stainless steel diaphragms. The results of this program indicated that the Kapton material has a greater cycle life capability than the stainless steel material. However, because of cost and schedule impacts resulting from changing the diaphragm material and more realistic assessment of mission cycle life requirements, the production pressure switch was considered qualified at a reduced number of cycles. Also, the pressure switch talk-back parameters were not critical to mission success and the nominal mission cycle prediction was less than the demonstrated cycle life of the production units.

2.2.2 Pressure Sphere Assembly Development and Qualification Test Programs

Development test program.- The only component in the pressure sphere assembly requiring development testing was the bimetal joint. The purpose of the development test program was to verify the capability of the design configuration to meet the Skylab mission environment and operating requirements. Specific areas investigated were the redundancy of the joint, pressure and load capabilities, weld joint and sphere neck configuration, and tooling and welding procedures. Six test specimens were successfully tested to demonstrate the acceptability of the bimetal joint configuration for production and flight usage.

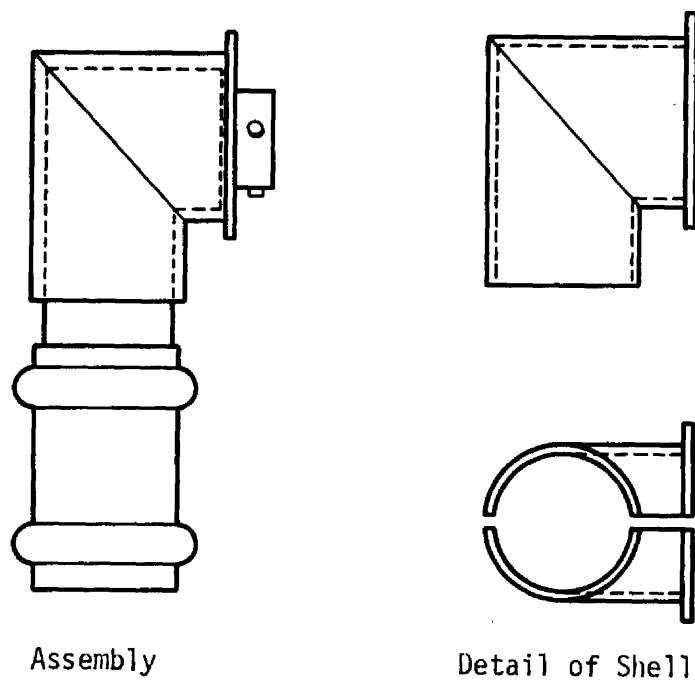


Figure 16.- Temperature Transducer Stainless Steel "Clamshell" Doubler

Qualification test program.- The purpose of the pressure sphere assembly qualification program was to qualify the pressure sphere installation for Skylab usage. The test specimen included a pressure sphere assembly with temperature transducer, bimetal joint, and a segment of the thrust structure. The hardware was qualified without any problems.

2.2.3 Flight System Checkout Tests

The flight checkout tests of the TACS were accomplished at Kennedy Space Center (KSC). Two relatively minor anomalies were noted during checkout testing. One of the sphere mounted temperature transducers failed to meet the specification leakage rate requirements when checked with a mass spectrometer operating in the vacuum mode. The magnitude of the leak did not justify removal of the transducer from the system. Extensive tests were performed to quantify the maximum leakage rate possible through existing leak paths to ensure flight worthiness. The results of the tests and the magnitude of the flight transducer leakage indicated that this leakage would not be detrimental to the mission, and no further action was required.

During component inspection of backup vehicle hardware, the pressure switches were found to be contaminated with mercury. It was postulated that the flight vehicle pressure switches were also contaminated. Since mercury forms an amalgam with gold, which is used in the braze alloy material, the possibility existed that the structural integrity of the system might be compromised. To preclude loss of structural strength, clamshell doubler assemblies were epoxy bonded over most of the braze fittings in the areas adjacent to the pressure switches. One fitting at each thruster location was inaccessible for retrofit. Also, extensive tests were performed to evaluate the effect mercury contamination has on the properties of the braze alloy used. The tests did not reveal any detrimental short term effect on the strength of the braze fittings.

3. THRUSTER ATTITUDE CONTROL SYSTEM MISSION SUPPORT EFFORT

This section describes the mission support effort relating to TACS performance assessment, real-time problem solving, flight anomalies, and the daily system evaluation.

3.1 THRUSTER ATTITUDE CONTROL SYSTEM PERFORMANCE PROGRAM

This computer program analyzed the performance of the TACS. The performance program combines logic, which describes the gas storage and delivery parameters, with a thruster performance program to obtain overall system performance. Nozzle performance parameters evaluated include thrust, specific impulse, flow rate, thrust coefficient, throat state, and exit velocity and state. Also, the system parameters of total impulse and GN_2 mass were calculated. Input to the program consisted of the stored GN_2 pressure and temperature. Pressure loss in transporting the GN_2 from storage spheres to the thrusters and storage volume variation with pressure were included.

The thruster performance program was developed by McDonnell Douglas Astronautics Company (MDAC). A principal feature of this program is its employment of the latest National Bureau of Standards (NBS) real gas properties for N_2 . An isentropic flow process is used in the single phase (superheat) region, and a shift is made to the homogeneous equilibrium assumption for expansions below the saturation line. Also, a two-phase expansion efficiency factor is used in the two-phase region to account for the nonisentropic phase change process.

A general description of the operation of the TACS performance program is:

1. For a given (input) storage gas temperature and pressure, the mass of gas is calculated, utilizing the real gas equation of state from the NBS real gas properties for N_2 .
2. A conversion to a selected base storage gas temperature is performed holding mass constant, thus providing a constant base temperature for all performance calculations.
3. Small pressure increments are selected according to the base thermodynamic state calculated in No. 2.
4. Thruster performance and system mass calculations are made for each pressure increment, beginning with no pressure and ending at the base thermodynamic state. Total impulse increments are obtained by multiplying average specific impulse by the mass increment, and a summed total is maintained for each pressure level.

5. The system performance parameters are printed at each pressure level. These results provide a history of total impulse and thruster performance as mass is expended from the base thermodynamic state calculated in No. 2.

Typical performance curves that were generated using this program are presented in Figures 17, 18, 19, and 20.

3.2 SPECIFIC IMPULSE PERFORMANCE VERIFICATION

Preflight predictions of specific impulse were based on a detailed analysis of real gas effects on the GN_2 expansion in the thruster nozzle. The analysis could not be verified since there were no data available from this program or other sources to determine the effect on performance of condensation in the nozzle.

During the mission, detailed analyses of the flight momentum data were performed to get an empirical assessment of the specific impulse performance. The data analyzed were limited to CMG reset maneuvers with no data dropouts. It was believed that this was the only situation in which the impulse imparted to the cluster could be determined accurately. Ten reset maneuvers were found to be usable for this analysis.

The first eight reset maneuvers analyzed occurred during the SL-2 manned mission. The results for these cases indicated that the apparent specific impulse was significantly higher than had been predicted at the measured module inlet temperatures. Even with the estimated error band of over 10 percent for each point (caused by effects of gravity gradient torques, rate gyro inaccuracies, data sampling intervals and resolution, uncertainties in cluster mass properties, and mass flow rate), the specific impulse data for some cases fell above the maximum preflight predictions.

Another analysis of apparent specific impulse was performed using data from the SL-3 manned mission. Flight momentum data for two reset maneuvers involving 80 firings were used along with thruster flow rate data from qualification testing. The results of this analysis indicate that the average specific impulse was 2 percent higher than the nominal preflight predictions on the hot side of the vehicle and 7 percent higher on the cold side of the vehicle, based on a 70 percent two-phase efficiency factor. The estimated accuracy of the results is ± 6 percent. It is believed that this analysis is more accurate than the previous one because of the increased performance stability of the astronaut installed "six-pack" rate gyro assembly during the SL-3 manned mission. Based on these results, use of the nominal preflight specific impulse predictions was continued for the duration of the mission.

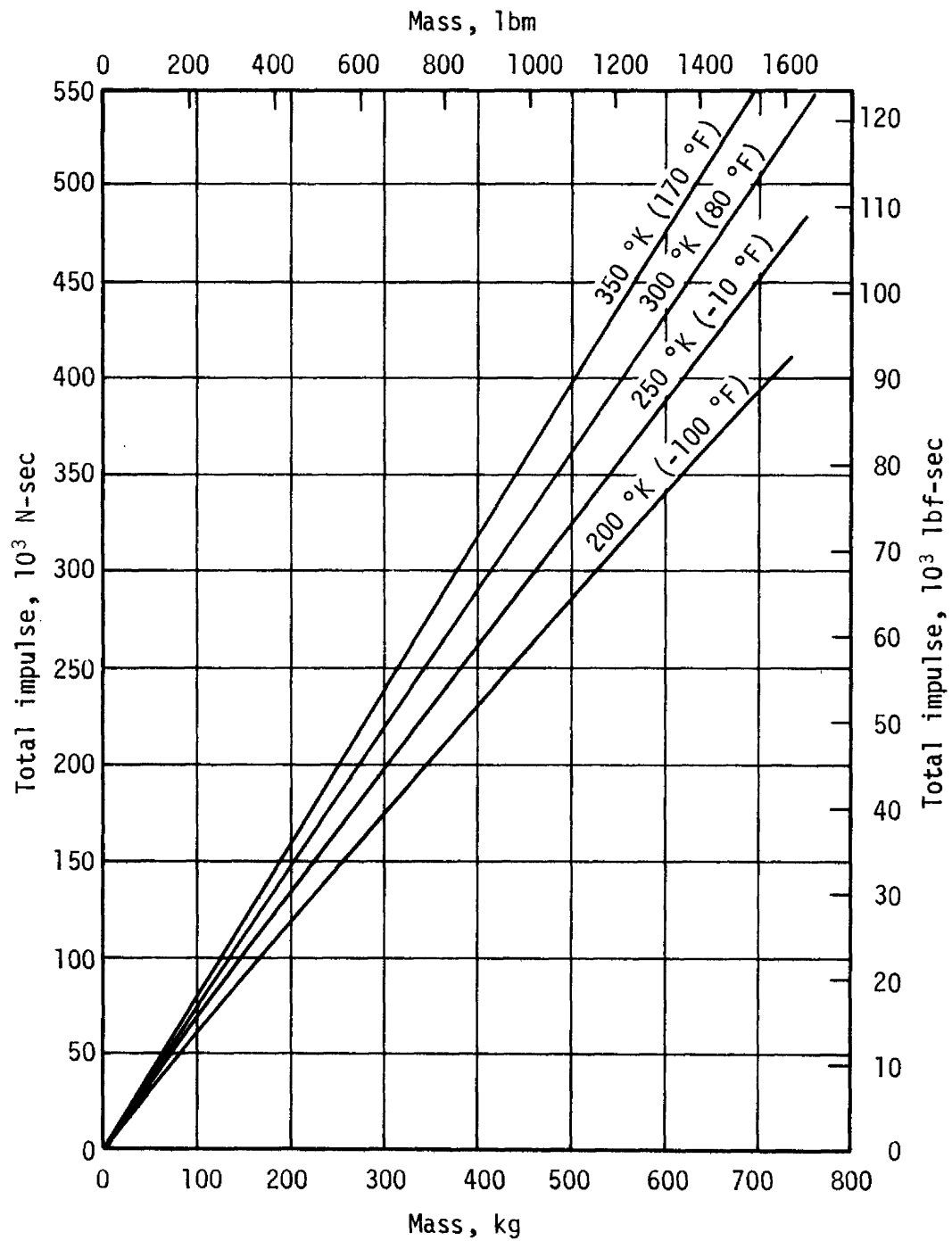


Figure 17.- Total Impulse Variation With Mass and Temperature

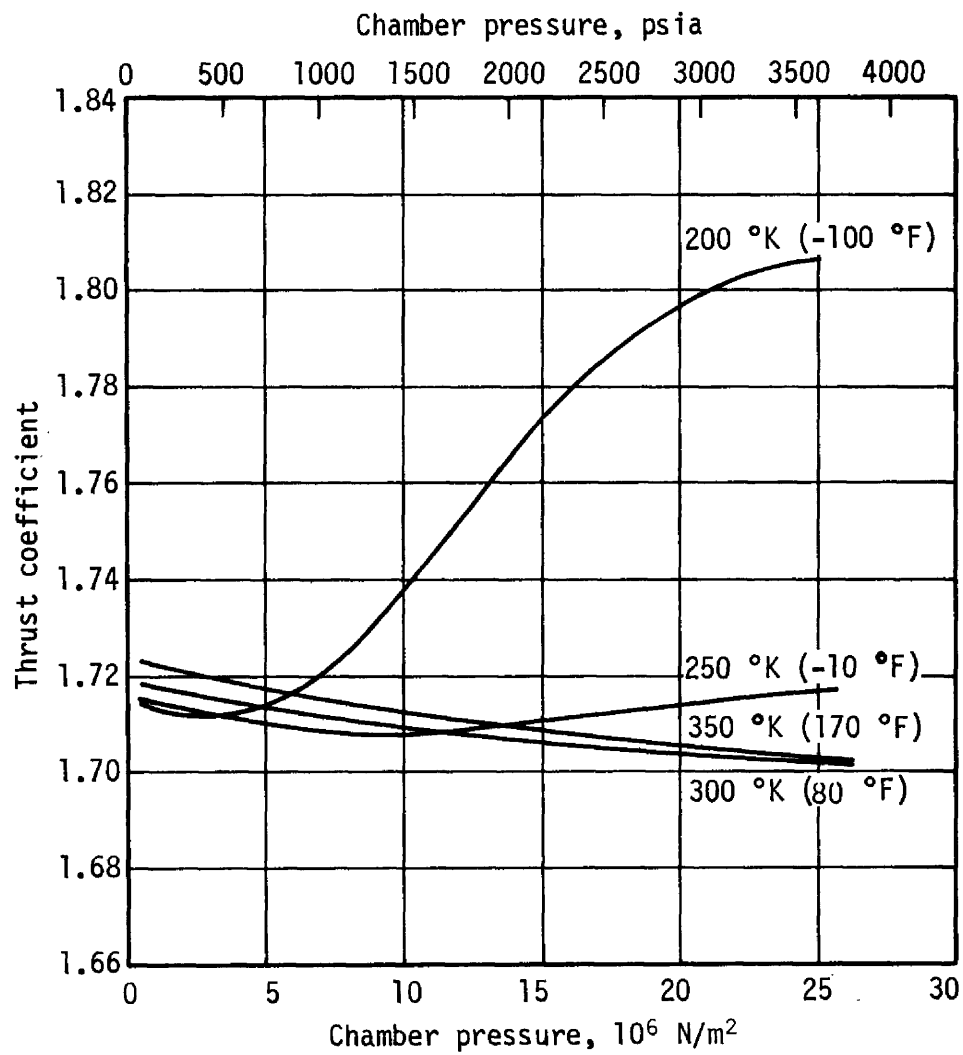


Figure 18.- Thrust Coefficient Variation With Chamber Pressure and Temperature

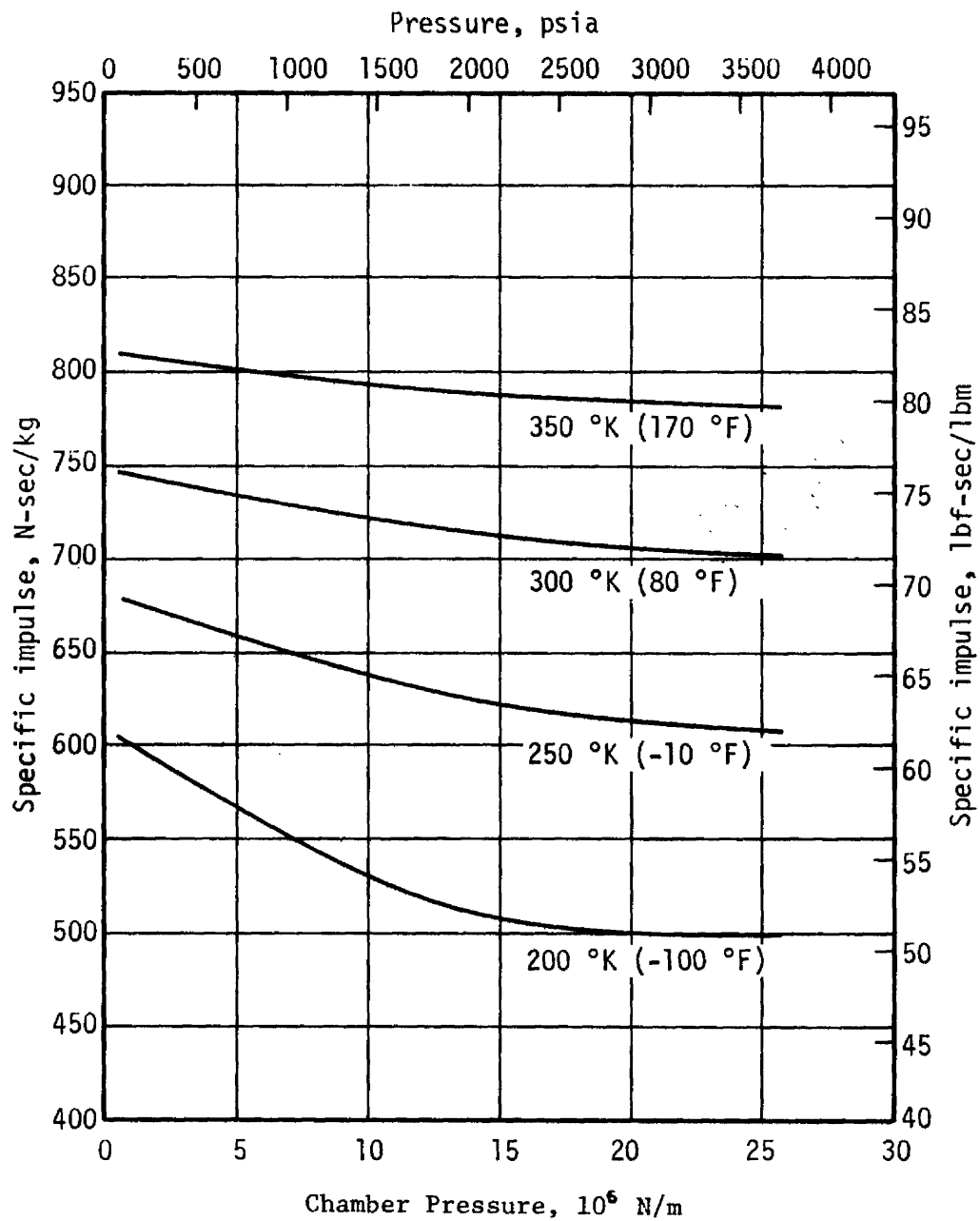


Figure 19.- Specific Impulse, 70% Two-Phase Efficiency

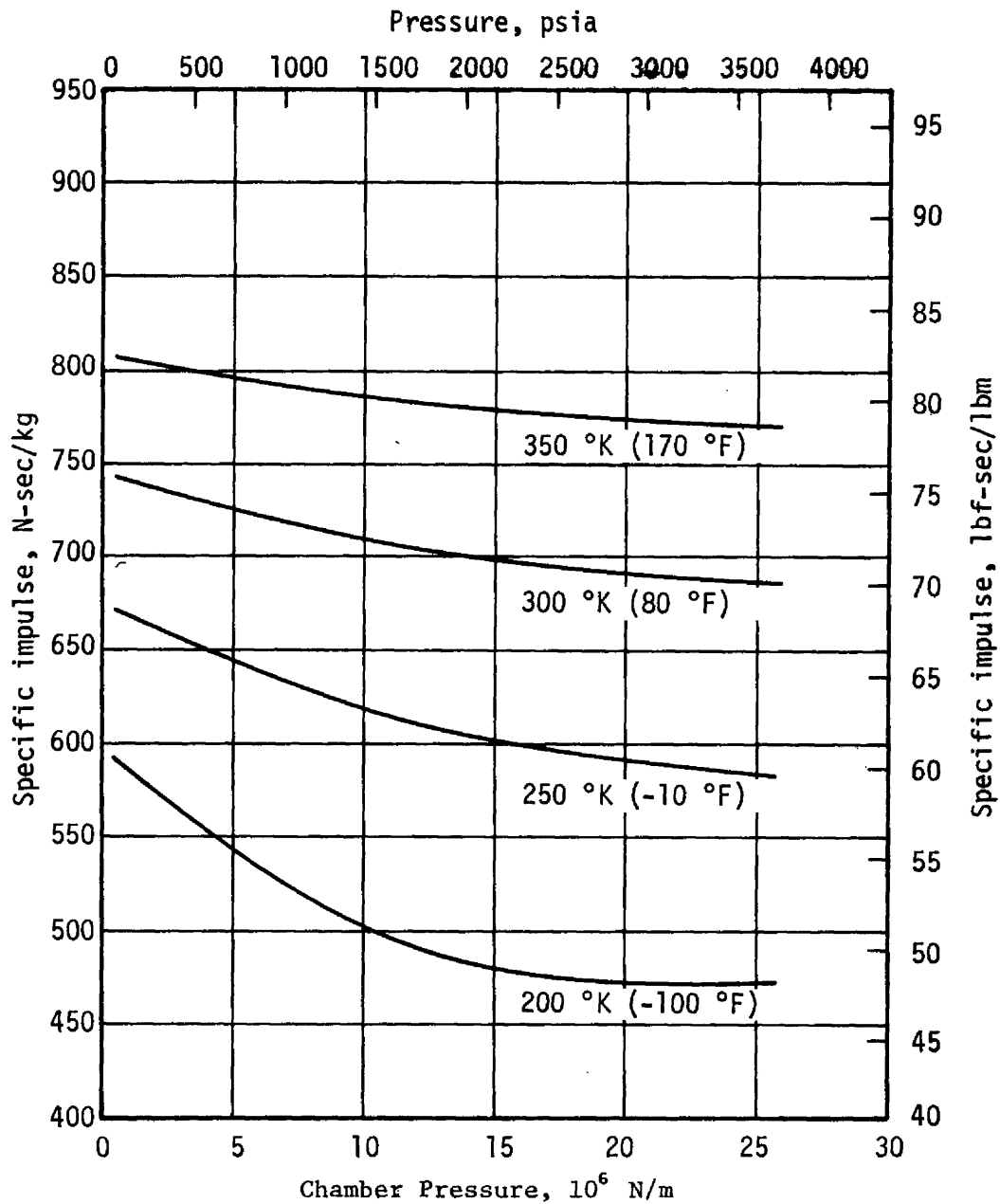


Figure 20.- Specific Impulse, 50% Two-Phase Efficiency

3.3 SOLENOID VALVE COMPUTER MODEL

During development testing of the thruster module assembly, analysis of the test data revealed that when four valves were operated in the series parallel configuration, the opening response of the downstream valves was erratic (see paragraph 2.2.1). The identical behavior was observed for two valves in series, but not in single valve operation. Therefore, a detailed computer modeling effort for the four-valve configuration was initiated.

Two potential causes of the problem were identified: bending of the plunger flange and leakage behind the lip seal retainer. The computer model verified that either of these mechanisms could lead to the anomalous response behavior and that an empirical solution discovered in testing (delaying the opening of the upstream valve relative to the downstream) would tend to eliminate the problem.

The computer model simulated the electrical, mechanical, pneumatic, and body forces acting on the moving parts of each valve. Real gas properties were included in determining the flow rates and pressures in the various valve compartments; and nonlinear effects of electromagnetic losses, back EMF, and hysteresis were included in the electrical portion of the model. The mechanical portion of the model included the effect of external acceleration loads as well as sliding friction forces affecting the motion of the valve parts. An algorithm monitored and controlled the mechanical motion of the three mechanical parts to keep the motion of these parts within specified design travel limits. Surface coefficients of restitution for hard and soft surfaces were included to simulate the dynamics of impacting valve parts.

The input routine was set up to permit investigation of the sensitivity of valve performance to dimensions (flow passages, solenoid air gap, etc.); operating conditions (pressure, temperature, voltage, etc.); and other variables such as friction coefficients. Selected output variables, including pressures and currents, were plotted by the computer and used for comparison with available test data. Other variables, including valve stroke and valve forces, were output to give the designer a better understanding of the current signature traces. Comparison of test data with the computer program output verified the program's effectiveness to predict valve performance and operation.

3.4 THERMAL ANALYSIS UPDATE

TACS hardware was designed and qualified for a maximum temperature of 347 °K (165 °F). Since the solenoid control valves were critical to system operation, valve performance or anything that might affect performance was closely monitored. Analysis of flight data obtained during the SL-2 manned mission indicated that the valves at Position Plane I had reached their maximum qualification test levels during a high beta angle period. The premission thermal analysis had not predicted such an occurrence and,

therefore, an investigation was initiated to determine the cause of the difference between the analytical and actual temperature values. Correlation between the flight data and the analytical prediction was obtained by assuming that the aft skirt white paint solar absorptivity, α_s , was degraded by retrorocket plume contamination. By varying α_s from a design value of 0.31 maximum to 0.34 and using an actual waste tank temperature value of 322 °K (120 °F) rather than the original prediction of 300 °K (80 °F), the thermal model predictions agreed closely with the actual valve module temperatures. Photographs of the aft skirt area obtained by the first crew further verified the optical degradation of these surfaces. The increased α_s had resulted in higher temperatures than originally predicted.

Based on the above flight data correlations, predictions for the third and final manned mission (SL-4) indicated that the qualification maximum temperatures would be exceeded during the orbits where the vehicle was continuously exposed to the sun during the periods of minimum beta angle. This could be caused by: increased solar intensity in the November-January period as the earth approached and receded from perihelion and by further degradation of the solar absorptivity, α_s , as the sun exposure time increased. A worst case temperature of 369 °K (204 °F) was predicted for the negative beta angle periods. Maximum, minimum, and nominal thermal predictions for the third manned mission time period are shown in Figure 21. Actual flight temperature data are also plotted for the Position Plane I module inlet. The maximum temperature actually observed was approximately 353 °K (175 °F), indicating that the paint did not degrade as much as assumed in the worst case prediction.

3.5 SOLENOID VALVE THERMAL TEST PROGRAM

An analysis of the basic valve design was performed to assess the valve's capability to withstand the high temperatures predicted for the final manned mission (see paragraph 3.4). The analysis included evaluation of clearances between moving parts, electrical characteristics, material properties of the valve components, and areas of concern relative to valve operation at elevated temperatures. Although the analysis did not reveal any definite problems, the interaction of individually insignificant geometric changes in the valve was considered to have potential effects which might adversely affect valve operation. As a result, a test program was initiated to verify valve operational integrity at elevated temperatures.

The objective of the test program was to determine the effects of the elevated temperatures on valve response times and leakage characteristics at environmental conditions predicted for the SL-4 manned mission maximum heat flux periods. Tests were performed on a thruster module assembly at room temperature to establish a base line with which to compare test results from other test phases. The tests performed were electrical, proof pressure, external leakage, response at three pressure levels and nominal operating voltage, and internal leakage prior to and after each response test for each pressure level.

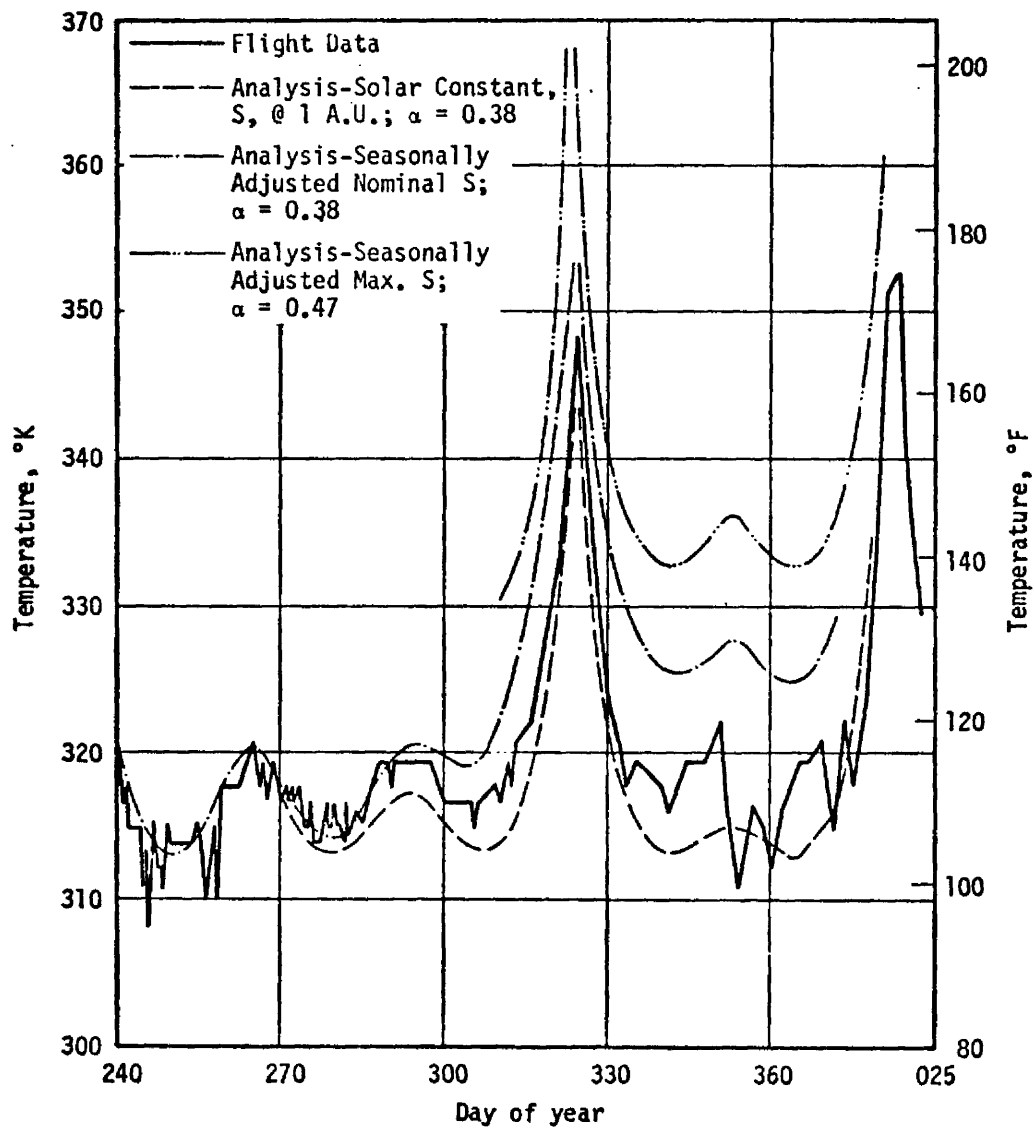


Figure 21.- Position Plane I Thruster Module Inlet Temperature

High temperature testing was conducted which consisted of soaking the thruster module at approximately 369 °K (205 °F) for 28 hours with 9.653×10^6 N/m² (1400 psig) inlet pressure. During the soak period the valves were cycled to determine their response characteristics, and internal leakage measurements were taken prior to and after each specified number of cycles. After the cycling and soak test was completed, tests were performed at room temperature to provide data for comparison with the base line data.

Additional high temperature soak tests were performed at approximately 369 °K (205 °F) and a module inlet pressure of 2.068×10^6 N/m² (300 psig) to simulate maximum temperature and minimum pressure conditions that might exist near the end of the mission. This test was also followed by room temperature checks for base line comparison purposes.

Extensive analysis of the test data indicated that the thruster module assembly performed normally throughout all phases of the testing. Internal leakage measurement results obtained during the test program were within specification requirements. The response characteristics of each valve at high temperatures were comparable to those observed in the room temperature and initial qualification test program high temperature testing. All the electrical and pneumatic response characteristics were within specification requirements. In view of the expedient test facility thermal control method employed, the actual temperature of each valve ranged from 366 °K (200 °F) to 378 °K (220 °F). One noteworthy observation was current fluctuations that were recorded during both room temperature and high temperature testing. Similar anomalies were also observed during the initial qualification testing. Based on an analysis of the data, the current fluctuations were not related to the thermal conditions. The rapid current change indicates that the valve poppet moved toward the closed position momentarily and then returned to a full open position. This movement of the valve poppet did not manifest itself in a change in thruster chamber pressure, and consequently module performance was unaffected.

3.6 ALTERNATIVES TO PRECLUDE SOLENOID VALVE THERMAL PROBLEMS

Concurrent with the TACS valve thermal test program which is discussed in paragraph 3.5, a study of options or means for avoiding the high valve temperatures was initiated. The objective of the study was to establish the most feasible means to protect the valves from high temperature exposure in the event the valve testing revealed that temperature related problems existed. The options were divided into those which avoided the use of the valves during the high temperature periods and those which reduced the valve temperature. The options are summarized in the following paragraphs.

Based on a November 11 SL-4 launch date, and assuming that the Attitude and Pointing Control System (APCS) was operating properly, the TACS was only needed for CMG momentum relief. Operational failure modes could be avoided by inhibiting the thruster system during the high temperature periods. This plan could have impacted nominal flight plan activities by

eliminating maneuvers out of solar inertial, eliminating Extravehicular Activity (EVA) and minimizing vent disturbances and momentum dump inhibits. Because the thruster system would be required for docking, inhibiting the thrusters during the high temperature period would necessitate a launch delay until more acceptable conditions were present. Thus a launch delay was a possible option.

If testing revealed a high temperature failure could occur, even if the valves were not operated, several methods of thermal shielding were investigated. Three of these methods involved the crew physically modifying the structure around the Position Plane I thruster nozzles. The necessary hardware and procedures would have been developed on the ground and flown up with the crew. These options were:

1. A sheet metal shield which would be attached to the aft skirt around the thruster valves. Weight and volume for CSM stowage were disadvantages.
2. Application of a thermal paint using either an aerosol can, brush, or cloth. Technique of application was the biggest disadvantage.
3. Application of aluminized tape to the aft skirt area around the valves. Adhering characteristics were unknown.

Two other concepts were suggested. The first was to control valve temperature to an acceptable level by maintaining a pitch attitude similar to that used during SL-1. This method would impact system usage for CMG momentum relief and the temperature of other cluster components. The final concept relied on the use of the N₂ gas supply to cool the hot valves. Since the average bulk gas temperature would be about 294 °K (70 °F) at minimum beta angles, a series of pulses generated by commanding small attitude maneuvers would allow this relatively cool gas to lower the valve temperature. High gas usage was a major concern with this method.

Of all the alternatives considered, the installation of the sheet metal heat shield by the crew appeared to be the best. However, following completion of the valve high temperature testing, a detailed review of data showed no indication of abnormal system performance. Consequently, no hardware or mission changes were made, and the TACS completed the Skylab program successfully.

3.7 SUPPLEMENTAL SYSTEMS STUDIES

The excessively high consumption of TACS propellant, GN₂, during the early part of the Skylab mission, prompted the initiation of studies of methods for either resupplying or supplementing the cold gas system. Various concepts were evaluated in an effort to determine the most feasible method of resupply/supplement. Certain candidate concepts, which are listed below, required extensive EVA and additional systems and component hardware to be carried up in subsequent Skylab launches:

Method 1 - Carry up a resupply module on SL-4, transfer module to Orbital Workshop (OWS) aft skirt and connect to the TACS fill line.

Method 2 - Carry up a resupply module on SL-4, leave module in CSM, and connect to TACS fill line using a long high pressure hose.

Method 3 - Connect onboard experiment gas (GN_2) tanks on Airlock Module (AM) to TACS using a long high pressure hose.

Method 4 - Same as Methods 1, 2, or 3 except hose would be connected to the pitch thruster, and gas backflowed through the thruster valves.

Method 5 - Same as Method 3 except onboard GN_2 from AM tanks would be used.

Method 6 - Install an adjustable thruster in the -Z axis Scientific Airlock (SAL) and utilize O_2 or N_2 from AM tanks.

Method 7 - Load additional propellants and use the CSM attitude control propulsion system as a supplemental OWS attitude control system.

Method 8 - Carry up an N_2 resupply in a cryogenic state and include systems for gasifying and transferring to the TACS.

Method 6 was selected as the best concept for supplementation based primarily on: use of excess onboard consumables, no requirement for EVA, minimum hardware requirements, and minimal crew training and installation time.

Initially, the thruster assembly design included provisions for use of both O_2 and N_2 gas supplies located in the AM. Further detailed analysis of the design revealed potential problems associated with compatibility of certain lubricants and seal materials with the O_2 . As a result, subsequent design and test activities concentrated on the N_2 system.

The maximum total impulse and thrust level obtainable with the SAL thruster assembly was 151,240 N-sec (34,000 lbf-sec) and 53.4 N (12 lbf), respectively. Using a rotatable thruster concept, the thruster assembly could be used to supplement the TACS during the EREP experiments and for desaturating the CMG's in attitudes where the gravity gradient dump scheme was not available.

The thruster assembly and the installation through the SAL are shown in Figure 22, which depicts the major components of the system. Maximum utilization of onboard hardware is illustrated in that only the thruster, valve assembly, boom assembly, and certain quick disconnects were to be carried up. All other hardware including the N_2 supply unit, experiment canister, and the water hose were onboard the OWS.

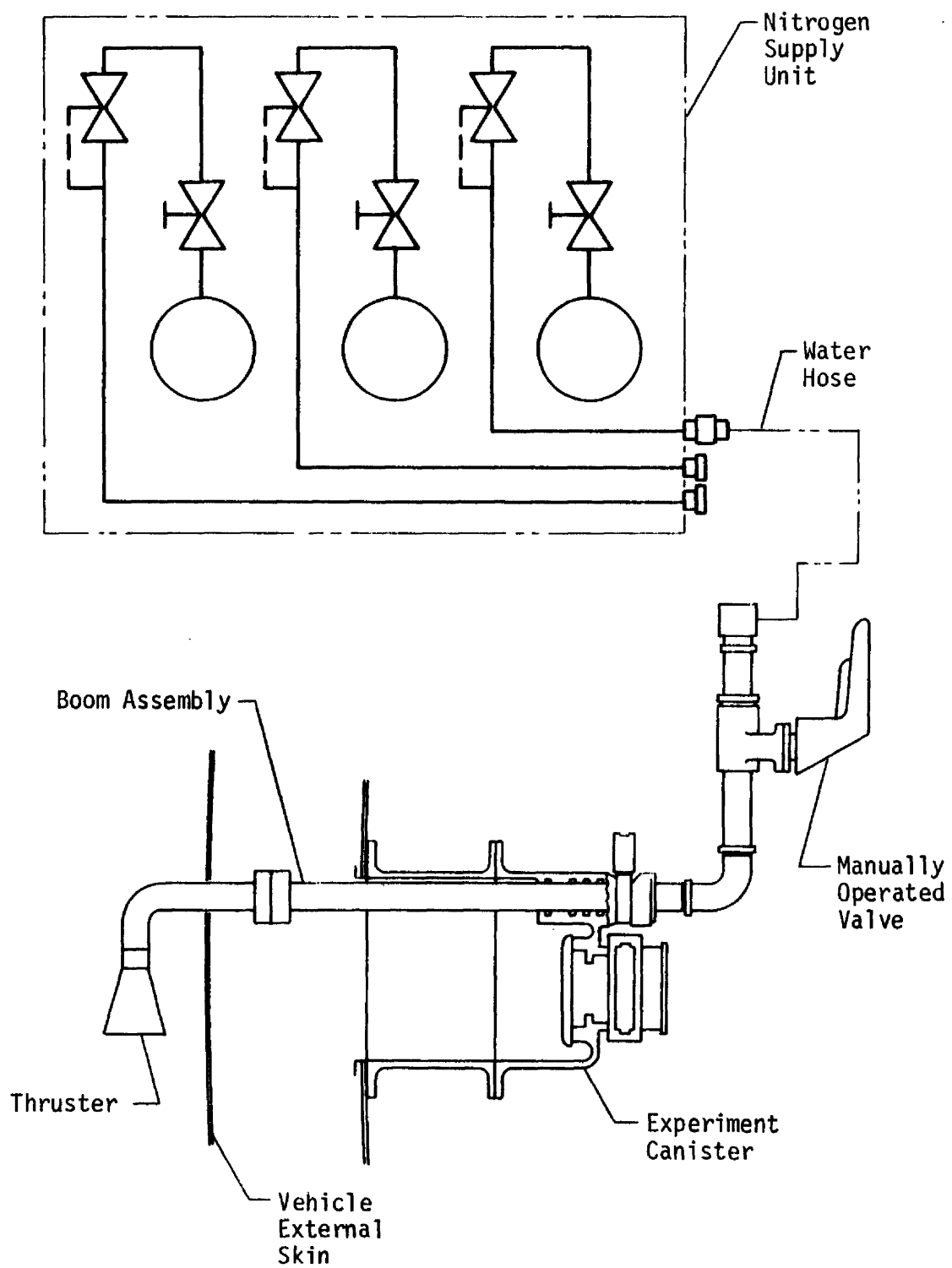


Figure 22.- Scientific Airlock Thruster System Schematic

Operation of the thruster assembly would require manual actuation of the valve by the astronaut for a predetermined period of time, depending on the impulse requirement. A disk indicator permitted orientation of the nozzle to the desired angular position to provide uncoupled torques about the roll, pitch, and yaw axes. Installation of the thruster assembly used procedures similar to those required for an onboard experiment.

Verification testing of the hardware included performance acceptance testing of the valve and the thruster assembly, O_2 compatibility, and lubricant tests. The hand operated ball valve was identical to that used onboard the OWS in the fecal dryer system. The higher operating pressure and increased cycle requirements for the thruster assembly application of the valve required that proof, leak, functional, cycle life, and burst tests be conducted to verify the valve integrity.

Mockup hardware was delivered to Johnson Space Center (JSC) for use in crew training exercises and flight hardware was delivered to KSC prior to the SL-3 launch. A systems status assessment of the APCS prior to the launch, and the more urgent need for other hardware items to be supplied to the workshop resulted in a decision not to use the SAL thruster assembly during the remainder of the Skylab mission.

3.8 MISSION SUPPORT

The Mission Support Team for the TACS manned the Huntsville Operations Support Center (HOSC) 24 hours per day, 7 days per week during SL-1, SL-2, SL-3, and SL-4. For the unmanned missions on-call personnel were available 24 hours per day, 7 days per week. A daily status report was submitted every day of the mission from the launch of the Skylab Cluster to completion of the APCS engineering tests at the end of the mission. With the exception of the SL-1 and SL-2 missions, each status report was coordinated with JSC mission support personnel whenever the system was active.

Prior to the Skylab mission, the performance of the TACS was analyzed and the curves were generated using the GN_2 performance computer program (see paragraph 3.1). These curves were used to determine the performance of the system during the mission, using real time telemetry data.

The JSC TACS consumable status was generated by a Hewlett-Packard computer program using real time data. The program's performance equations were mathematical curve fits of the performance curves generated at the Marshall Space Flight Center (MSFC) prior to start of the mission. The Hewlett-Packard computer's limited data storage capability required the use of compact equations. One obvious disadvantage of this method of computing the system status is the error introduced by use of the curve fit equations; however, the error was normally less than 3 percent.

Two methods were used to estimate total impulse remaining. One method was based on GN_2 mass calculations using telemetry real time data. Basically, this method employed the curves generated from the GN_2 performance computer

program or actually used the computer program to calculate mass and total impulse remaining at appropriate times during the mission. The latter approach was the most accurate method to determine system status. The other method utilized the minimum impulse bit (MIB) and was very useful for a quick determination of impulse usage. This method was based on estimating the total impulse per thruster firing and multiplying this by the number of firings. The total impulse per firing was calculated by the equation:

$$I_T = F_{avg}(t + \Delta t)$$

where

I_T = total impulse

F_{avg} = average thrust

t = command pulse width

Δt = time factor added to account for thrust tailoff.

The thrust level was determined from the performance curves as a function of flight system pressure and average module inlet temperature. The command pulse width was changed periodically as a function of the MIB required. The thrust tailoff time was varied from 25 to 10 msec during the final manned mission in an attempt to provide better correlation between the MIB and mass methods of calculating total impulse remaining. Comparison of total impulse remaining values computed near the end of the mission by the different methods indicated that a 15 msec tailoff factor more closely approximated the actual impulse expended.

Several problems were encountered during the mission support phase. One problem was the instrumentation transducer noise (see paragraph 3.9) that occurred during manned missions. The noise was of a sufficient random nature that averaging large numbers of data points created no difficulties, and the results were consistent enough to be beneficial. A second problem involved apparent excess mass consumption when performing mass calculations immediately after large system usage. The indicated mass of GN_2 remaining tended to increase with time until a stable condition was reached and repeatable results obtained. This phenomenon was associated with the existence of temperature gradients within each sphere (see paragraph 3.10) and was taken into account when applying the mass calculation results to system total impulse remaining determinations. Finally, the nonreal time data were of limited usefulness to the mission support effort. The All Digital Data Tape (ADDT) event data (thruster pressure switch actuations) were too noisy to have been of any practical benefit. The Mission Operations Planning System (MOPS) stored and processed data in a centrally located computer which was accessed through remote terminals. During the early part of the mission, these data were of limited usefulness because they were not usually available or were erroneous. However, during the latter part of the mission the data were more consistently available and accurate. In this case it did provide a meaningful supplement to the real time data system.

3.9 PRESSURE TRANSDUCER NOISE

The telemetry system pressure measurements were observed to fluctuate by as much as 4.137×10^5 N/m² (60 psia) just after the SL-3 CSM docking on Day of Year (DOY) 209. The fluctuations were not noted during the previous orbital stowage phase of the mission. Although the measurements remained within system tolerances, an investigation was made to determine the probable cause of the noise.

Review of data from DOY 208 through DOY 216 indicated that the data on two different multiplexers and their respective reference channels were stable until the manned phase. When the Skylab was manned, there was a noticeable increase in noise for the subject pressure measurements and their respective multiplexer reference channels. Three other reference channels were evaluated and they also showed increased noise content. Since the presence of the CSM with its associated electronic equipment may have caused the configuration of the radio frequency field to have changed following docking, the most probable cause for the fluctuations was that the signal lines were experiencing radio frequency interference.

The fluctuations of both pressure measurements continued throughout the manned phases of the mission. However, accurate mass calculations could still be made by averaging many data points to remove the random fluctuations caused by the noise. No further investigation or troubleshooting of the instrumentation system was necessary.

3.10 SPHERE TEMPERATURE ANOMALIES

It was noted during the mission support effort that mass calculations did not stabilize until some period of time after large gas usages. After equilibrium conditions were restored, the mass calculations yielded consistent results. An analysis of flight data was performed to determine possible means of eliminating this phenomenon from future missions and to evaluate its effect.

Calculations of the Raleigh Number indicated conduction to be the dominant heat transfer mode in the storage sphere since body forces acting on the gas were small except for brief periods when gas was being withdrawn. In most instances the rate of withdrawal of gas from the spheres and the rate of change of the radiation environment were small enough that heat transfer by conduction could maintain a state of near equilibrium between the gas and the metal sphere. However, during periods of large usage, the gas expansion tended to cause the gas to cool faster than the sphere, with the result that a nonequilibrium condition existed for some time after the usage. During this transient period, large temperature gradients could have existed within the gas.

The sphere temperature transducer installation was designed to minimize the effect of temperature gradients within the sphere by placing the sensing element at a point where it would read close to the mean gas temperature in

the sphere during the transient period. Since this mean temperature point could shift and methods for analyzing its location are not very accurate, it was to be expected that there would be some error inherent in the temperature data during the transient periods. Figures 23 and 24 show the approximate magnitude of this error for a representative gas usage period. The temperature during the transient period read higher than it should have based on calculations of mass from subsequent equilibrium data. This trend was observed during most periods of high gas usage. Mass calculations using pressure and temperature telemetry data performed during the transient period yielded erroneous results. These tended to indicate a greater mass usage than that calculated from equilibrium data.

The analysis indicated that the transducer sensing elements should have been located slightly farther from the wall to give a better estimate of the mean temperature during the transient period.

3.11 INSTRUMENTATION ERROR ANALYSIS

During the mission, the TACS pressure required to provide a minimum of 44.5 N (10 lbf) thrust was reassessed. To accomplish this task the accuracy of the system instrumentation, including telemetry, had to be more realistically determined.

Prelaunch loading requirements were based on an instrumentation error analysis. Individual instrumentation transducer accuracies (pressure and temperature) were obtained from a study which evaluated all onboard and ground support equipment components. These accuracies were used to develop a fill envelope which guaranteed that the minimum loaded GN₂ mass would meet all Contract End Item Specification and mission requirements.

During the mission, available total impulse remaining was calculated using system pressure and bulk gas temperature. The usable total impulse was obtained by subtracting an unusable amount from the available calculated total impulse. The unusable total impulse was originally based on a minimum system pressure required to provide 44.5 N (10 lbf) thrust, including instrumentation inaccuracies.

During the second manned mission, an analysis was performed to determine whether the usable total impulse could be increased by reducing the amount previously considered unusable. The analysis reviewed calibration and test data for the specific pressure transducers installed in the flight system. A 3- σ error band was determined for each transducer and then combined with the telemetry system errors to yield a pressure reading inaccuracy of $\pm 4.688 \times 10^5 \text{ N/m}^2$ ($\pm 68 \text{ psia}$). Also the telemetry bit size of approximately $1.034 \times 10^5 \text{ N/m}^2$ (15 psia) was included.

Using the results from the above analyses and the requirement to provide a minimum thrust level of 44.5 N (10 lbf) for a rescue mission docking, the minimum allowable system pressure was lowered from 3.020×10^6 to $2.530 \times 10^6 \text{ N/m}^2$ (438 to 367 psia). This represented a gain in usable total impulse of 14,283 N-sec (3211 lb-sec).

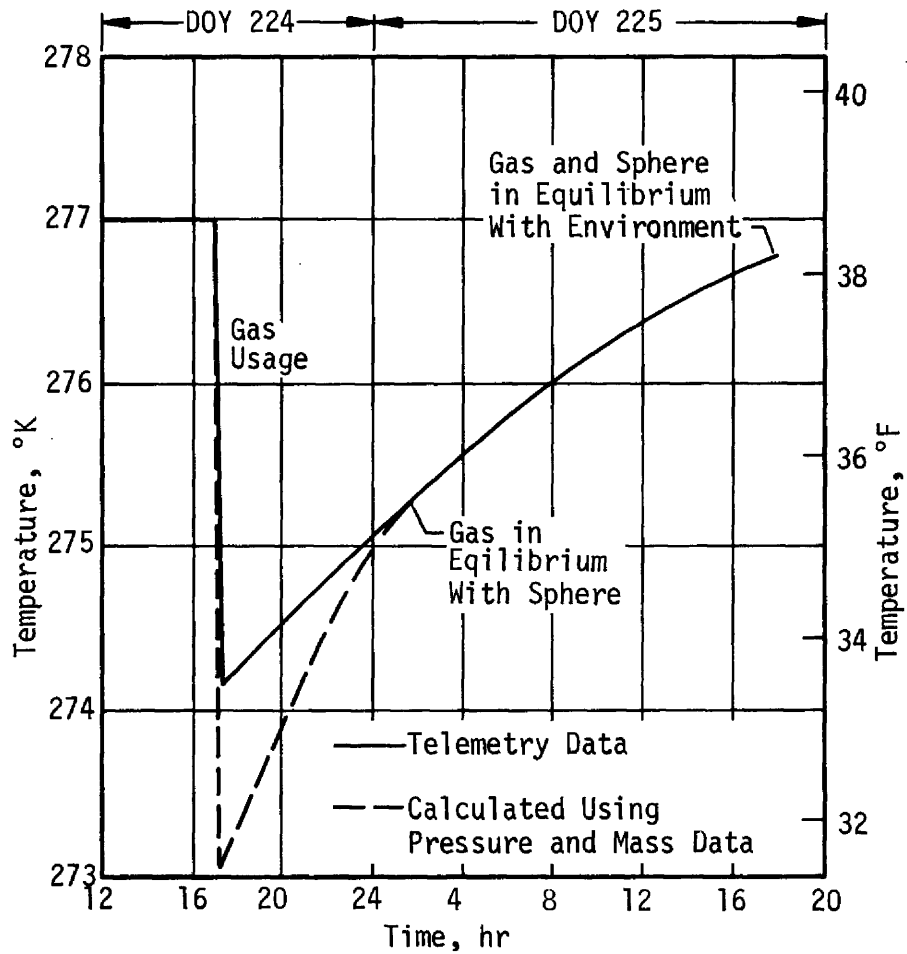
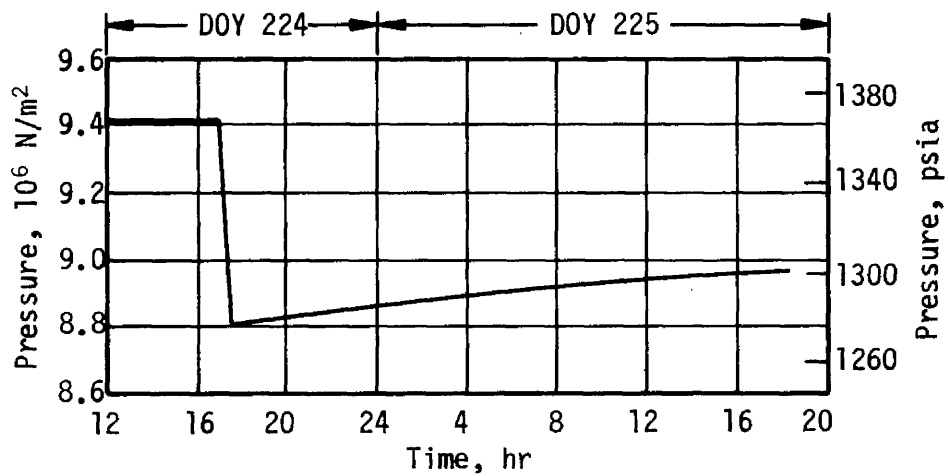
Figure 23.- Average GN_2 Bulk Gas Temperature

Figure 24.- Average System Pressure

3.12 THRUST LEVEL REQUIREMENTS

The premission thrust level requirements for the TACS are presented in Table 1. These requirements imposed a restriction on available TACS usable impulse. A system pressure of $2.53 \times 10^6 \text{ N/m}^2$ (367 psia) including allowance for telemetry and instrumentation inaccuracies (see paragraph 3.11) was required to provide a thrust of 44.5 N (10 lbf). Therefore, the total impulse remaining in the TACS when the pressure decays below $2.53 \times 10^6 \text{ N/m}^2$ (367 psia) is by definition unusable.

Since the potential to gain additional impulse existed by lowering the rescue mission thrust level and, therefore, the system pressure, a review of rescue and other mission thrust level requirements was initiated during the SL-3 mission. An analysis was performed to evaluate thrust level requirements for various mission events utilizing available flight and design data. The results of the analysis shown in Table 2 indicate that a rescue mission CSM docking in the radial port would require 44.5 N (10 lbf) which would not allow the premission thrust level requirement to be lowered.

Table 1.- TACS Premission Minimum Thrust Level Requirements

Mission Events	Newtons	Pounds-Force
Booster Separation Transients	222.4	50
Each Manned Mission CSM Docking	89.0	20
From Last Manned Mission Docking to End of Mission	44.5	10
Rescue Mission CSM Docking*	44.5	10

*This requirement appended to original premission thrust requirements.

Table 2.- TACS Minimum Thrust Level Requirements Analysis

Mission Events	Newtons	Pounds-Force
Earth Resources Experiment Pointing*	8.9	2
CMG Reset Maneuver*	8.9	2
Momentum Desaturation Maneuver*	8.9	2
Trim Burn--Four CSM Engines	89.0	20
Trim Burn--Two CSM Engines	44.5	10
Rescue Mission--Nominal End Port Docking	22.2-44.5	5-10
Rescue Mission--"Worst Case" Radial Port Docking	44.5	10

*This thrust level is not optimum but is usable. Lower thrust levels might be acceptable but were not studied because it required rescaling of the simulation.

4. THRUSTER ATTITUDE CONTROL SYSTEM DETAILED MISSION EVALUATION

This section contains the detailed flight evaluation of the TACS. The data are presented by mission phase for SL-1, SL-2, orbital storage, SL-3, orbital storage, and SL-4. The data presented for the orbital storage phases were kept at a minimum because the TACS was inactive.

4.1 FIRST UNMANNED ORBITAL STORAGE PERIOD, SL-1

The TACS was pressurized for flight to 2.083×10^7 N/m² (3021 psia) on April 30, 1973. Approximately 647 kg (1426 lbm) of ambient temperature GN₂ were loaded. The loading envelope showing the prelaunch temperature and pressure conditions at completion of system pressurization is presented in Figure 25.

The Skylab Cluster assembly was placed in earth orbit by a Saturn V launch vehicle on May 14, 1973. Lift-off occurred at 134:17:30:00 GMT. During the boost phase the dual purpose micrometeoroid/heat shield was separated from the vehicle by aerodynamic forces. Also, one of the solar array assemblies was severed from the OWS and the other was prevented from fully deploying.

The TACS was activated at 134:17:39:52 GMT, at which time firing commands were received from the Launch Vehicle Digital Computer (LVDC) located in the Instrument Unit (IU). The TACS functioned as the primary attitude control system until control was transferred to the Apollo Telescope Mount Digital Computer (ATMDC) at 134:22:20:05 GMT. At this time the CMG's were spinning up and had reached 25 percent of nominal momentum. The low momentum coupled with excessive rate gyro drift resulted in the automatic selection of "TACS Only" control. Because the heat shield was severed from the vehicle, the APCS was required to maintain a "thermal attitude" to keep workshop temperatures within acceptable limits. These thermal attitude maneuvers were performed using "TACS Only" control. CMG control was enabled with nominal momentum for the first time at 135:11:48:31 GMT.

The total impulse remaining for this initial unmanned period is presented in Figure 26. Large gas consumption on DOY's 134 and 135 resulted from removal of orbit insertion transients and operation in a "TACS Only" mode until transfer of control to the CMG's was effected. The total impulse usage rate remained high because the system was required to perform frequent CMG resets while maintaining the thermal attitude. A detailed listing of TACS usage is presented in Appendix B.

The system pressure decay and GN₂ mass are shown in Figures 27 and 28. Both parameters display blowdown characteristics similar to the total impulse remaining curve. The thrust level variation for this phase of the mission

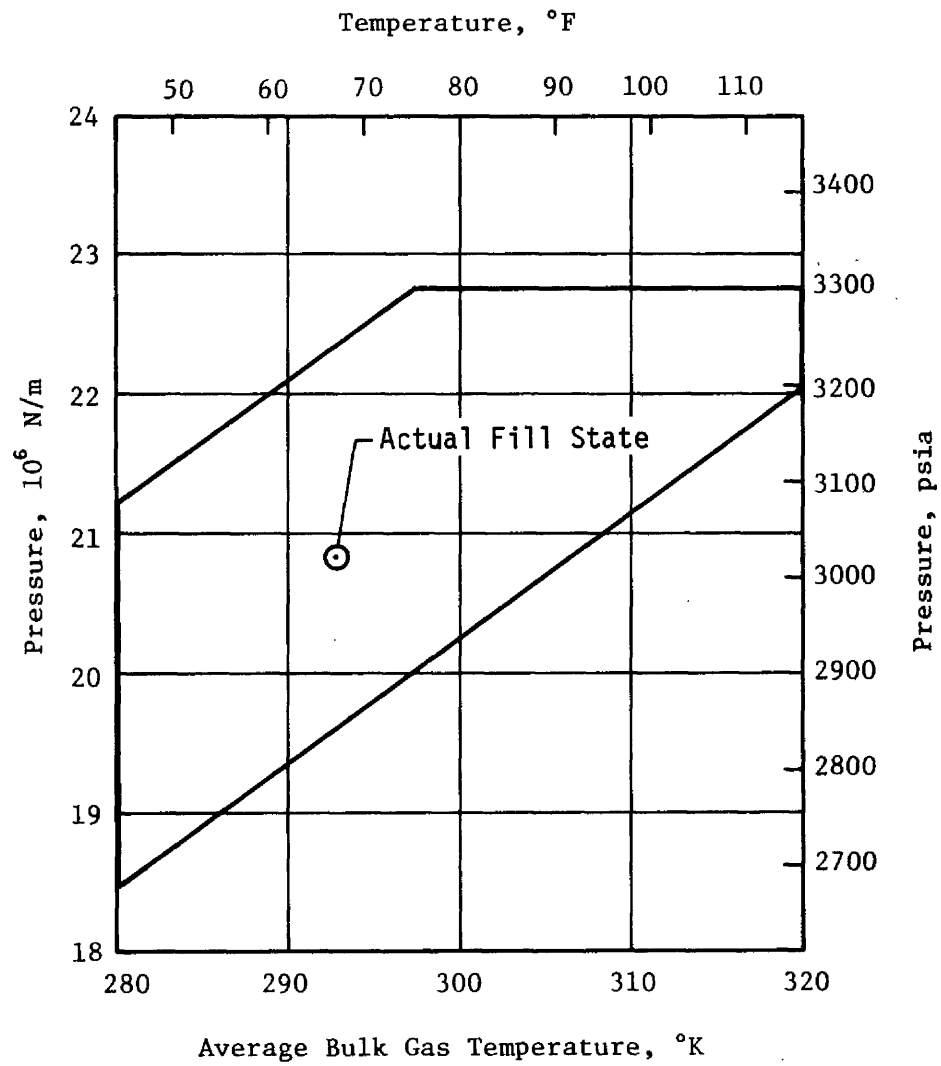


Figure 25.- Thruster Attitude Control System GN_2 Fill Envelope

is shown in Figure 29 and is compared to the thrust level stored in the ATMDC. The variation in MIB (Figure 30) also shows the times at which the ATMDC command pulse width was updated. With the exception of a brief period during DOY 136 and early in the mission when the system pressure was high, the MIB was maintained at approximately 27 N-sec (6 lbf-sec) for efficient vehicular momentum management.

Figures 31 and 32 present MIB and full-on firing histories during ATMDC control (the firing history while on IU control was not recorded). A full-on firing is defined as a firing of 1 sec command pulse width duration. Firings of longer duration are counted as individual 1 sec full-on firings equal to the number of seconds of the firing command.

The average bulk gas temperature is presented in Figure 33. The average bulk gas temperature is the arithmetic average of the six temperature transducers located in equally spaced storage spheres on the aft structure. The beta angle variation is shown in Figure 34. Beta angle describes the orientation of the orbital plane with respect to the sun vector. Positive values of beta angle are defined as the orientation of the orbital plane when the apparent orbital rotation of the spacecraft is in a clockwise direction when viewed from the sun. Negative beta angles are defined by the apparent orbital rotation of the spacecraft in a counterclockwise direction. Note that during most of this phase of the mission, the average bulk gas temperature does not increase as is expected with a decrease in negative beta angle; this is attributable to cooling of the bulk gas after orbital insertion. Orbital thermal equilibrium was established at approximately DOY 142, thereafter the bulk gas temperature responded to the changes in beta angle.

The module inlet gas temperatures and the average module inlet temperature are presented in Figure 35. In solar inertial attitude, Module One is located on the hot side of the vehicle at Position Plane I and Module Two is located on the cold side of the vehicle at Position Plane III. Cooling of the hardware and gas occurred at these positions after orbital insertion until thermal equilibrium was established. The process was similar to that occurring in the storage spheres.

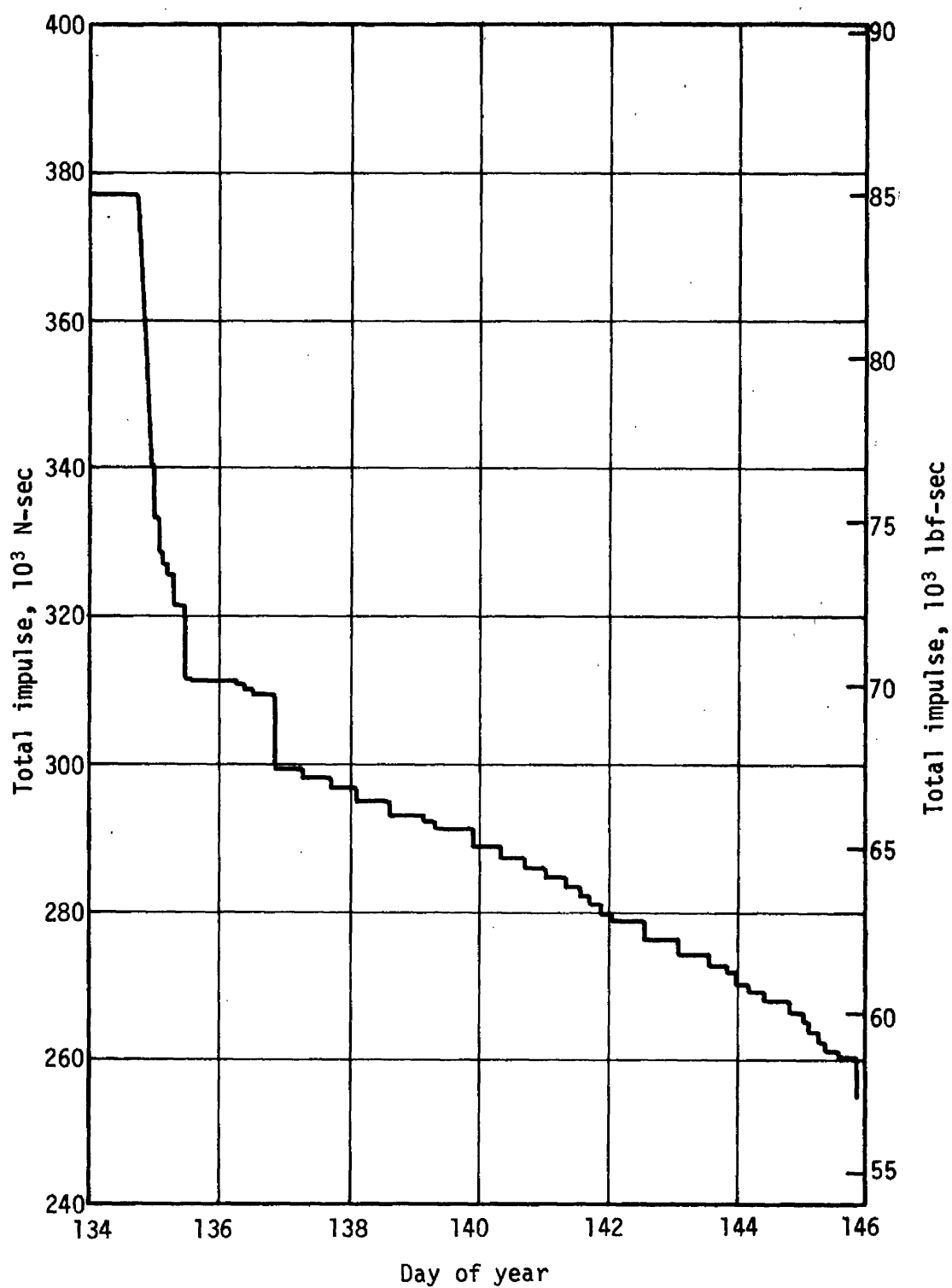


Figure 26.- Usable Total Impulse Remaining, SL-1

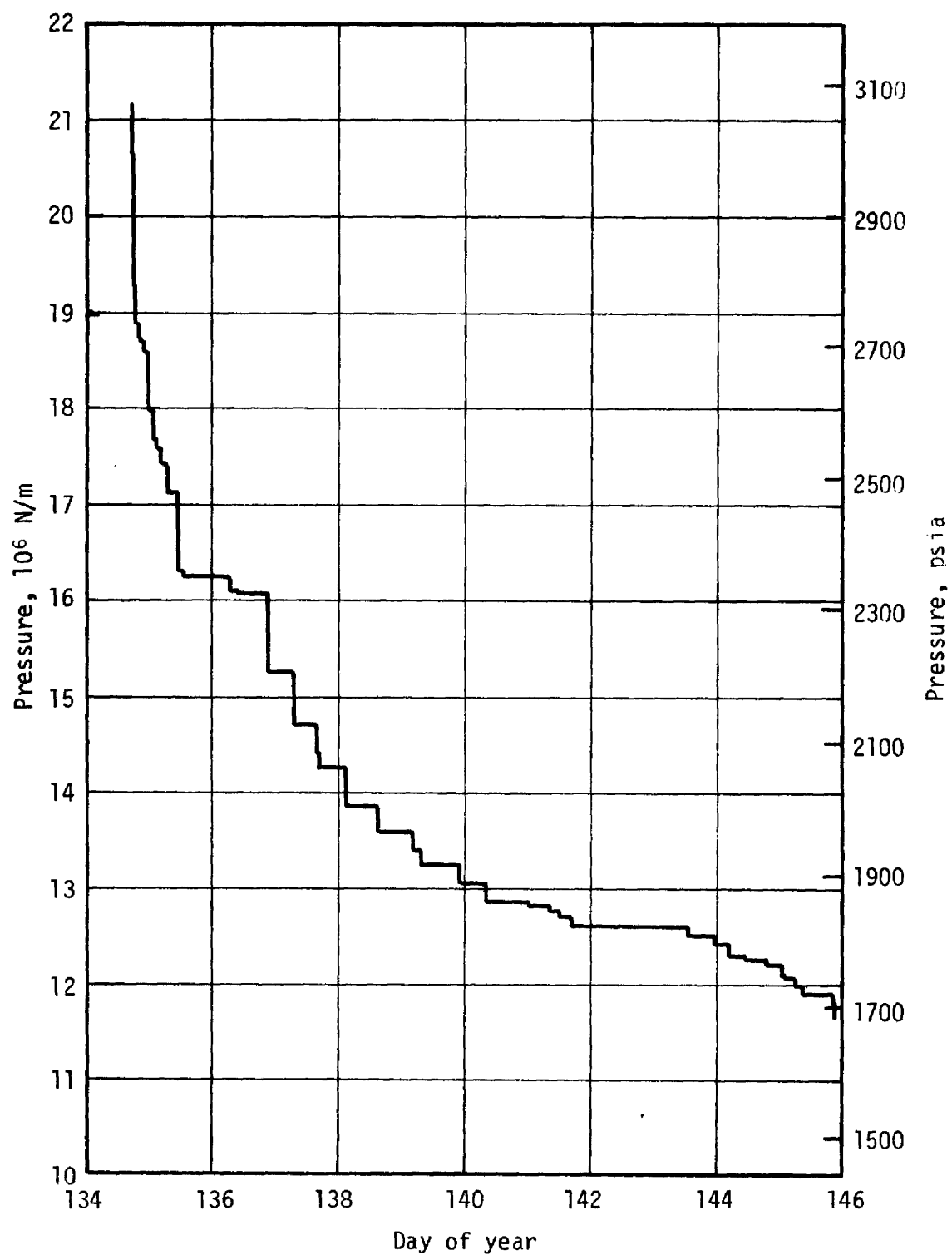


Figure 27.- GN₂ Pressure, SL-1

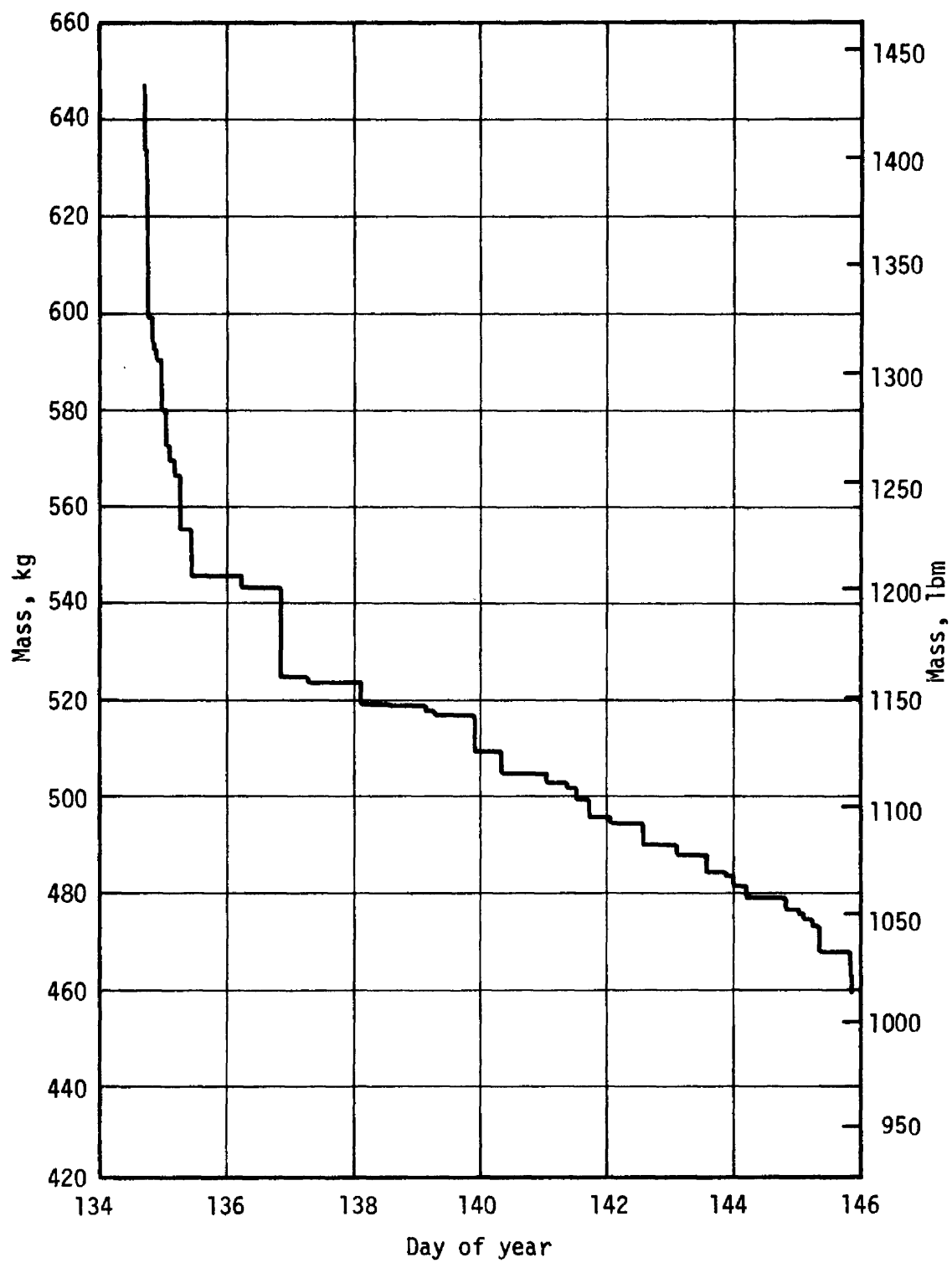


Figure 28.- GN₂ Mass, SL-1

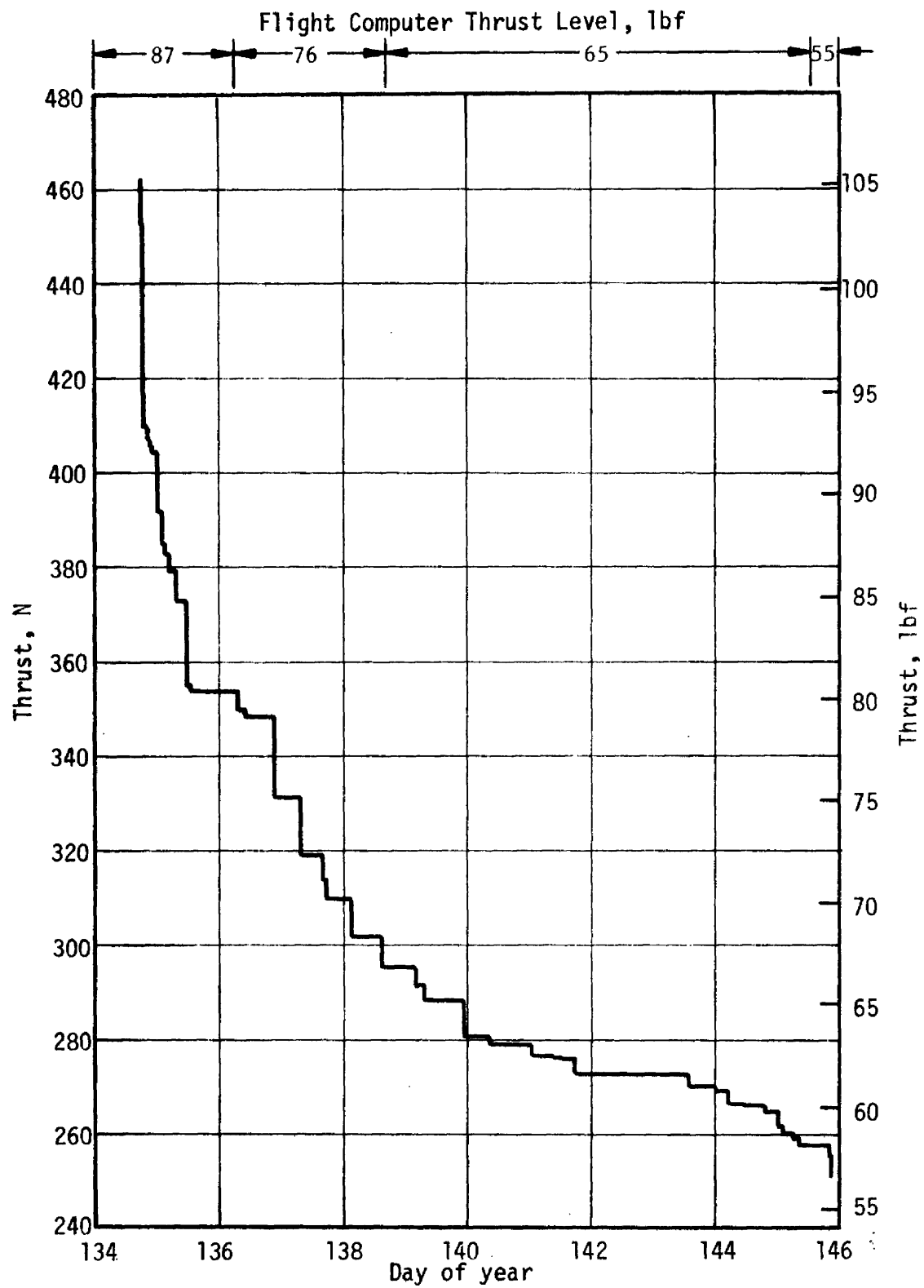


Figure 29.- Thrust, SL-1

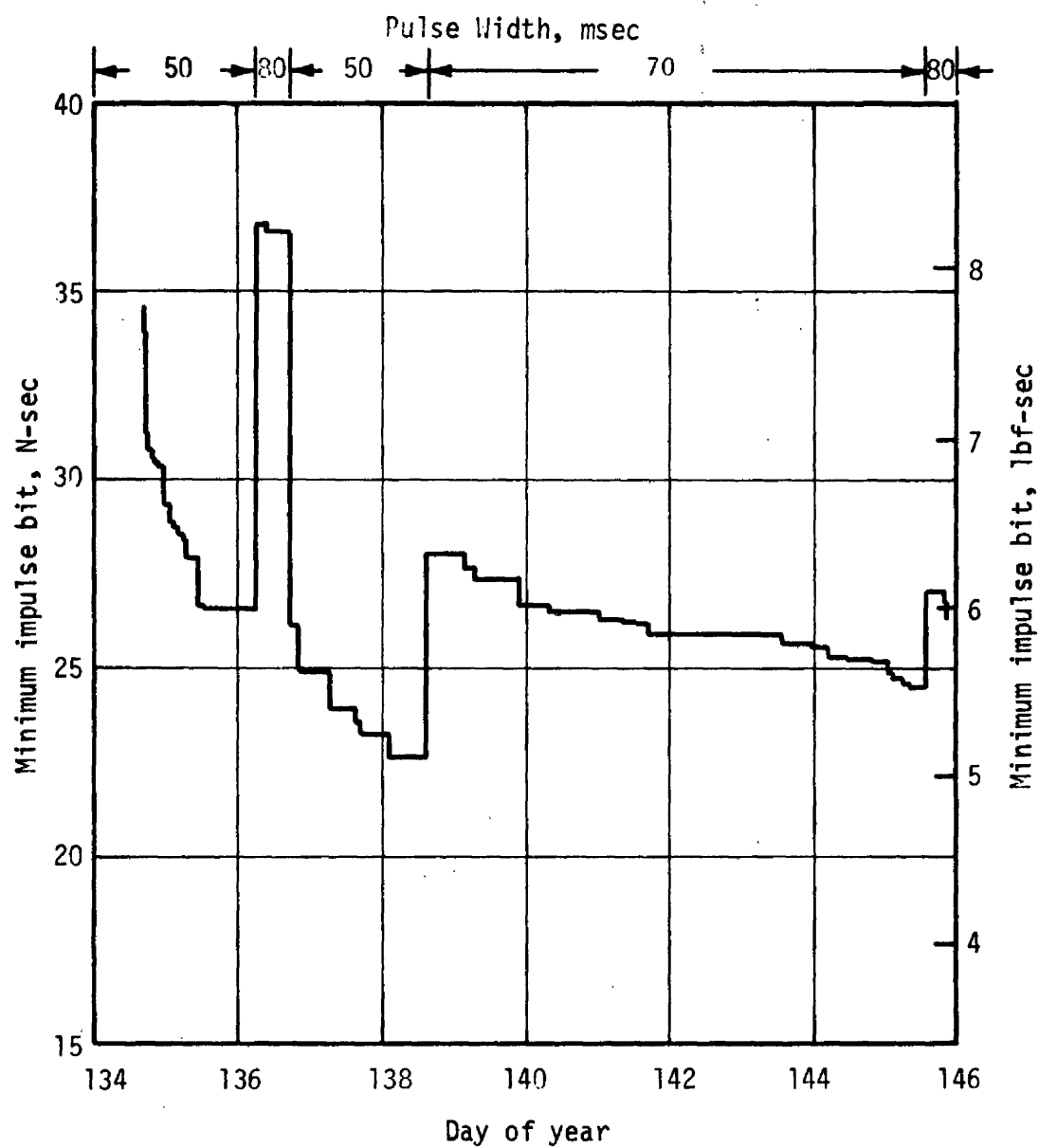


Figure 30.- Nominal Minimum Impulse Bit, SL-1

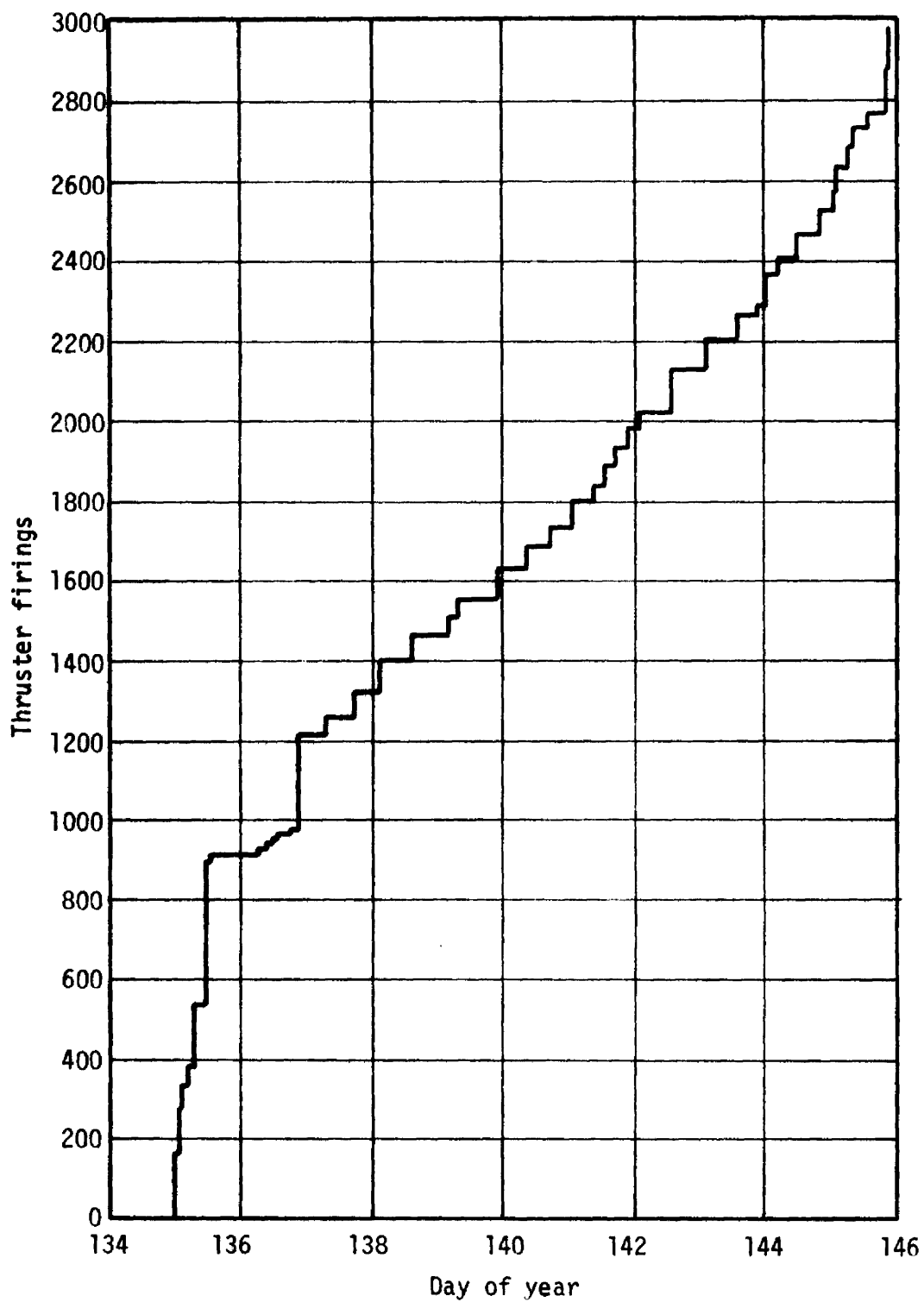


Figure 31.- Accumulated Minimum Impulse Bit Firings, SL-1

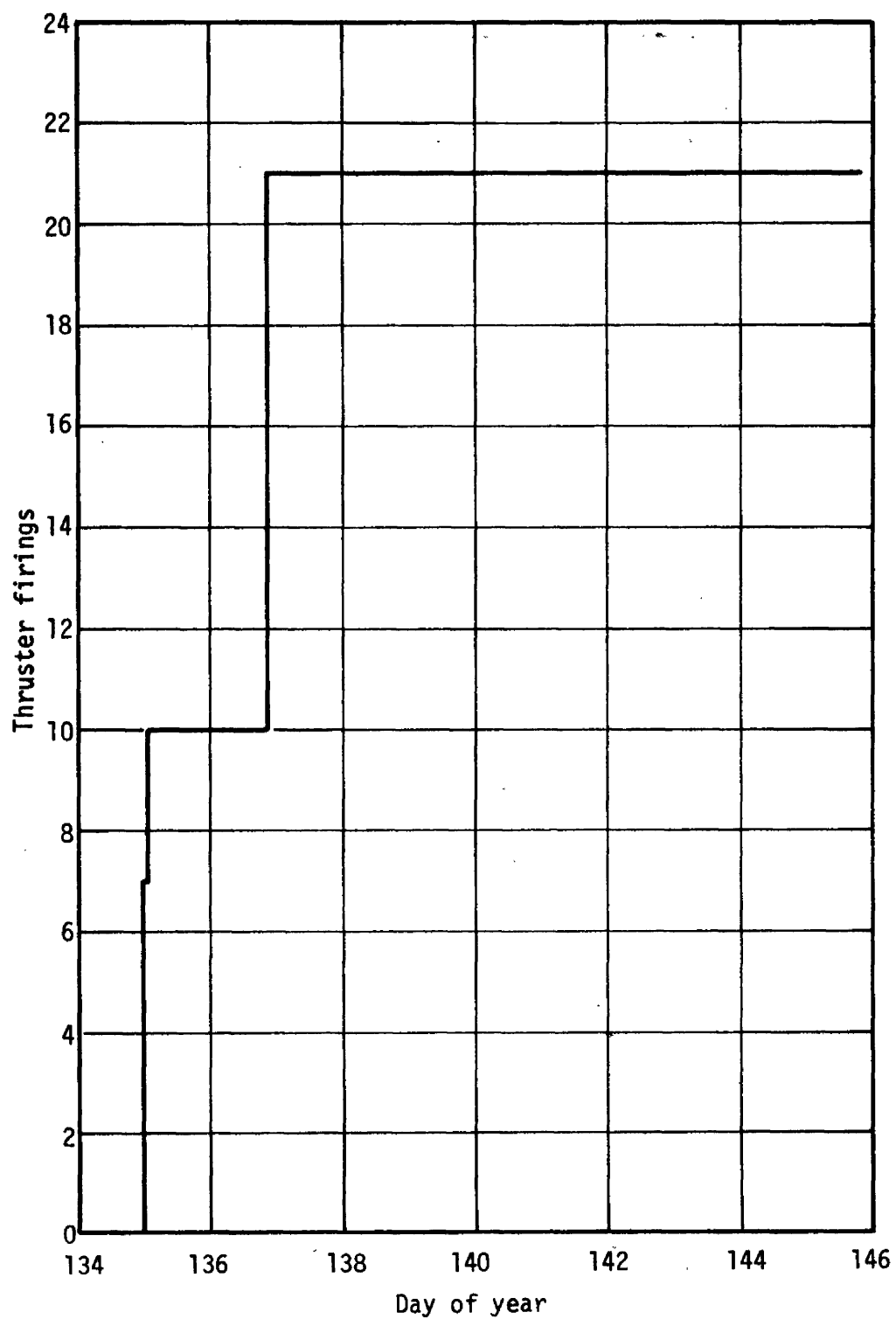


Figure 32.- Accumulated Full-On Firings, SL-1

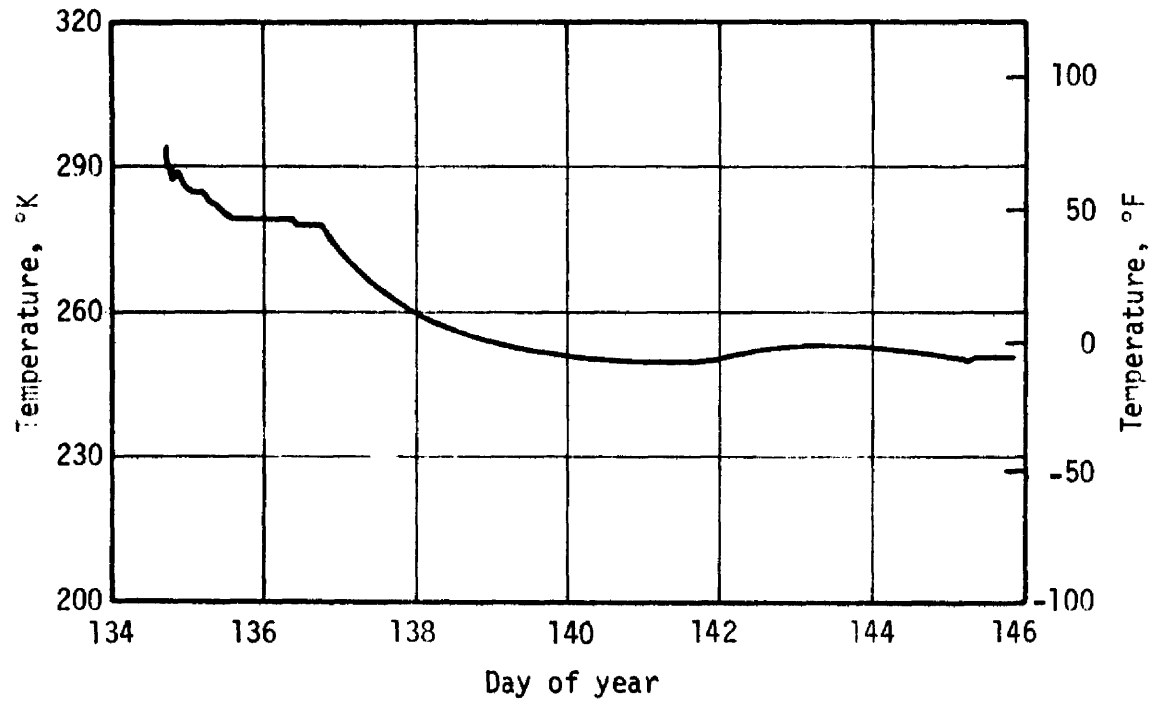


Figure 33.- Average GN₂ Bulk Gas Temperature, SL-1

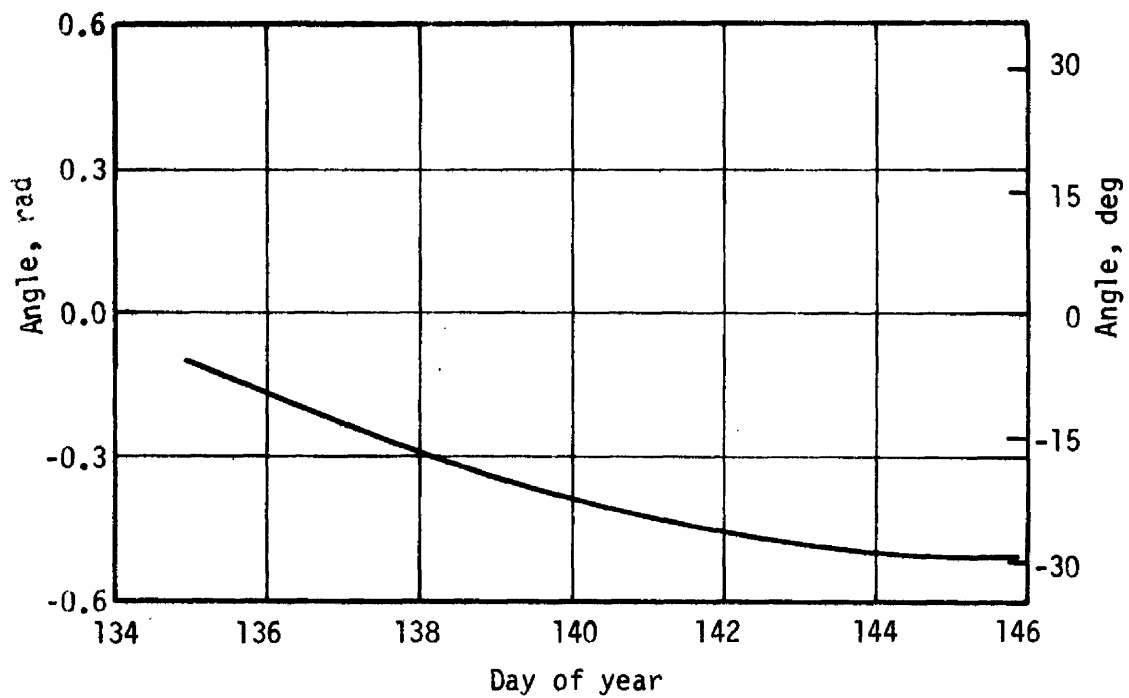


Figure 34.- Beta Angle, SL-1

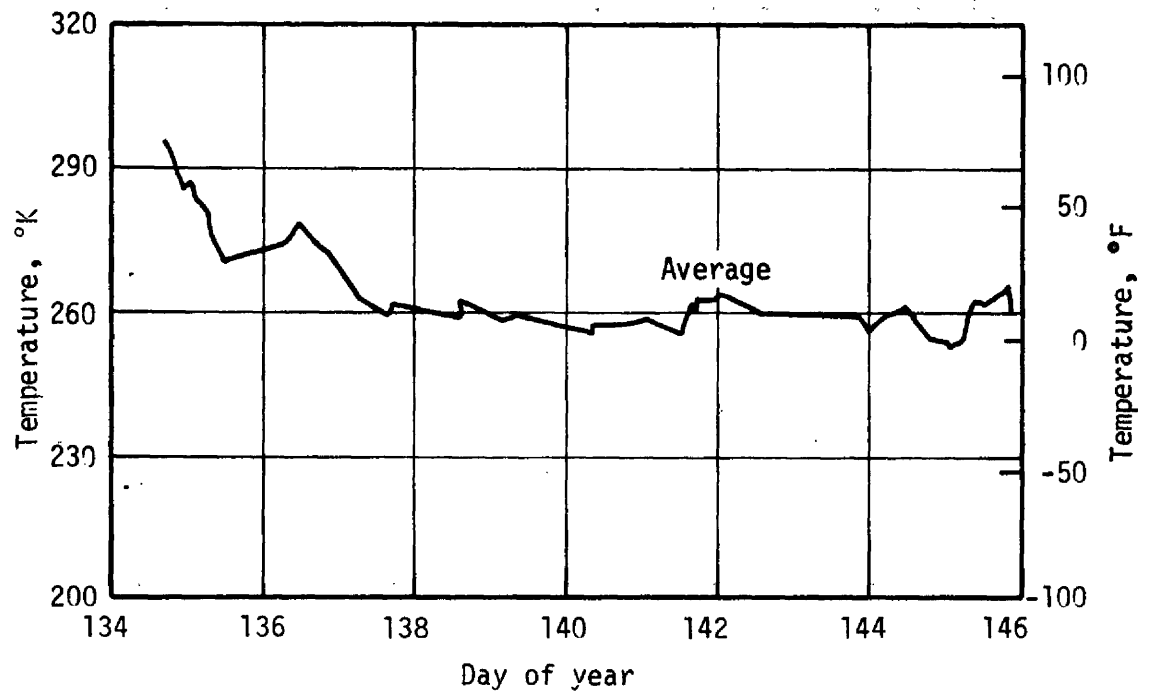
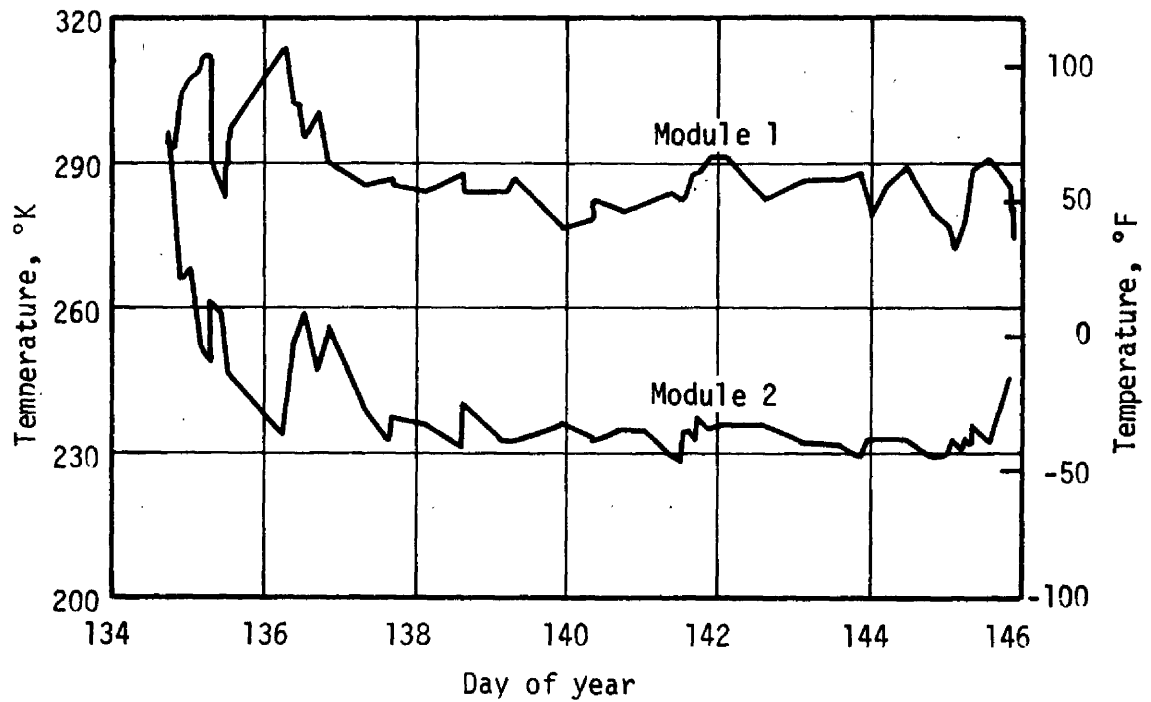


Figure 35.- Module Inlet Temperatures, SL-1

4.2 FIRST MANNED MISSION, SL-2 (28 DAYS)

The first three man Skylab crew was launched from KSC on May 25, 1973. Lift-off occurred at 145:13:00 GMT. The CSM docked with the orbiting Skylab Cluster at 146:03:40 GMT. Two EVA's were performed during this phase of the mission: one on DOY 158 and one on DOY 170. Crew accomplishments include deployment of the sunshade and freeing of the solar array so that it could fully deploy. CSM undocking occurred at 173:08:55 GMT.

The TACS was utilized extensively during the first 5 days of this initial manned phase. The total impulse remaining is presented in Figure 36. It can be seen that the system usage was reduced after DOY 150 because of decreased impulse demands. A detailed listing of all usage for this period is presented in Appendix B.

The system pressure decay and GN_2 mass are shown in Figures 37 and 38. The thrust level variation for this phase of the mission is shown in Figure 39 and is compared to the thrust level stored in the ATMDC. The variation in MIB (Figure 40) also indicates the times at which the ATMDC command pulse width was updated. The MIB was maintained at approximately 22 N-sec (5 lbf-sec).

Figures 41 and 42 present thruster firing histories for this mission phase. The MIB firings and full-on firings are shown separately. The large usages early in the mission are associated with the stand-up EVA to free the partially deployed solar array and several docking attempts before final hard dock was achieved.

The average bulk gas temperature is presented in Figure 43. The beta angle variation is shown in Figure 44 for this mission phase. Note that the temperatures responded to the changes in beta angle during this period of time because orbital thermal equilibrium conditions had been established. The module inlet gas temperatures and the average module inlet temperature are presented in Figure 45.

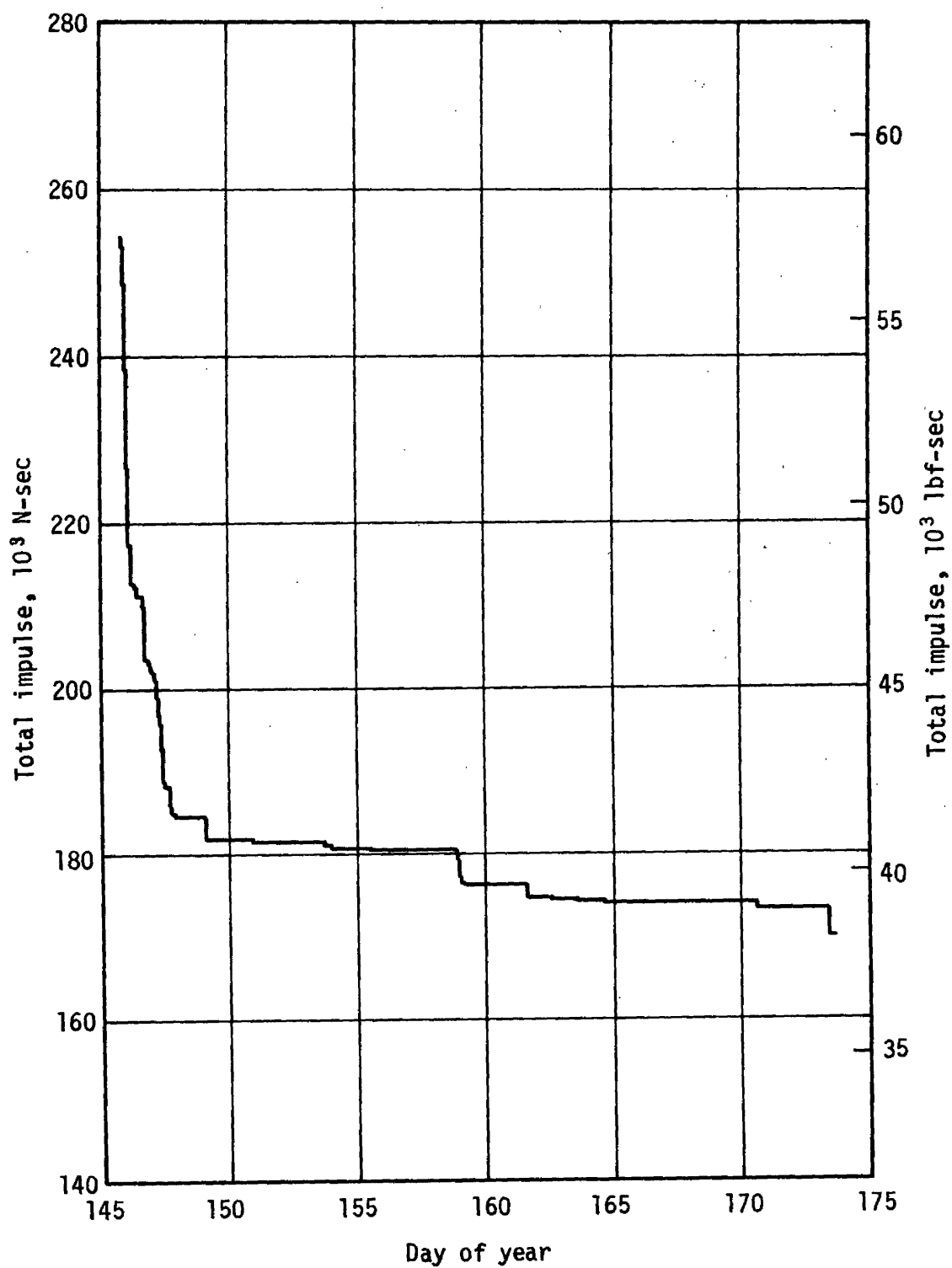


Figure 36.- Usable Total Impulse Remaining, SL-2

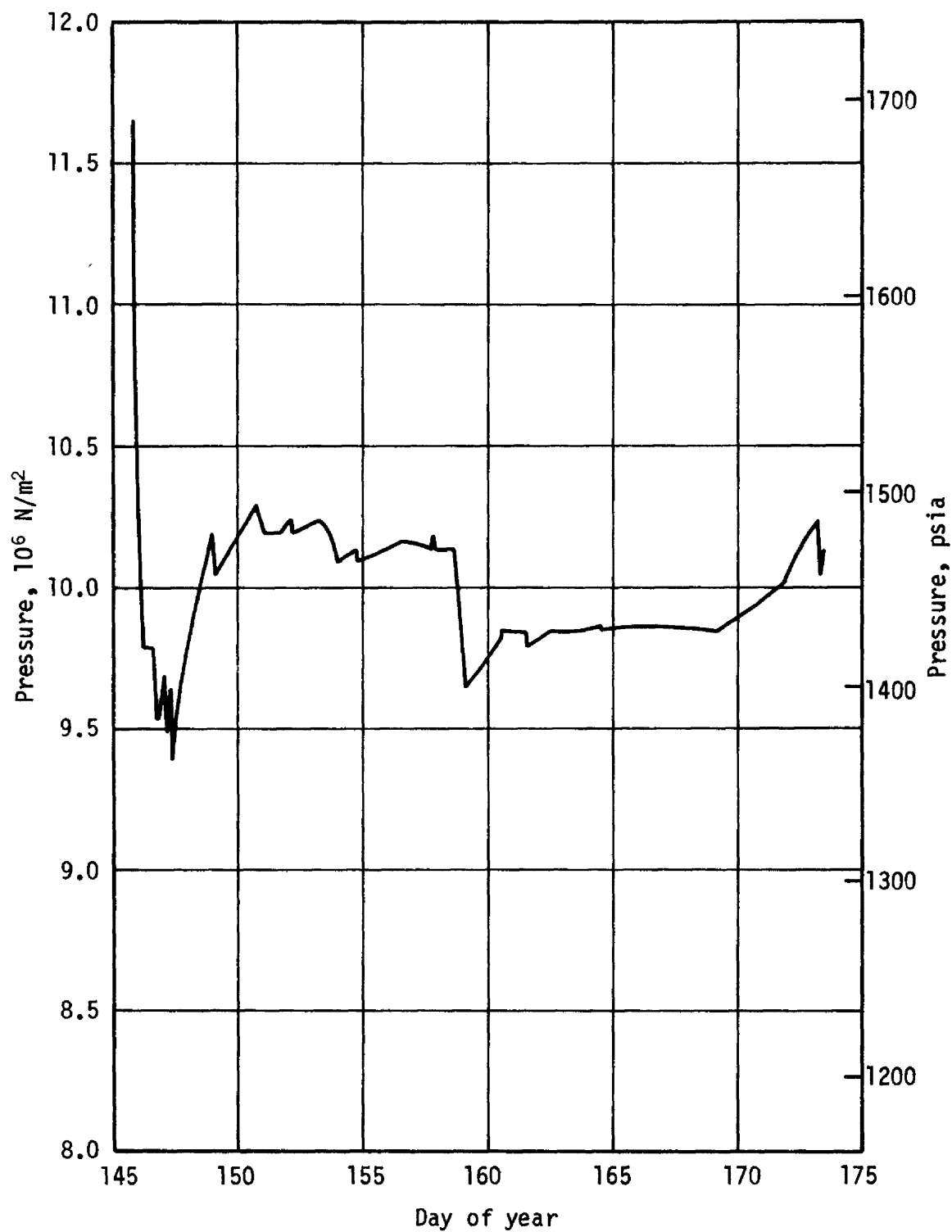
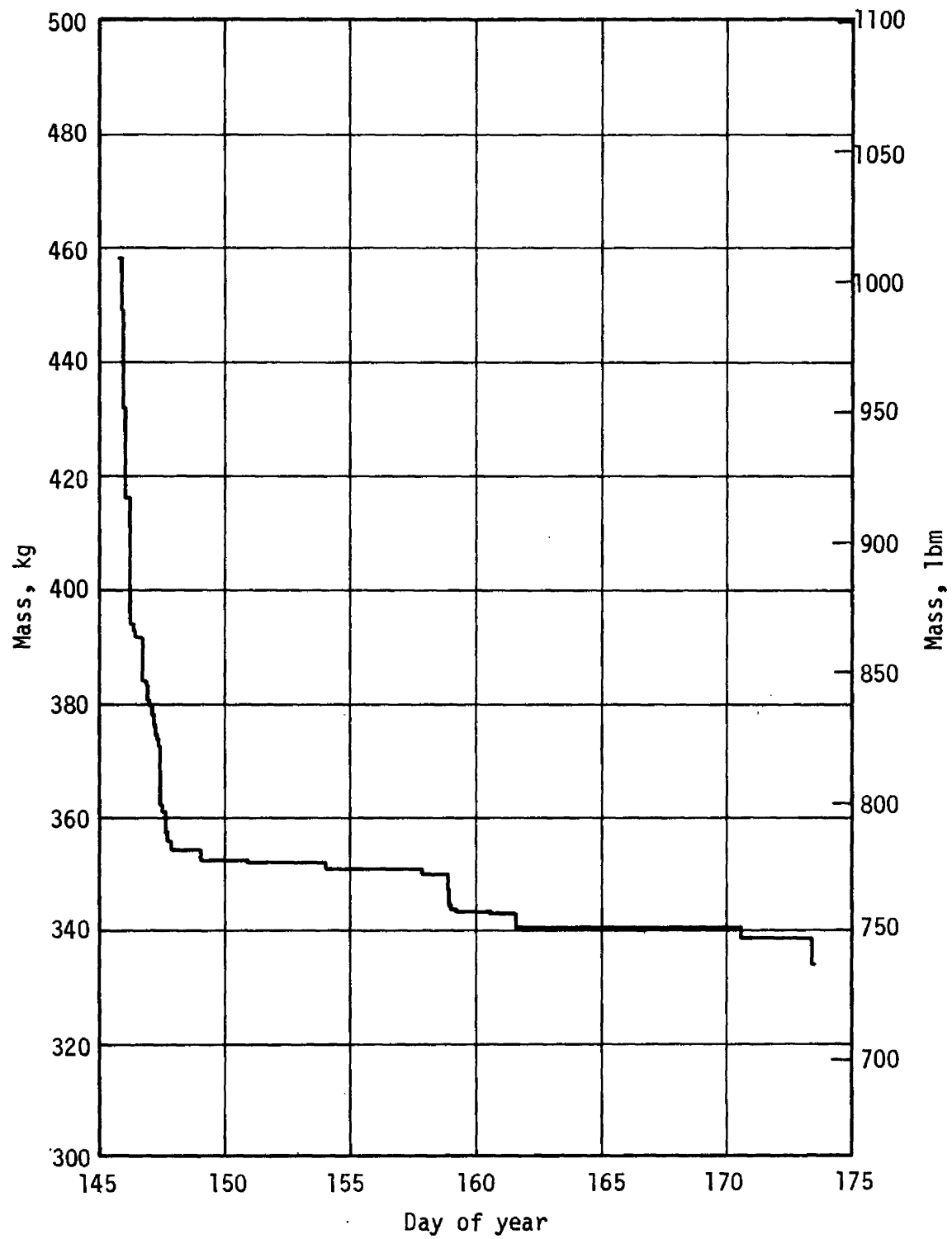


Figure 37.- GN₂ Pressure, SL-2

Figure 38.- GN₂ Mass, SL-2

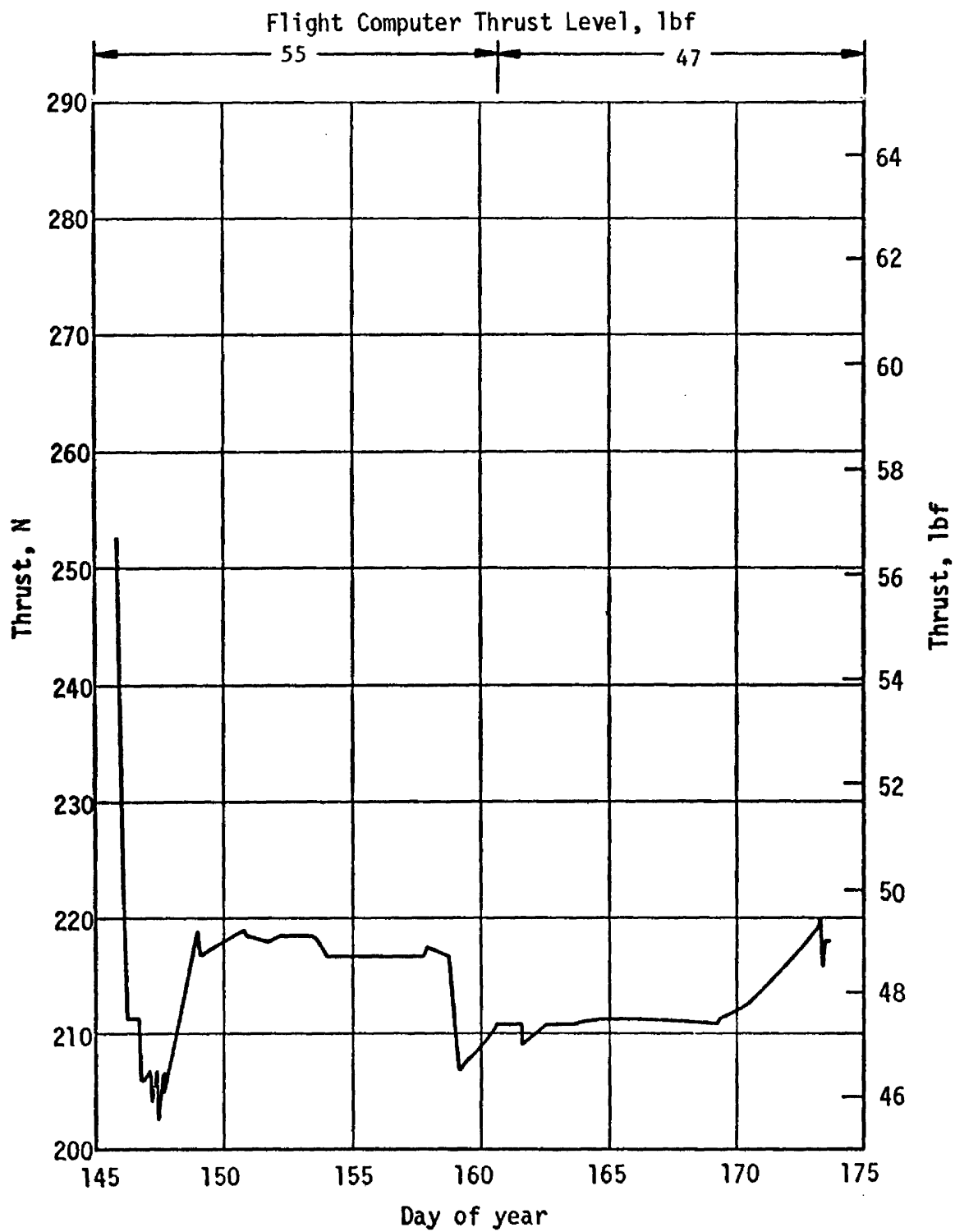


Figure 39.- Thrust, SL-2

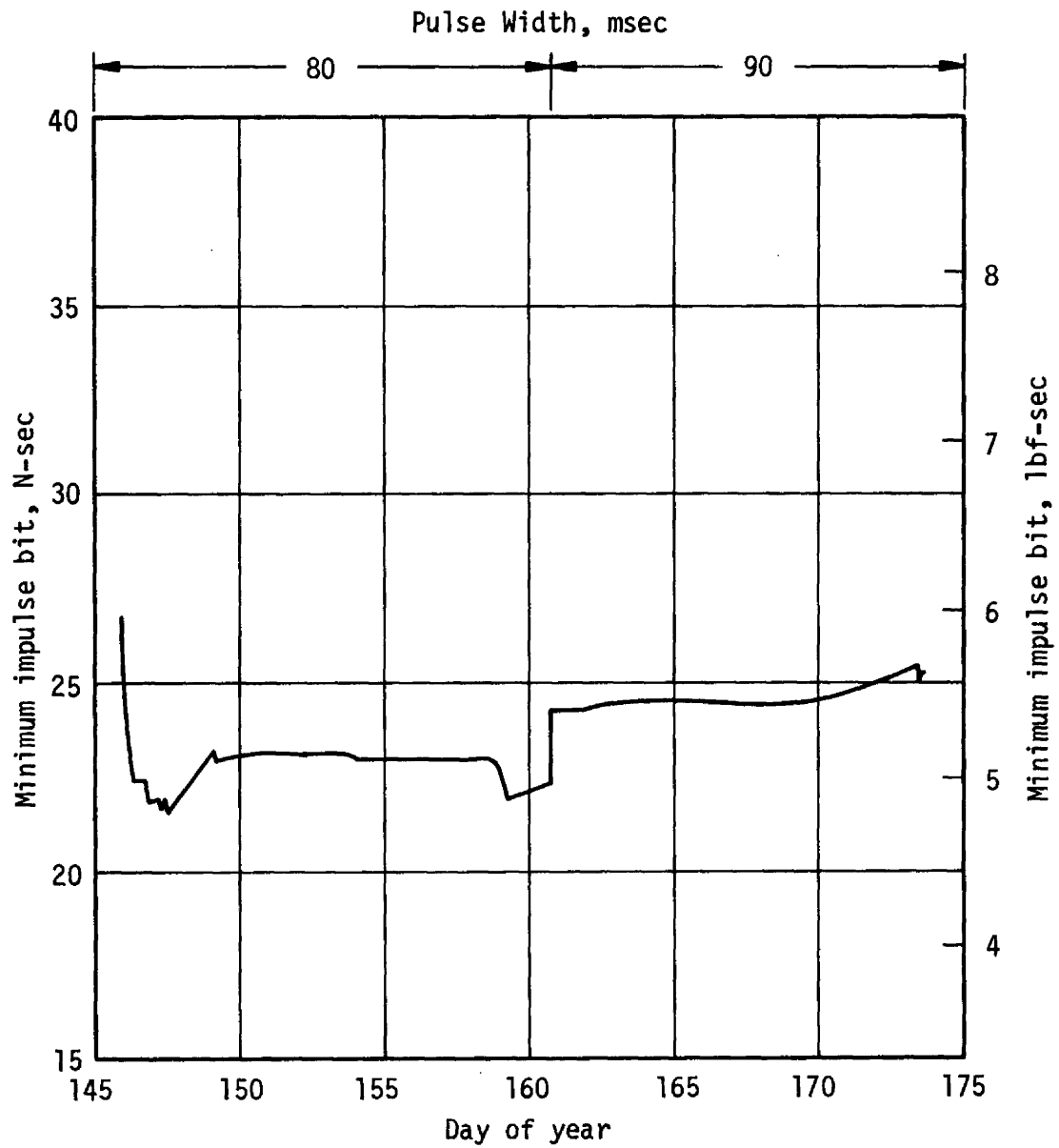


Figure 40.- Nominal Minimum Impulse Bit, SL-2

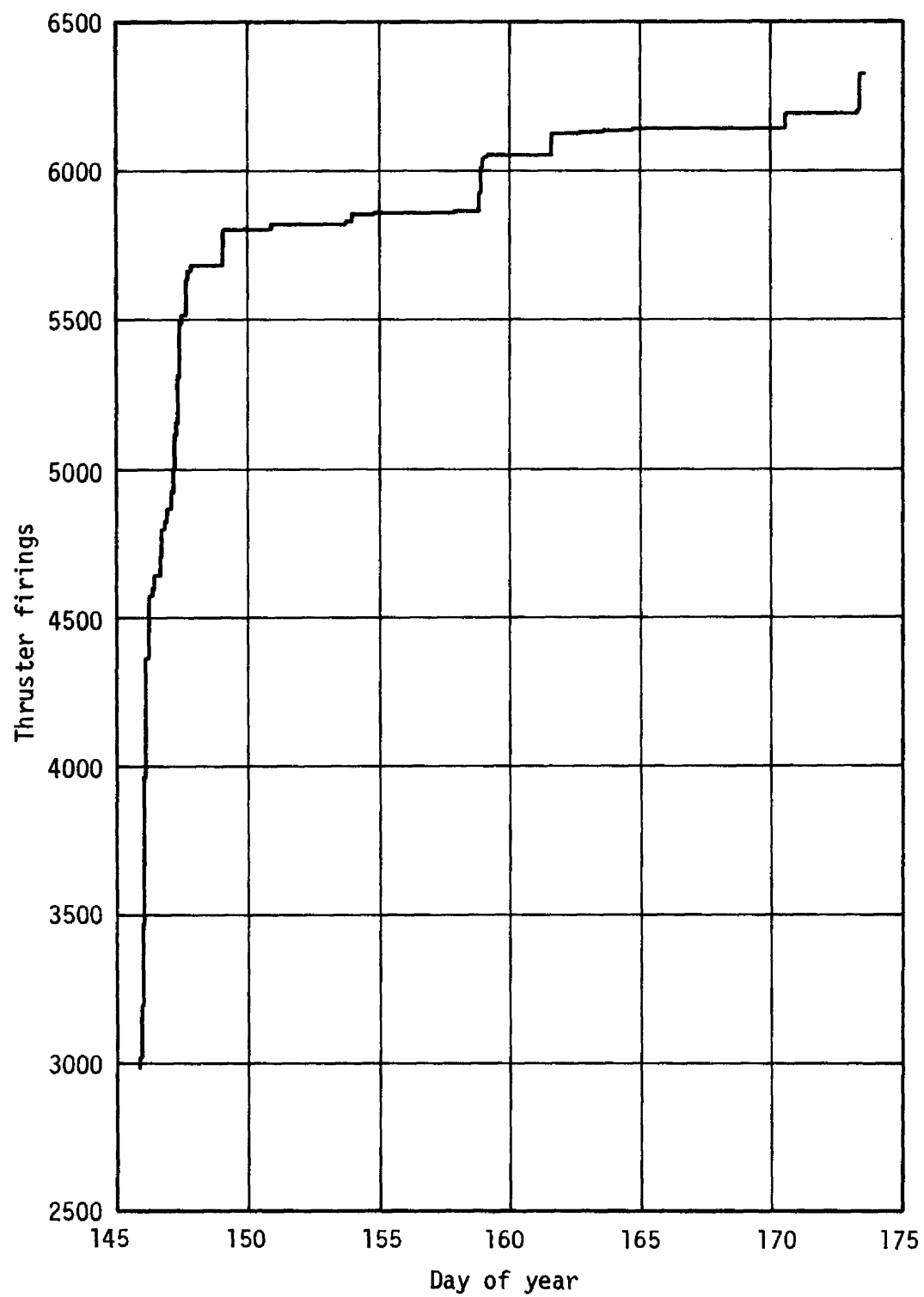


Figure 41.- Accumulated Minimum Impulse Bit Firings, SL-2

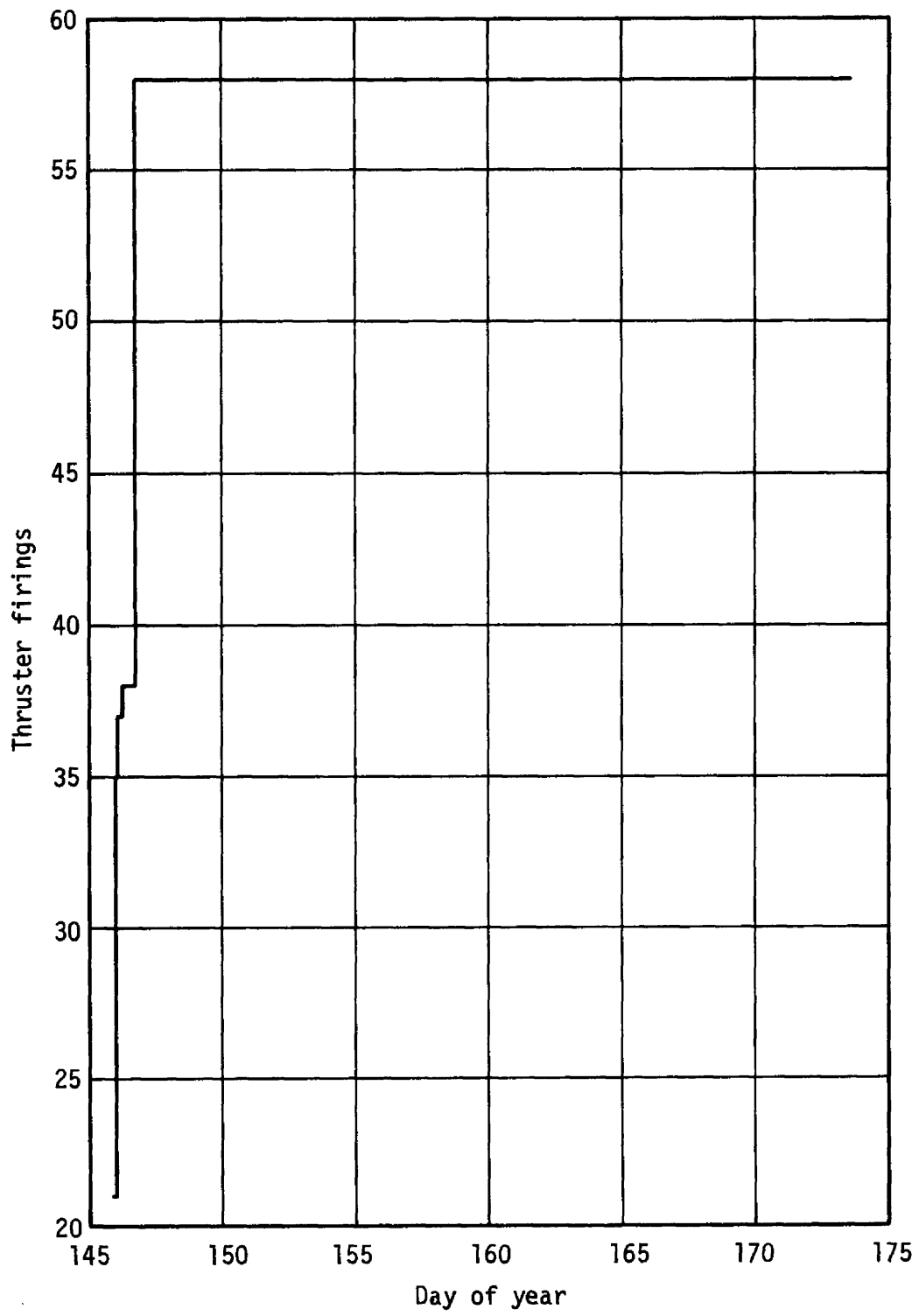


Figure 42.- Accumulated Full-On Firings, SL-2

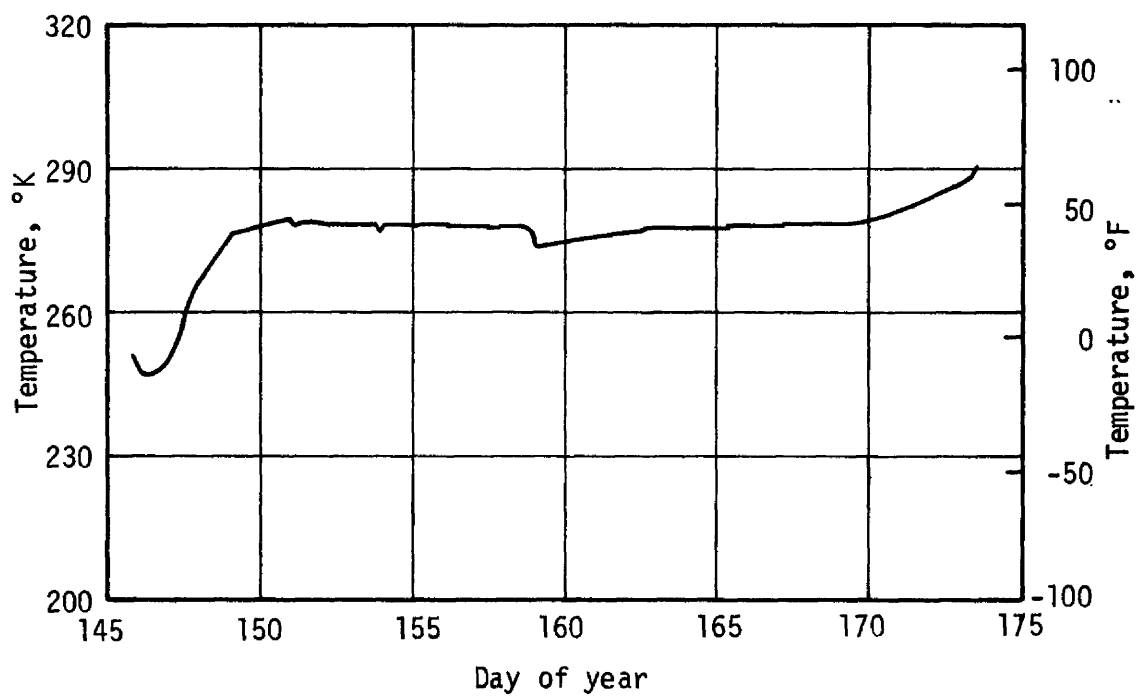


Figure 43.- Average GN₂ Bulk Gas Temperature, SL-2

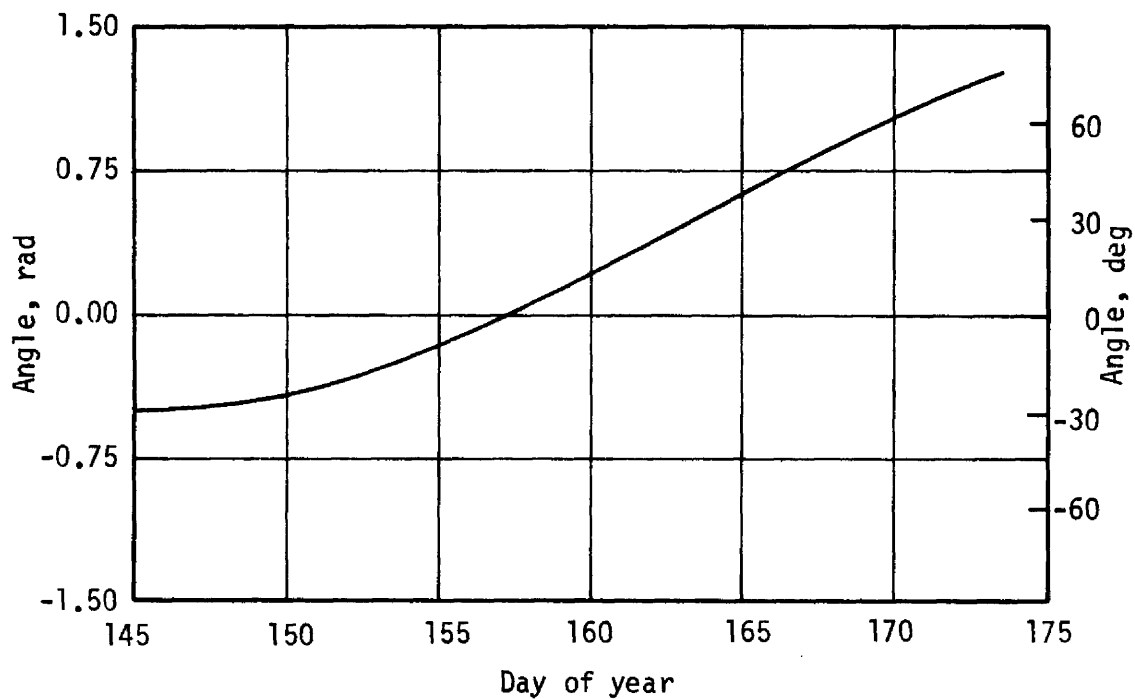


Figure 44.- Beta Angle, SL-2

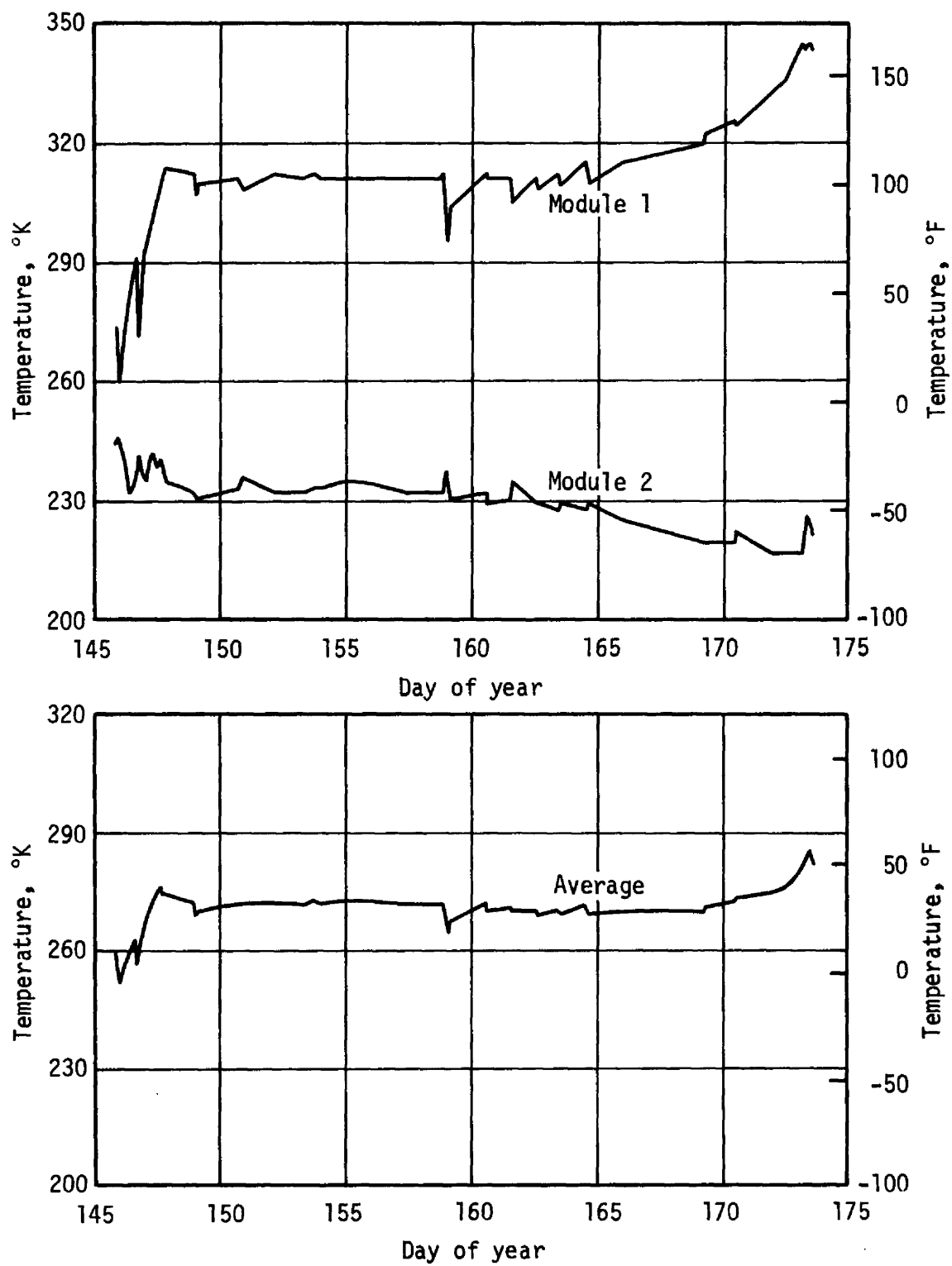


Figure 45.- Module Inlet Temperatures, SL-2

4.3 SECOND UNMANNED ORBITAL STORAGE PERIOD

The TACS was inactive throughout the orbital storage period from approximately DOY 173 to 209. Consequently, the total impulse remaining, the GN_2 mass, the MIB firings, and the full-on firings were constant. The variation in system pressure resulting from changes in bulk gas temperature with beta angle is shown in Figure 46.

The beta angle variation and the average system bulk gas temperature are shown in Figures 47 and 48. Average module inlet temperature and the individual module inlet temperatures are shown in Figure 49.

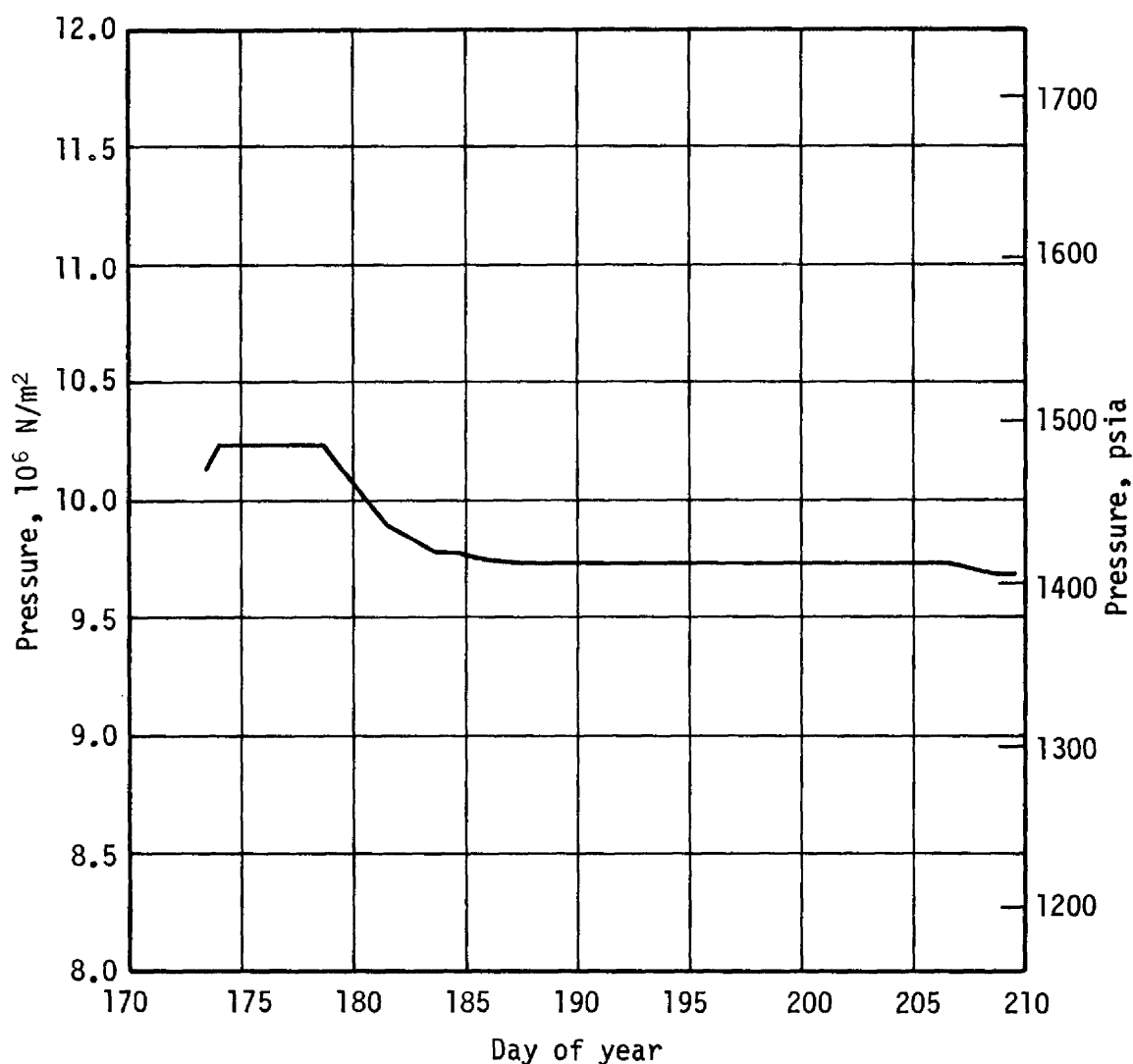


Figure 46.- System GN_2 Pressure, Second Unmanned Phase

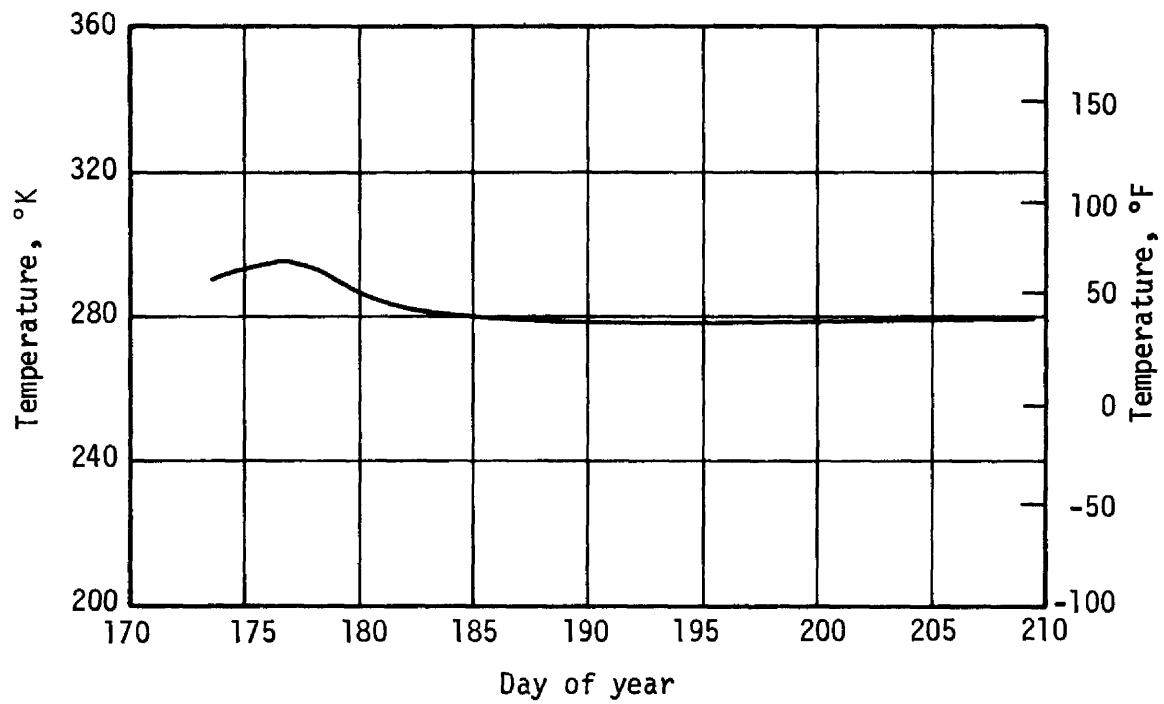


Figure 47.- Average GN_2 Bulk Gas Temperature, Second Unmanned Phase

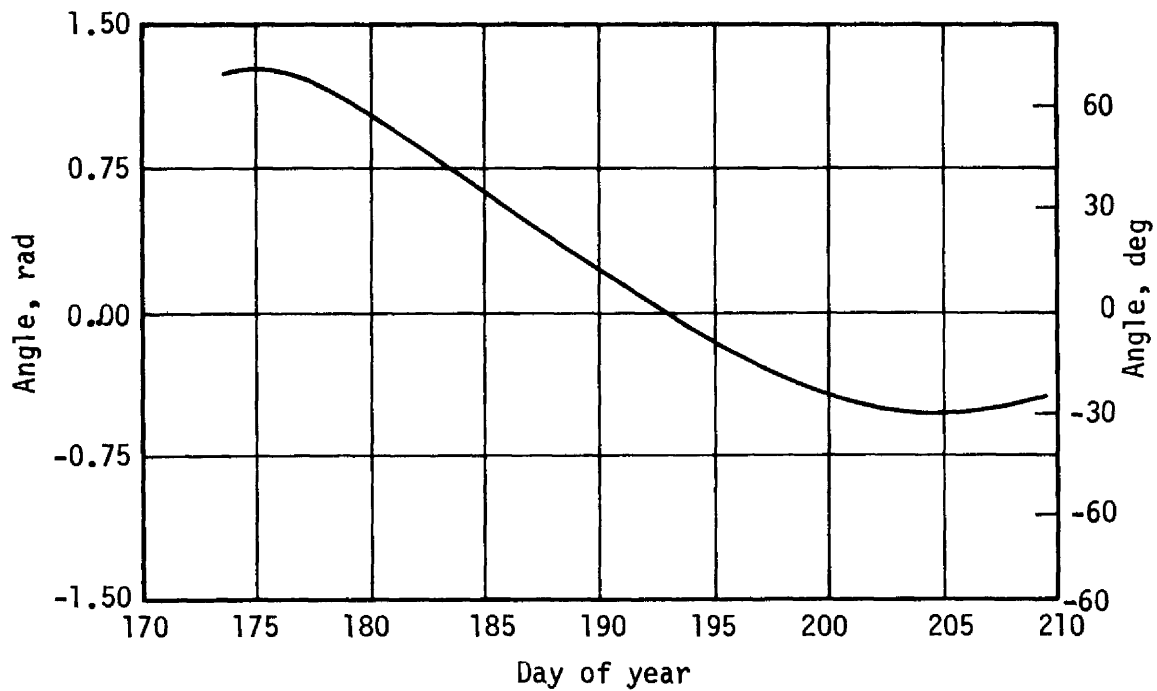


Figure 48.- Beta Angle, Second Unmanned Phase

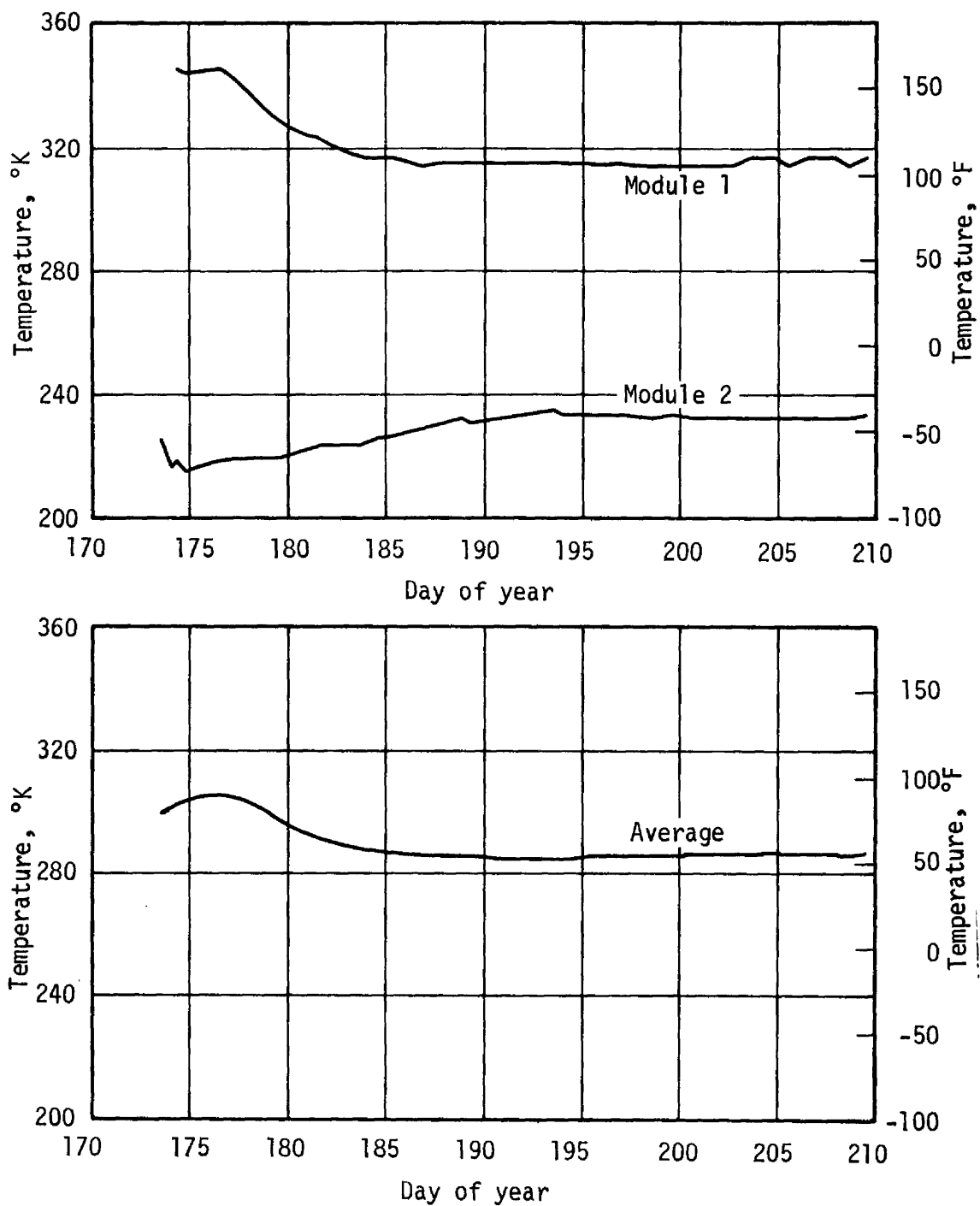


Figure 49.- Module Inlet Temperatures, Second Unmanned Phase

4.4 SECOND MANNED MISSION, SL-3 (59 DAYS)

The second three man crew was launched from KSC on July 28, 1973. Lift-off occurred at 209:11:10:50 GMT. The CSM achieved final docking to the Skylab Cluster at 209:19:39 GMT. Three EVA's were performed during this mission on DOY's 218, 236, and 265. Crew achievements included the deployment of a sun shield over the parasol sun shield installed by the first crew and the installation of the rate gyro "six pack". The CSM undocked from the Skylab Cluster at 268:19:49 GMT at the completion of this mission.

The TACS total impulse remaining for this second manned mission is presented in Figure 50. A detailed listing of TACS usage for this time period is presented in Appendix B.

The system pressure decay and GN_2 mass are shown in Figures 51 and 52. The thrust level variation for this phase of the mission is shown in Figure 53 and is compared to the thrust level stored in the ATMDC. The variation in MIB (Figure 54) also indicates the times at which the ATMDC command pulse width was updated. The MIB was maintained at approximately 22 N-sec (5 lbf-sec). The MIB and full-on firing histories are shown in Figures 55 and 56.

The average bulk gas temperature is presented in Figure 57. The beta angle variation is shown in Figure 58. The module inlet gas temperatures and the average module inlet temperature are presented in Figure 59.

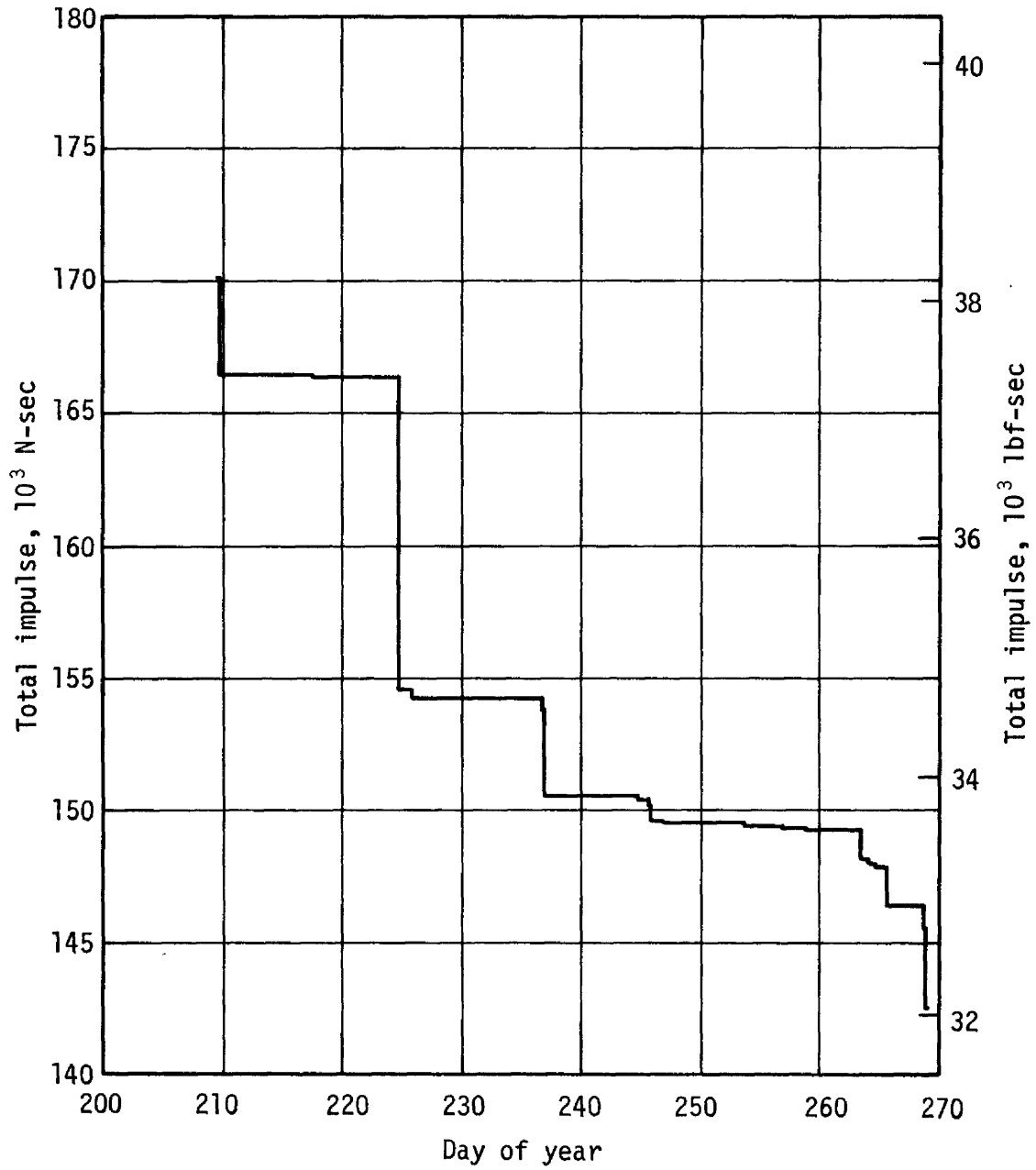


Figure 50.- Usable Total Impulse Remaining, SL-3

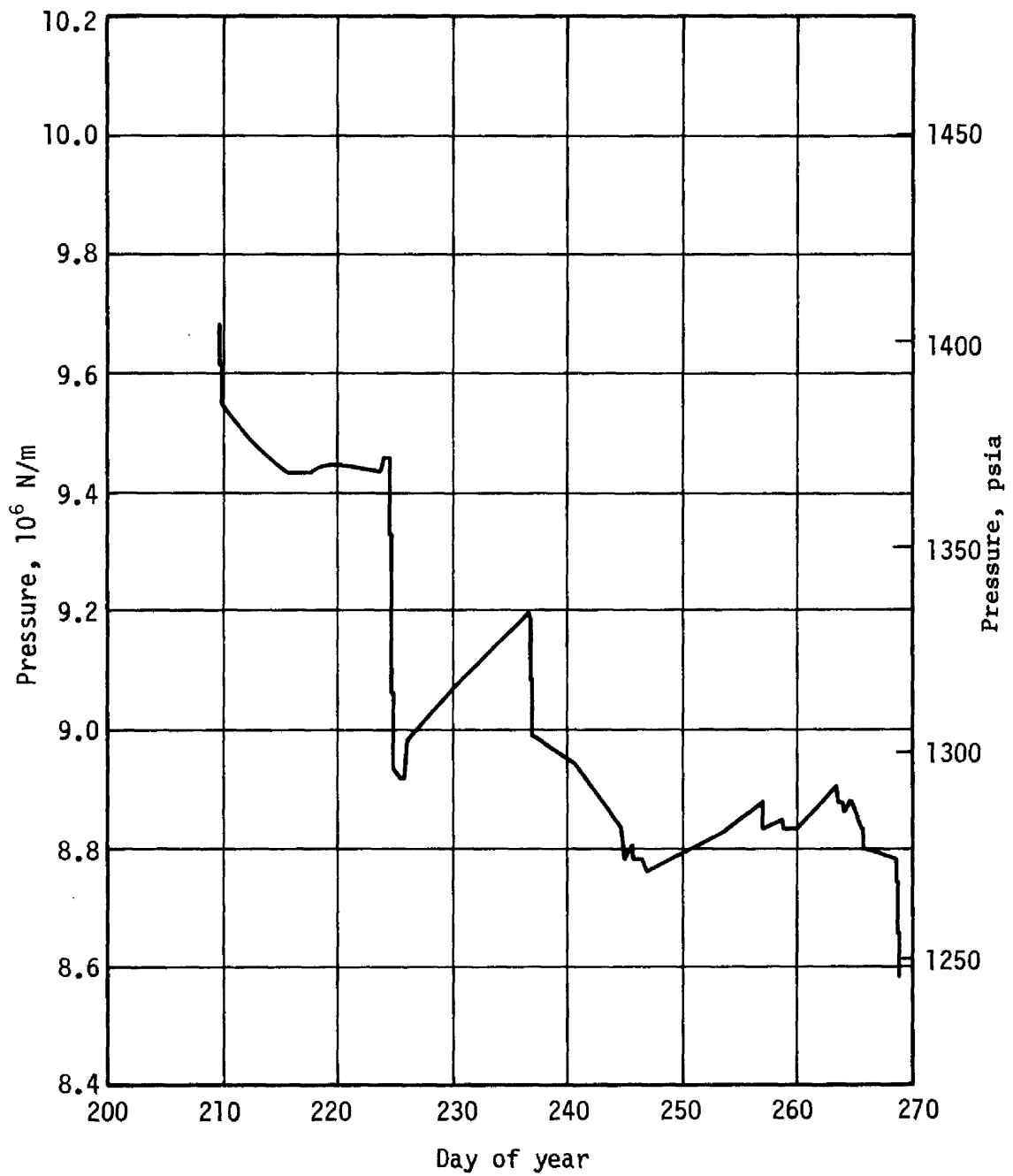
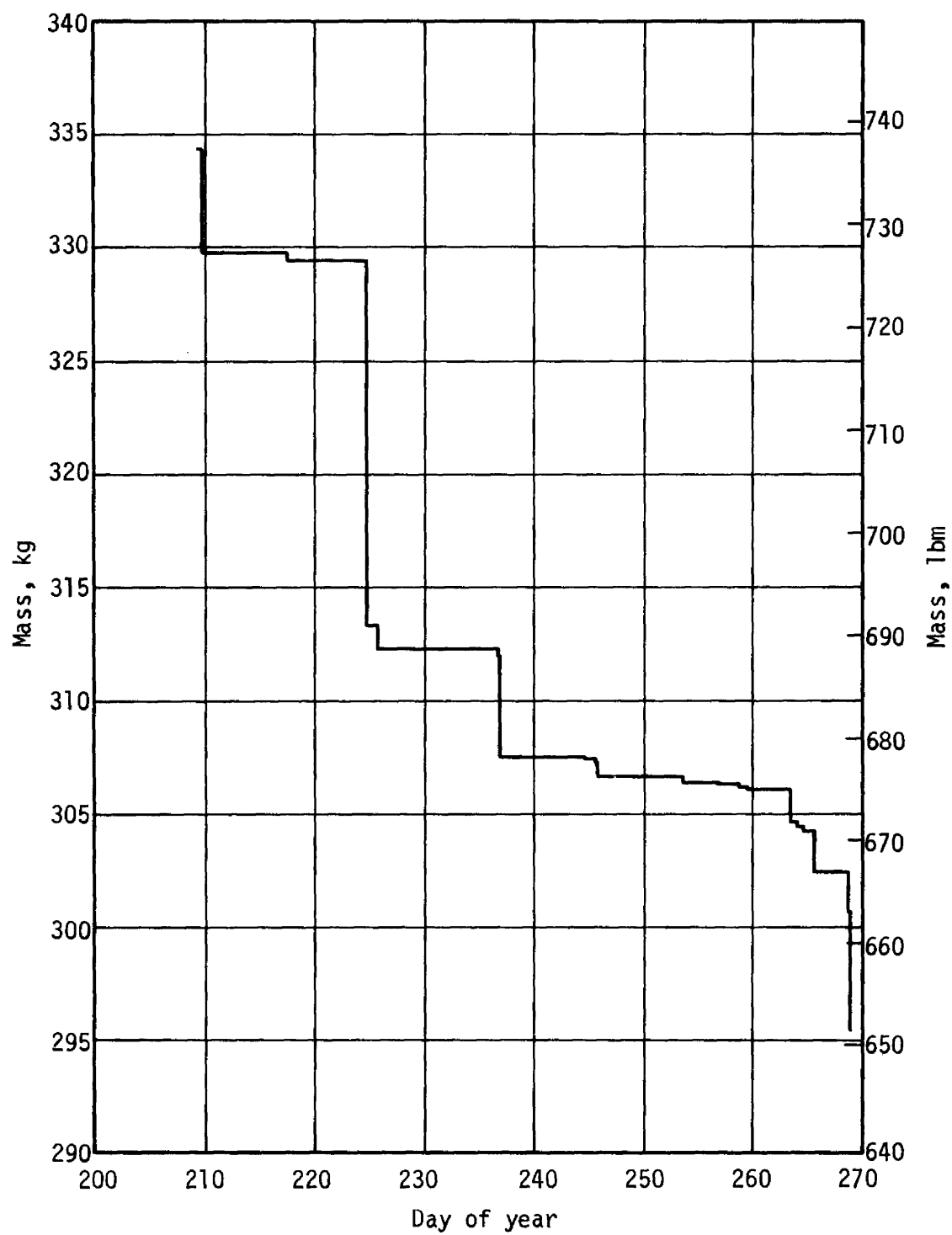


Figure 51.- GN₂ Pressure, SL-3

Figure 52.- GN₂ Mass, SL-3

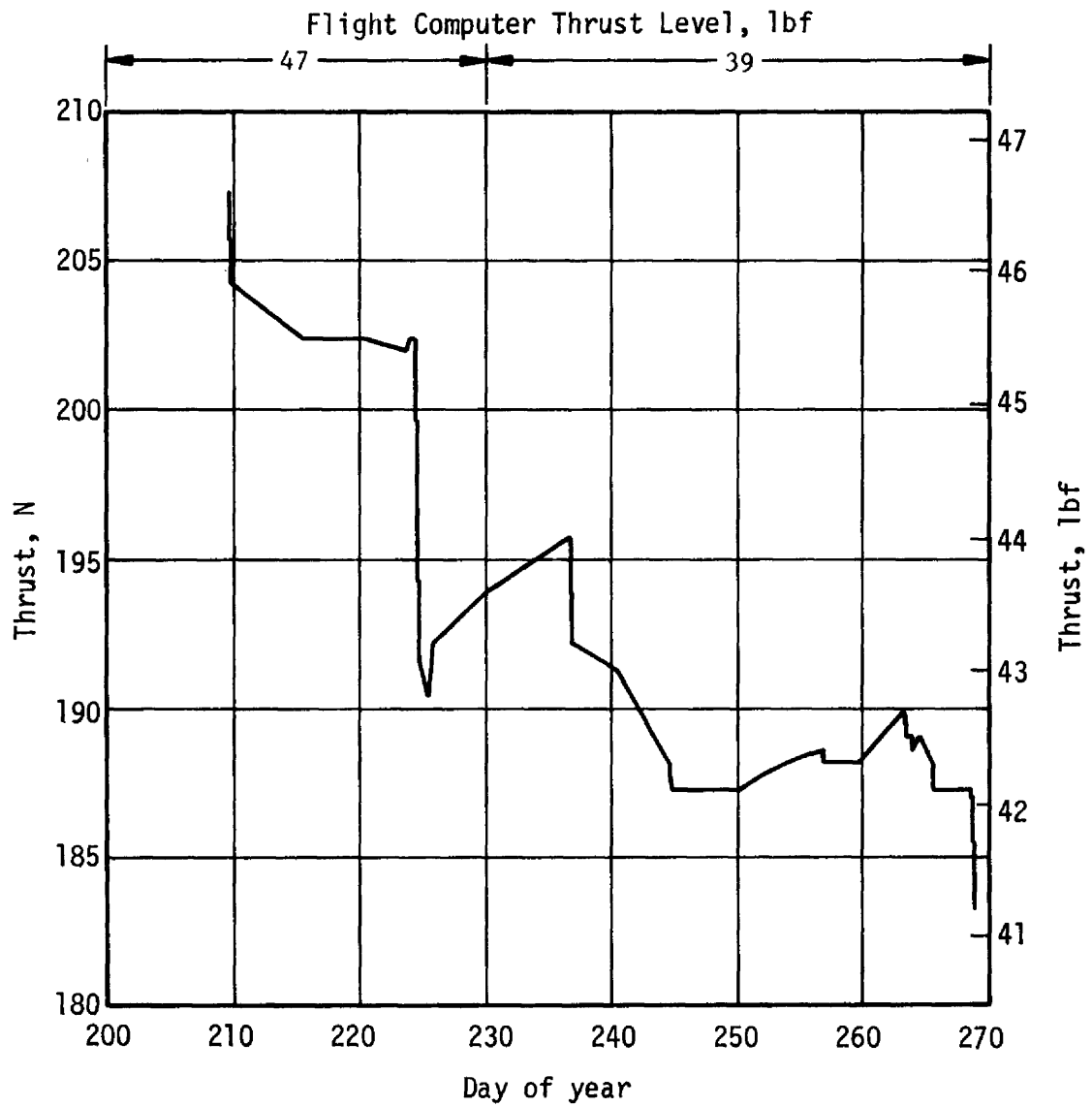


Figure 53.- Thrust, SL-3

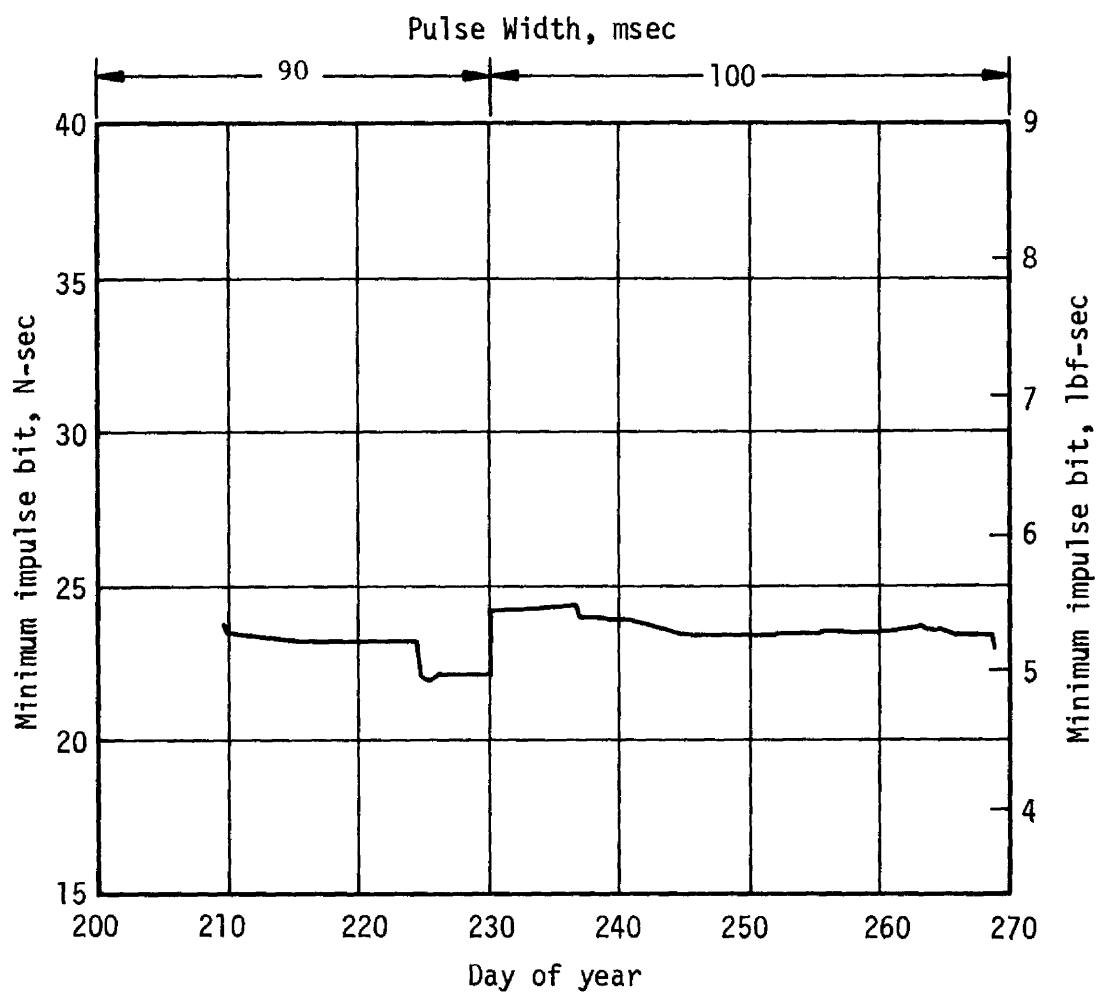


Figure 54.- Nominal Minimum Impulse Bit, SL-3

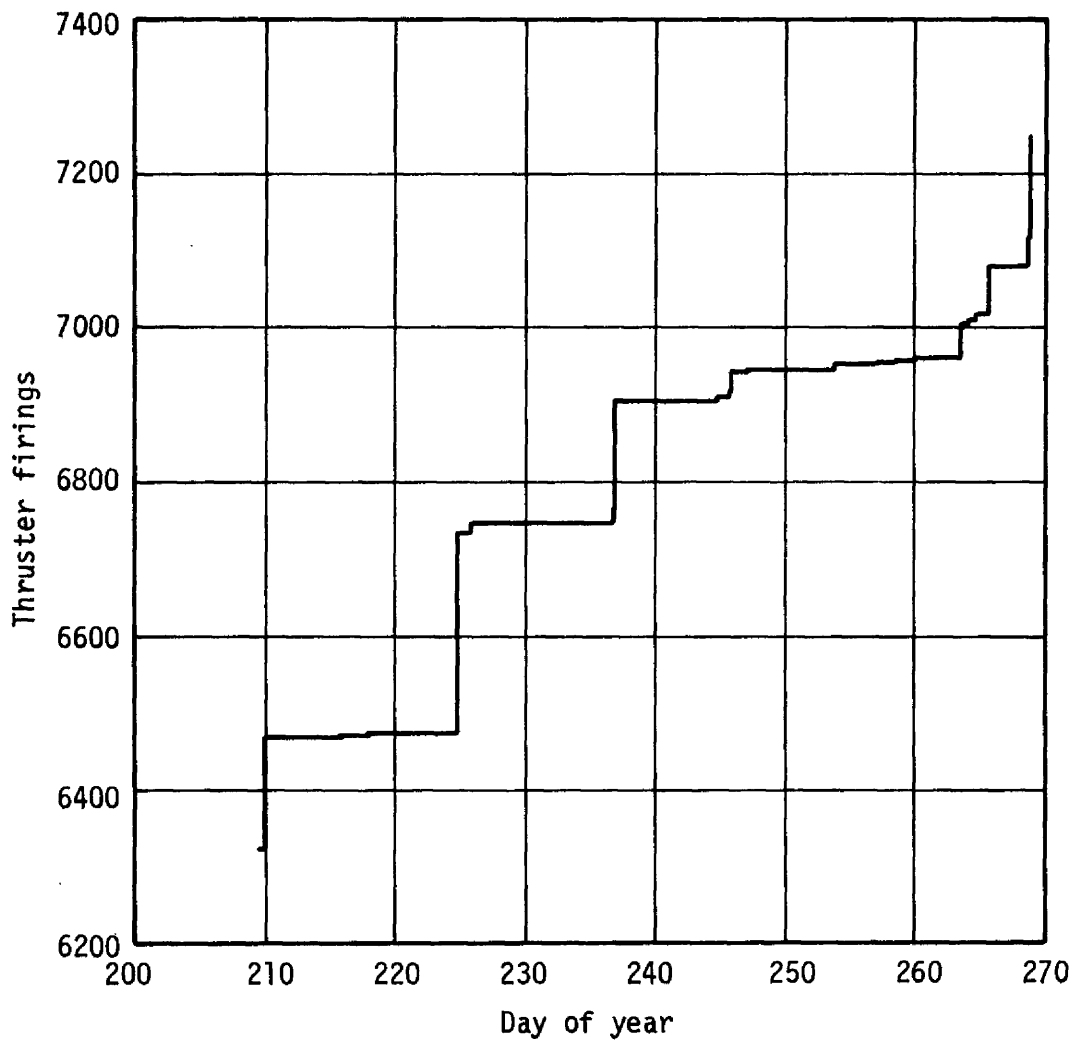


Figure 55.- Accumulated Minimum Impulse Bit Firings, SL-3

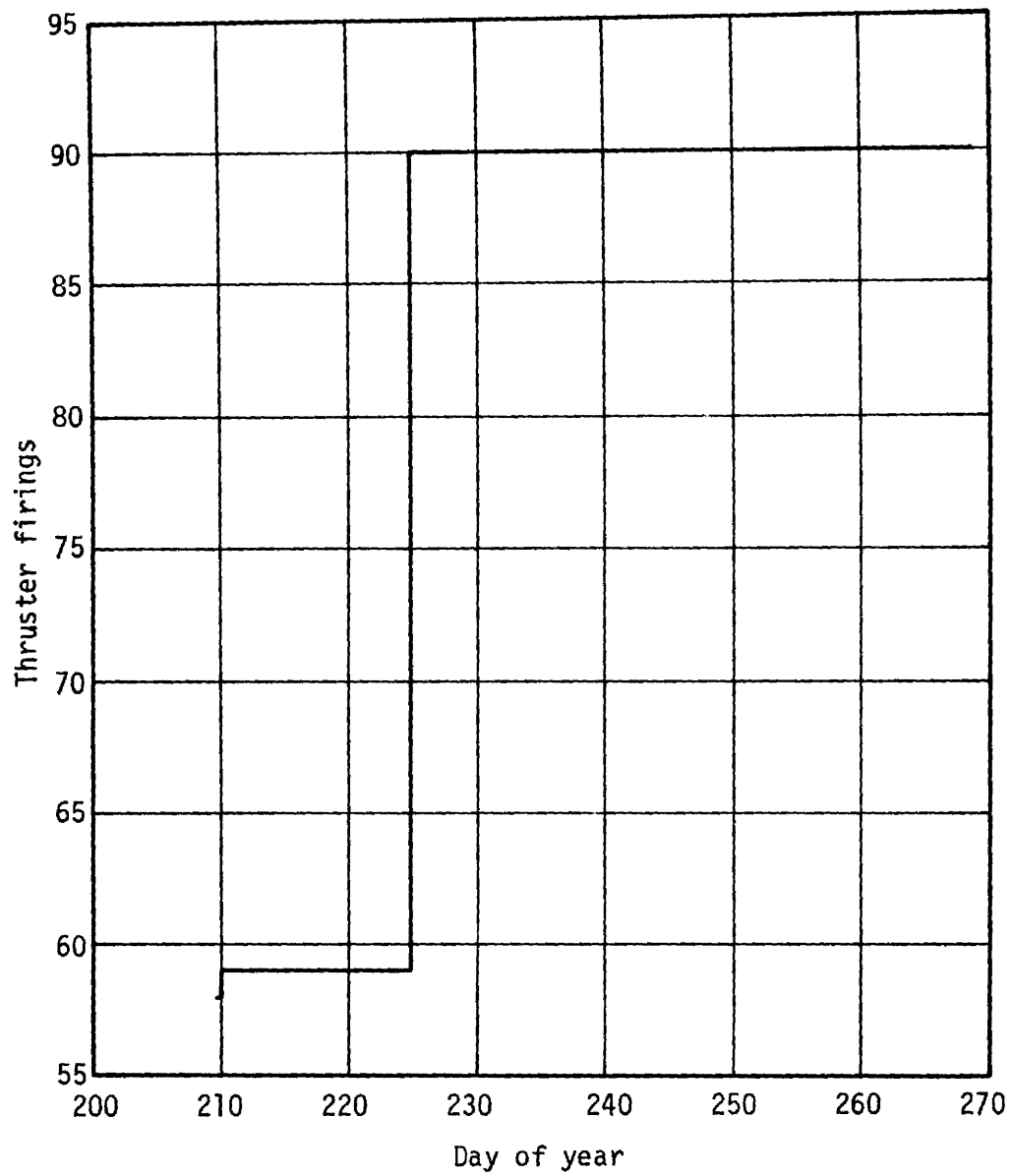


Figure 56.- Accumulated Full-On Firings, SL-3

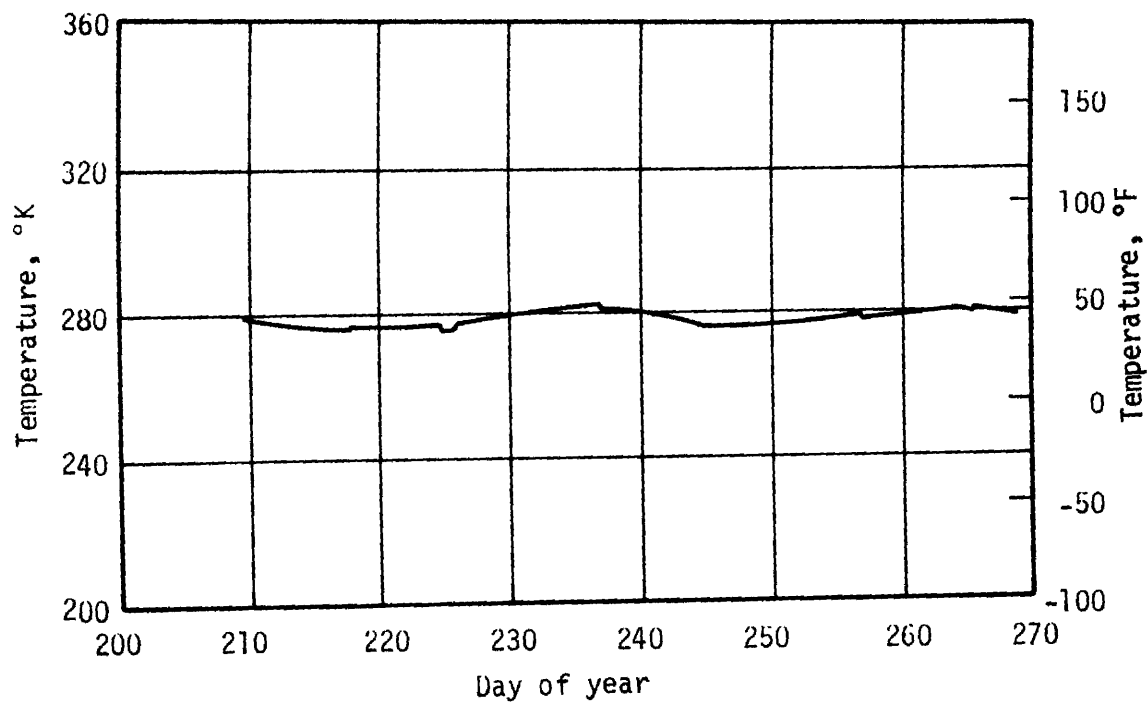


Figure 57.- Average GN_2 Bulk Gas Temperature, SL-3

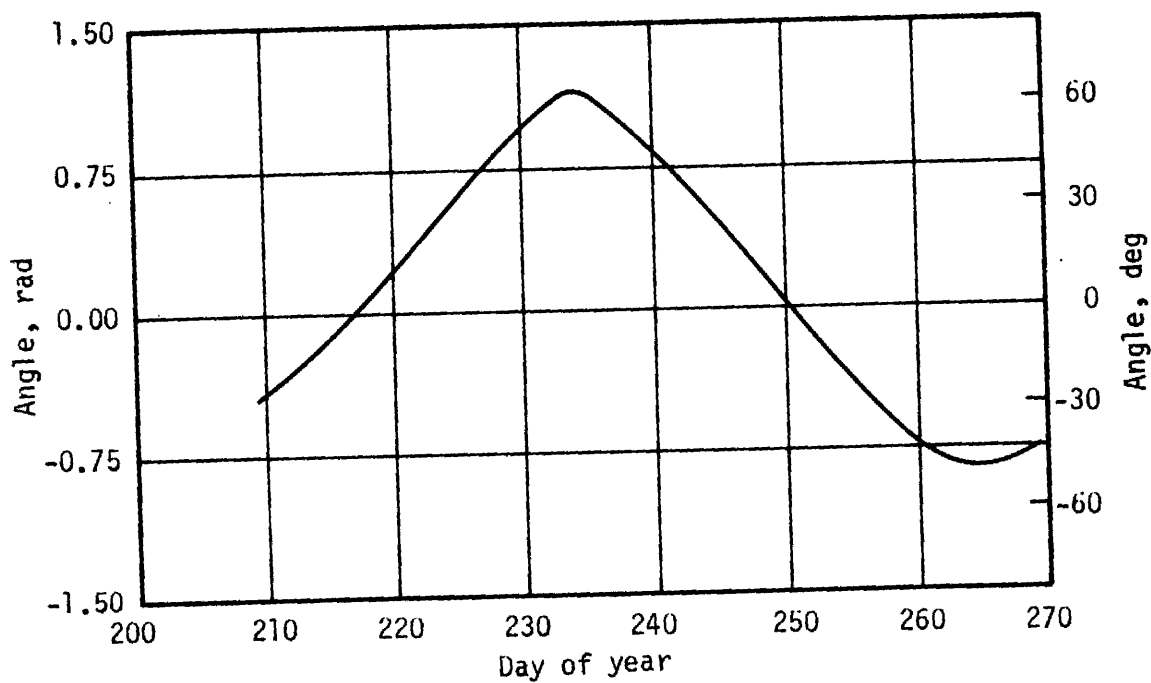


Figure 58.- Beta Angle, SL-3

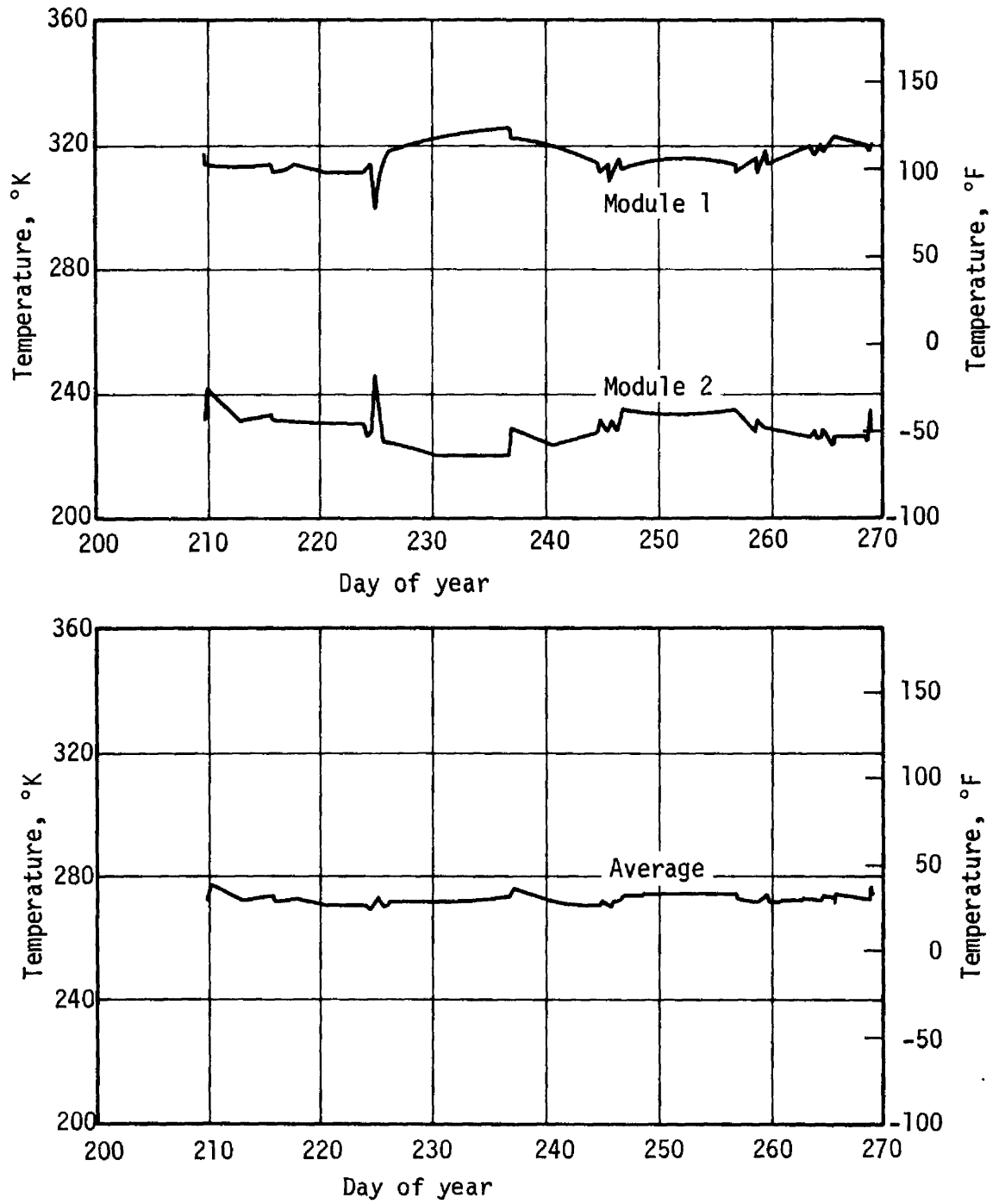


Figure 59.- Module Inlet Temperatures, SL-3

4.5 THIRD UNMANNED ORBITAL STORAGE PERIOD

The TACS was inactive throughout the orbital storage period from DOY 268 to 320. The total impulse remaining, the GN_2 mass, the MIB firings, and the full-on firings were constant. The variation in system pressure resulting from changes in bulk gas temperature with beta angle is shown in Figure 60.

The beta angle variation and the average system bulk gas temperature are shown in Figures 61 and 62. Average module inlet temperature and the individual module inlet temperatures are shown in Figure 63.

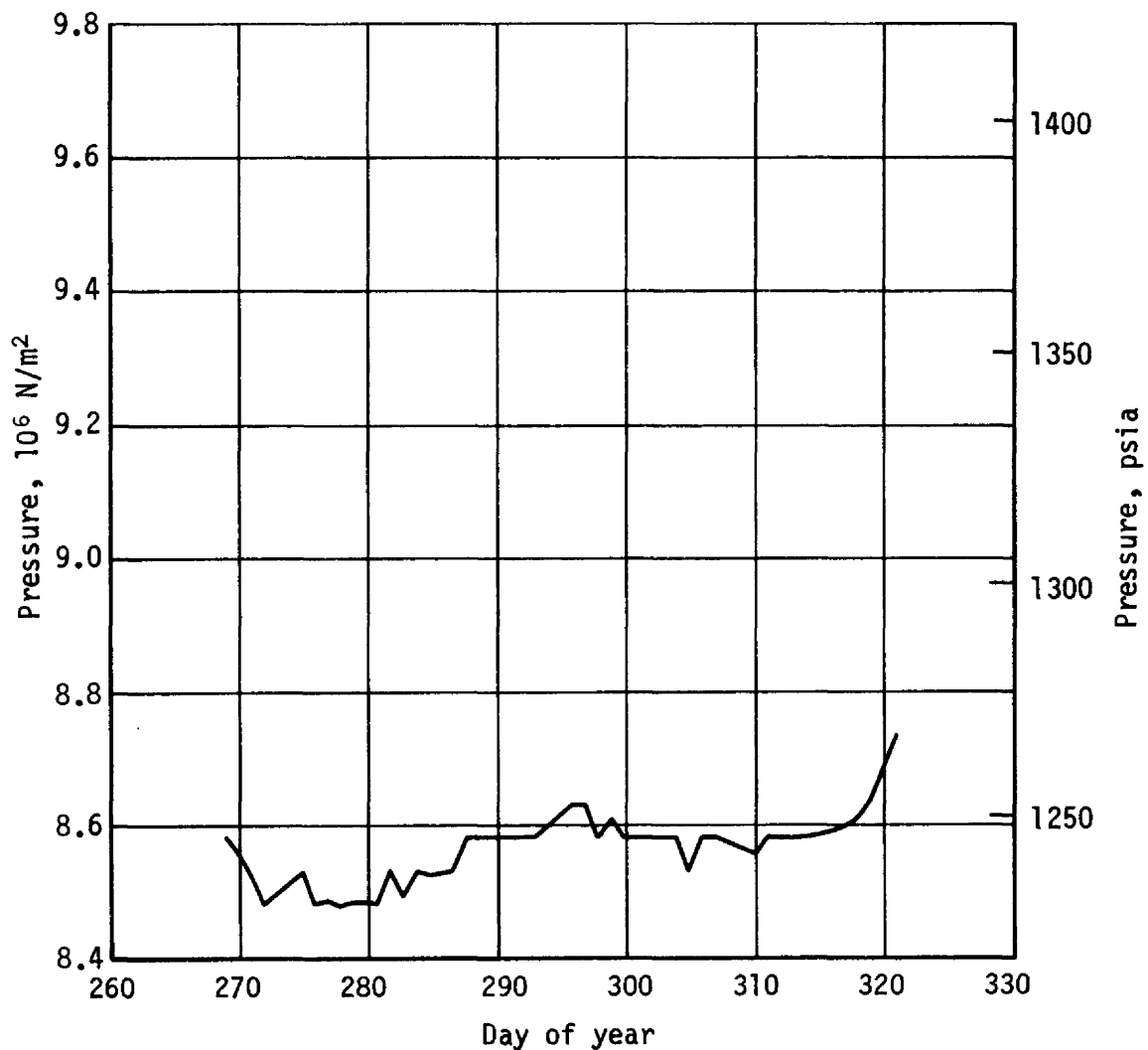


Figure 60.- GN_2 Pressure, Third Unmanned Phase

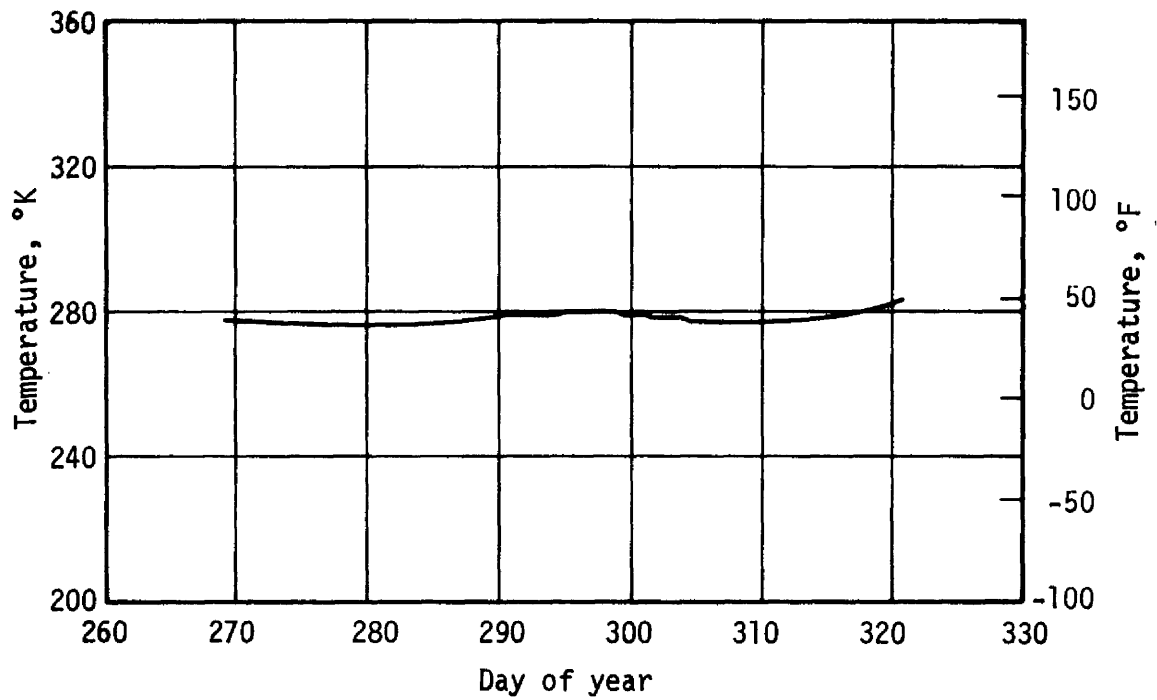


Figure 61.- Average GN₂ Bulk Gas Temperature, Third Unmanned Phase

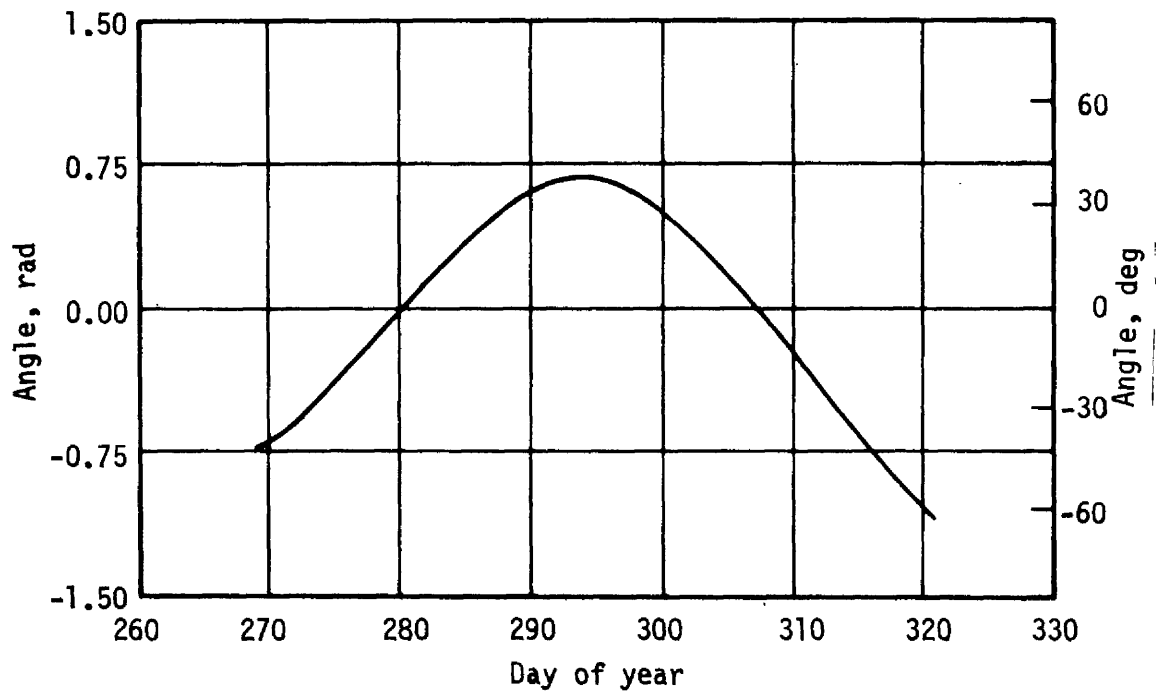


Figure 62.- Beta Angle, Third Unmanned Phase

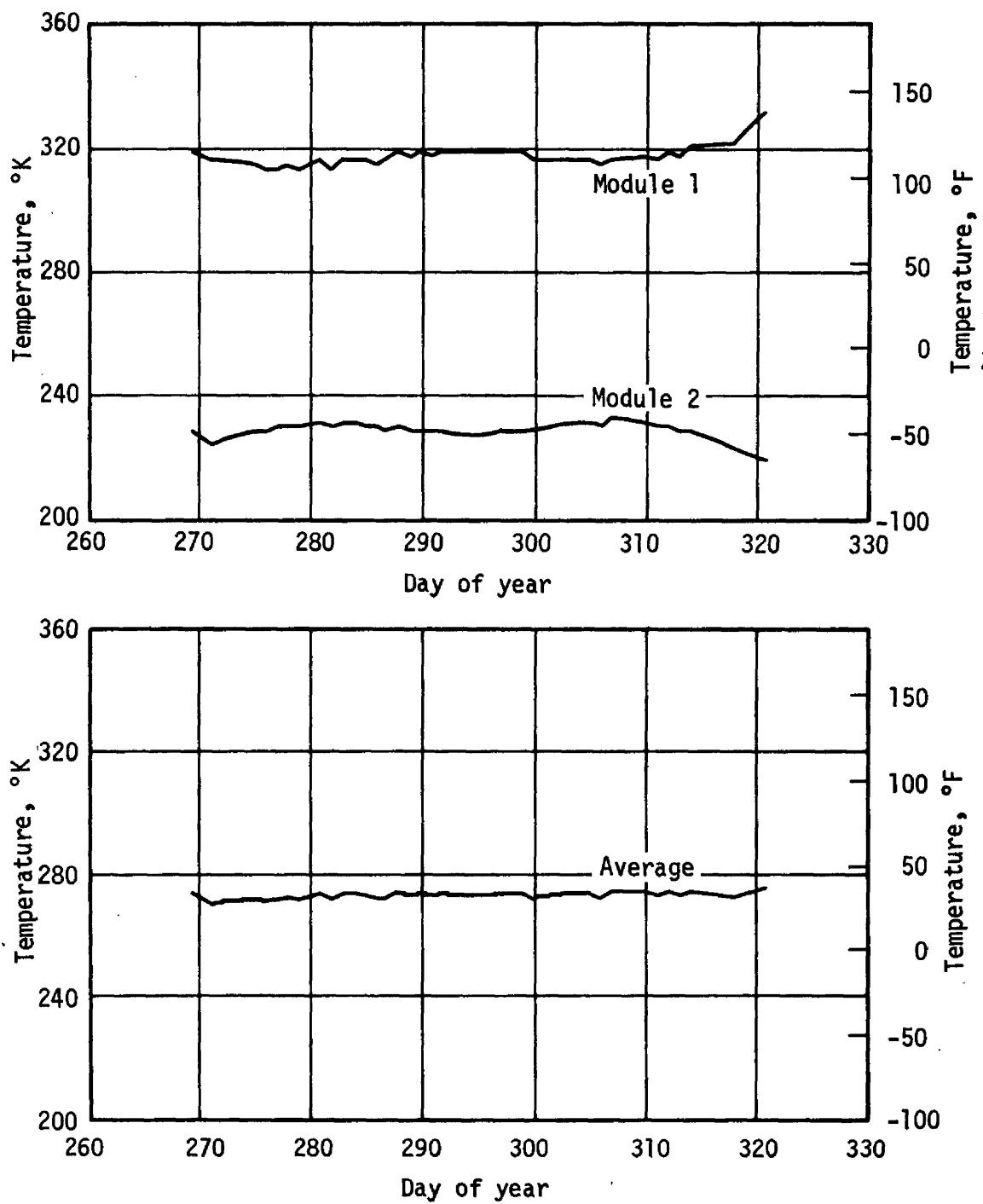


Figure 63.- Module Inlet Temperatures, Third Unmanned Phase

4.6 THIRD MANNED MISSION, SL-4 (84 DAYS)

The third and final three man crew was launched from KSC on November 16, 1973. Lift-off occurred at 320:14:03 GMT with docking of the CSM to the Skylab Cluster occurring at 320:21:41 GMT. Four EVA's were performed during the mission on DOY's 326, 359, 363, and 034. Comet Kohoutek science was added to the mission objectives because the comet perihelion and optimum viewing opportunities coincided with this mission phase. Although the Comet Kohoutek science did increase the projected TACS usage, of more significance relative to system usage was the loss of CMG No. 1 on DOY 326. The CSM undocked from the Skylab Cluster at 039:10:34 GMT in Year 1974. This completed the Skylab planned flight activities.

The total impulse remaining for this third manned mission is presented in Figure 64. A detailed listing of TACS usage for this time period is presented in Appendix B.

The system pressure decay and GN_2 mass are shown in Figures 65 and 66. The thrust level variation for this phase of the mission is shown in Figure 67 and is compared to the thrust level stored in the ATMDC. The variation in MIB (Figure 68) also shows the times at which the ATMDC command pulse width was updated. The MIB was maintained at approximately 22 N-sec (5 lbf-sec). The MIB and full-on firing histories are shown in Figures 69 and 70.

The average bulk gas temperature and the beta angle variation are shown in Figures 71 and 72. The module inlet gas temperatures and the average module inlet temperature are presented in Figure 73.

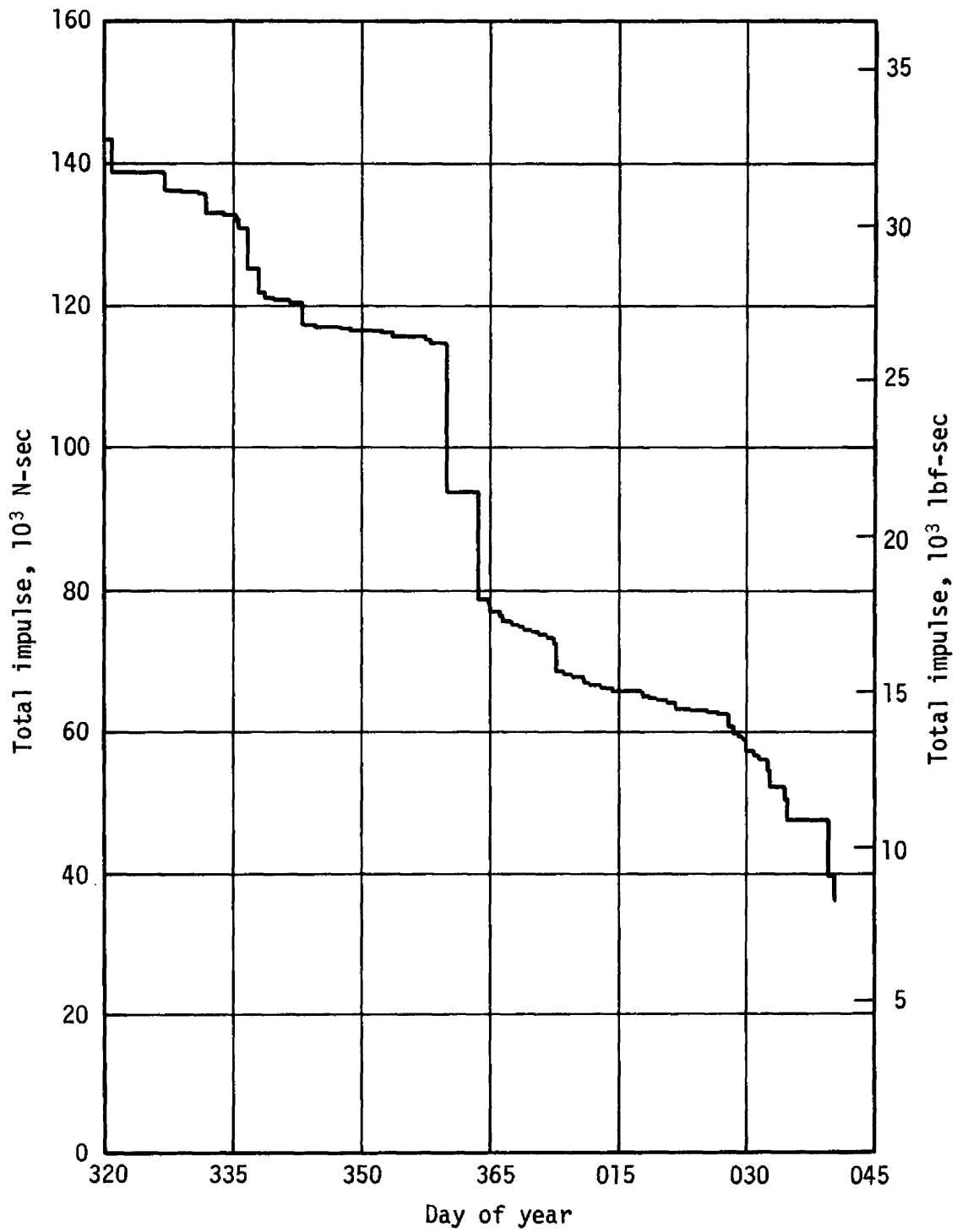
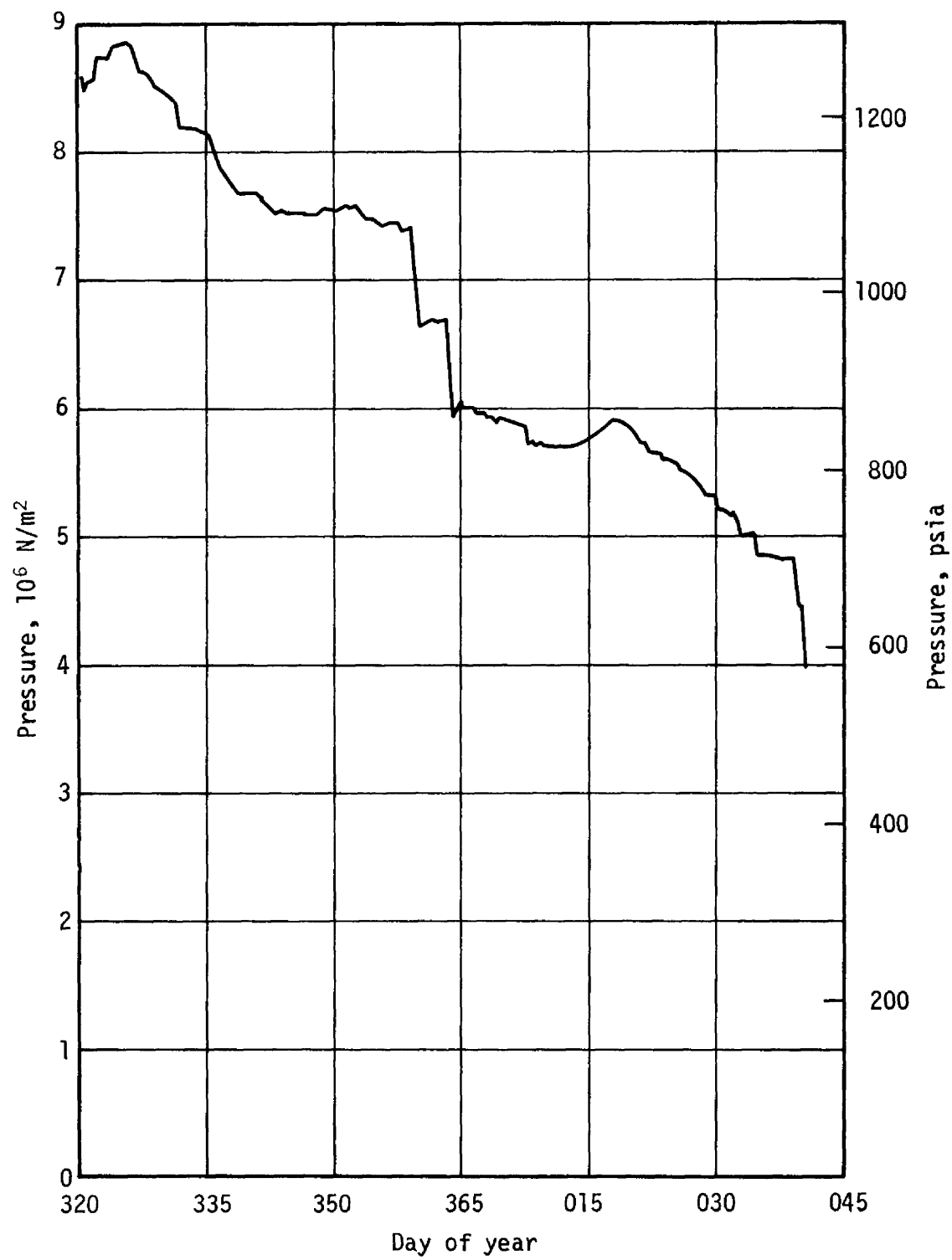
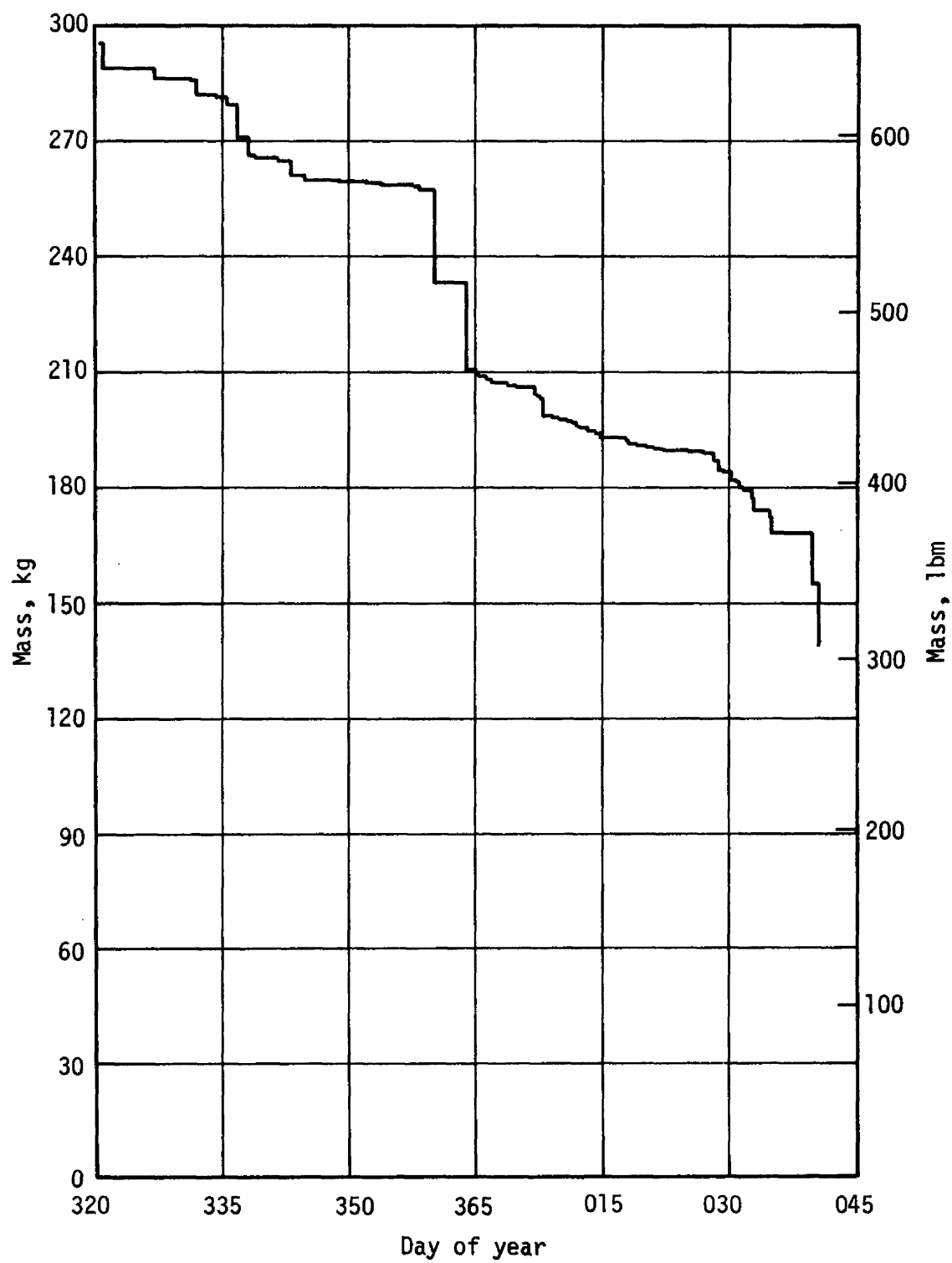


Figure 64.- Usable Total Impulse Remaining, SL-4

Figure 65.- GN₂ Pressure, SL-4

Figure 66.- GN₂ Mass, SL-4

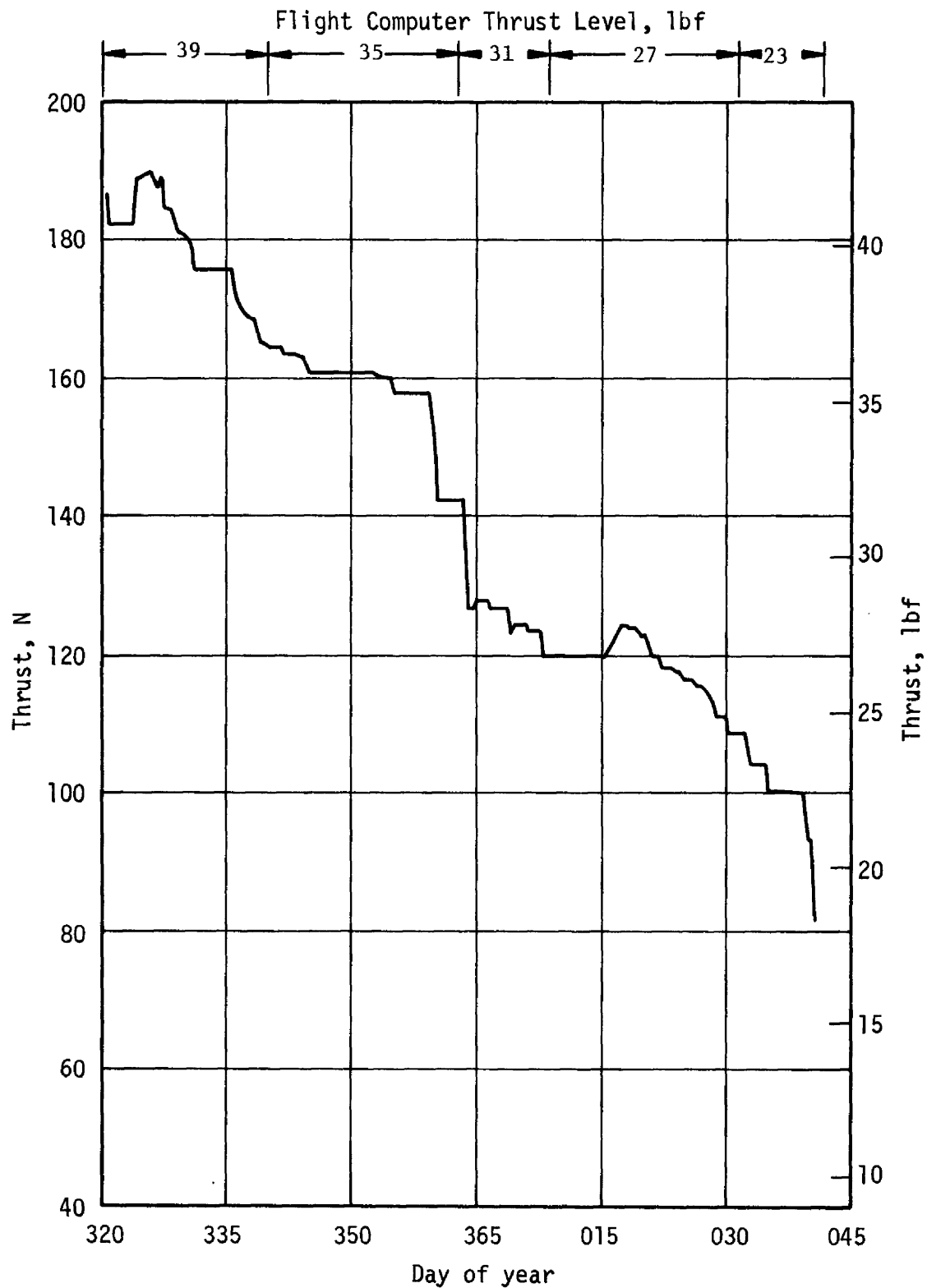


Figure 67.- Thrust, SL-4

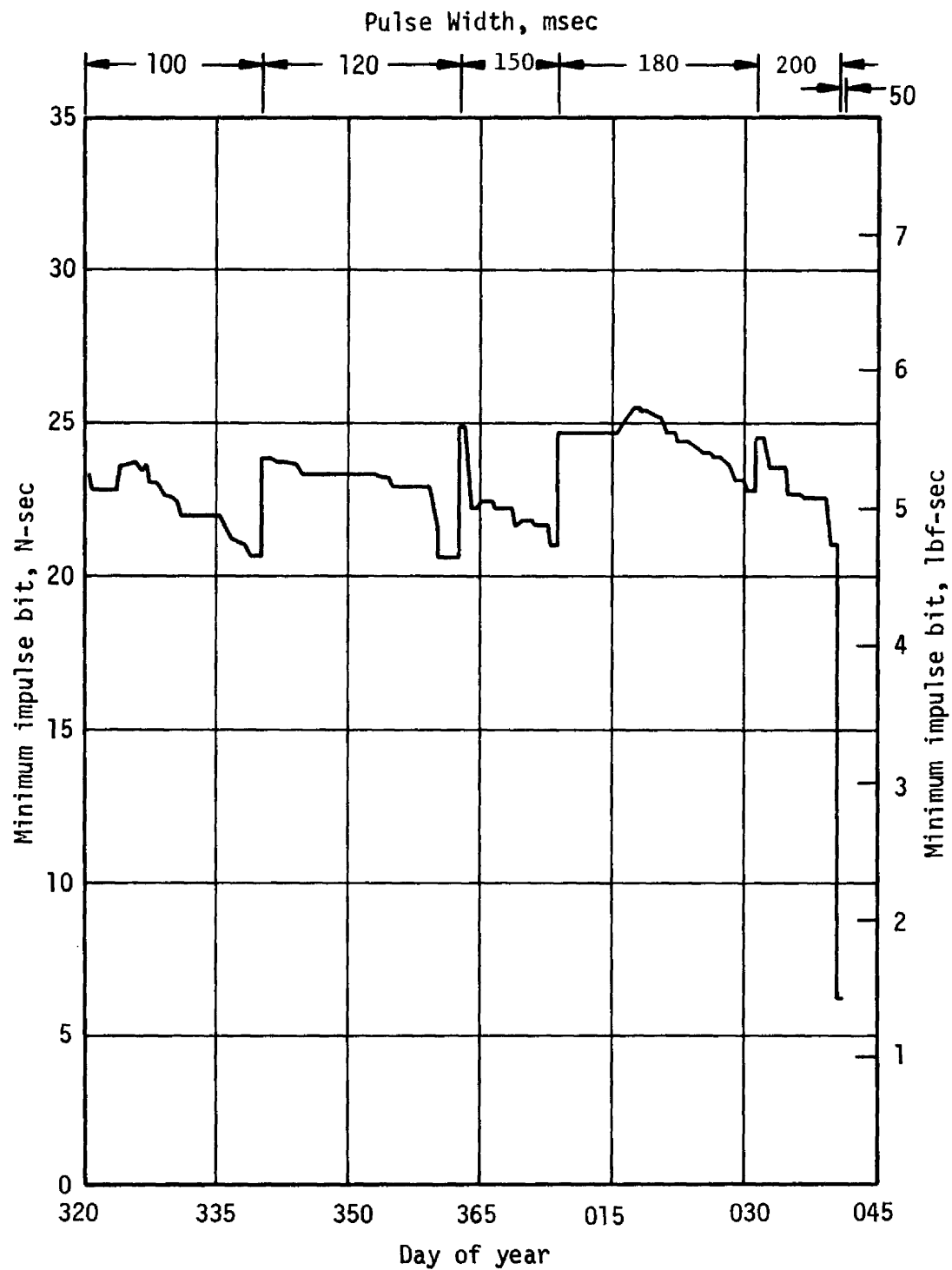


Figure 68.- Nominal Minimum Impulse Bit, SL-4

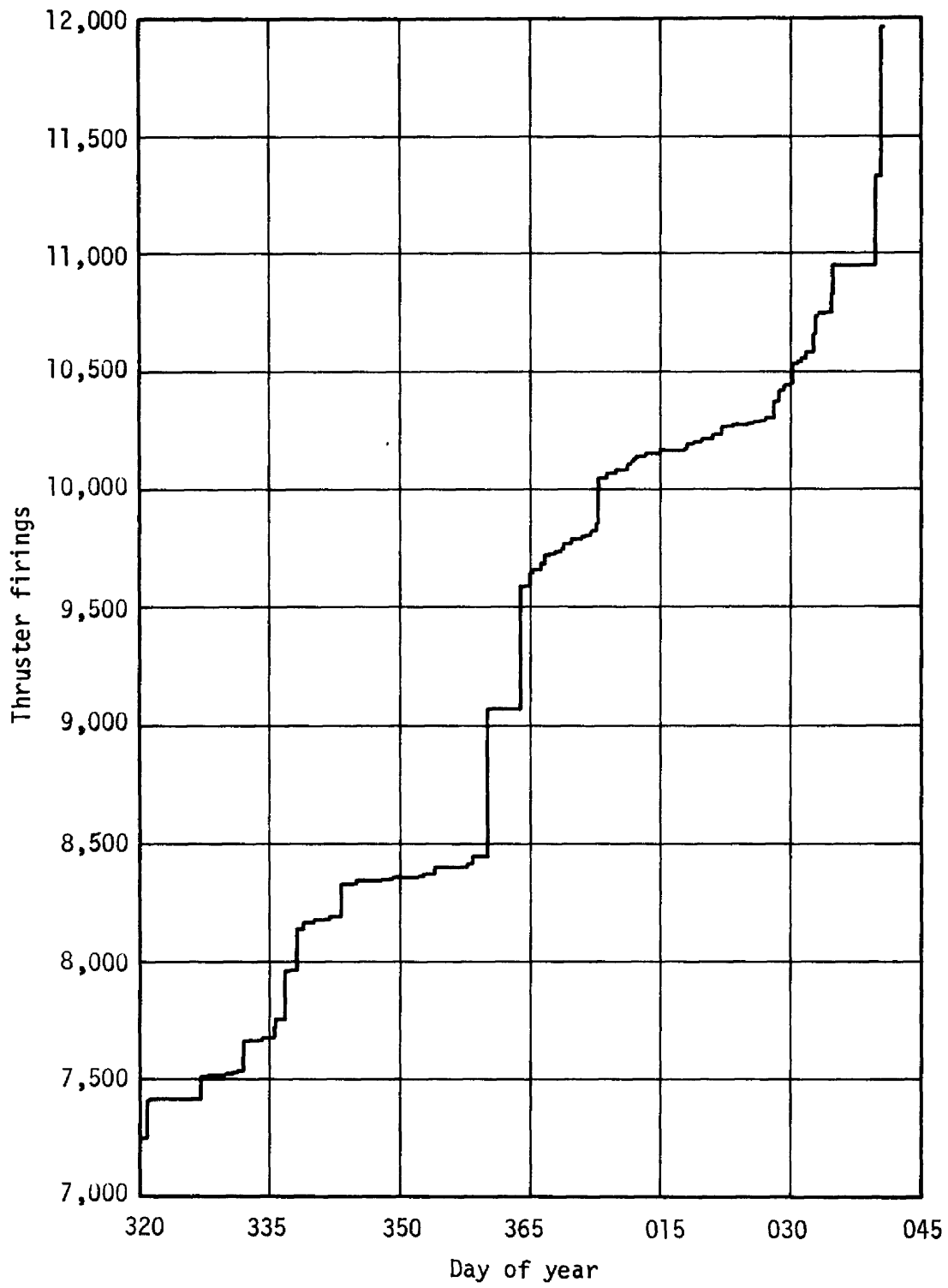


Figure 69.- Accumulated Minimum Impulse Bit Firings, SL-4

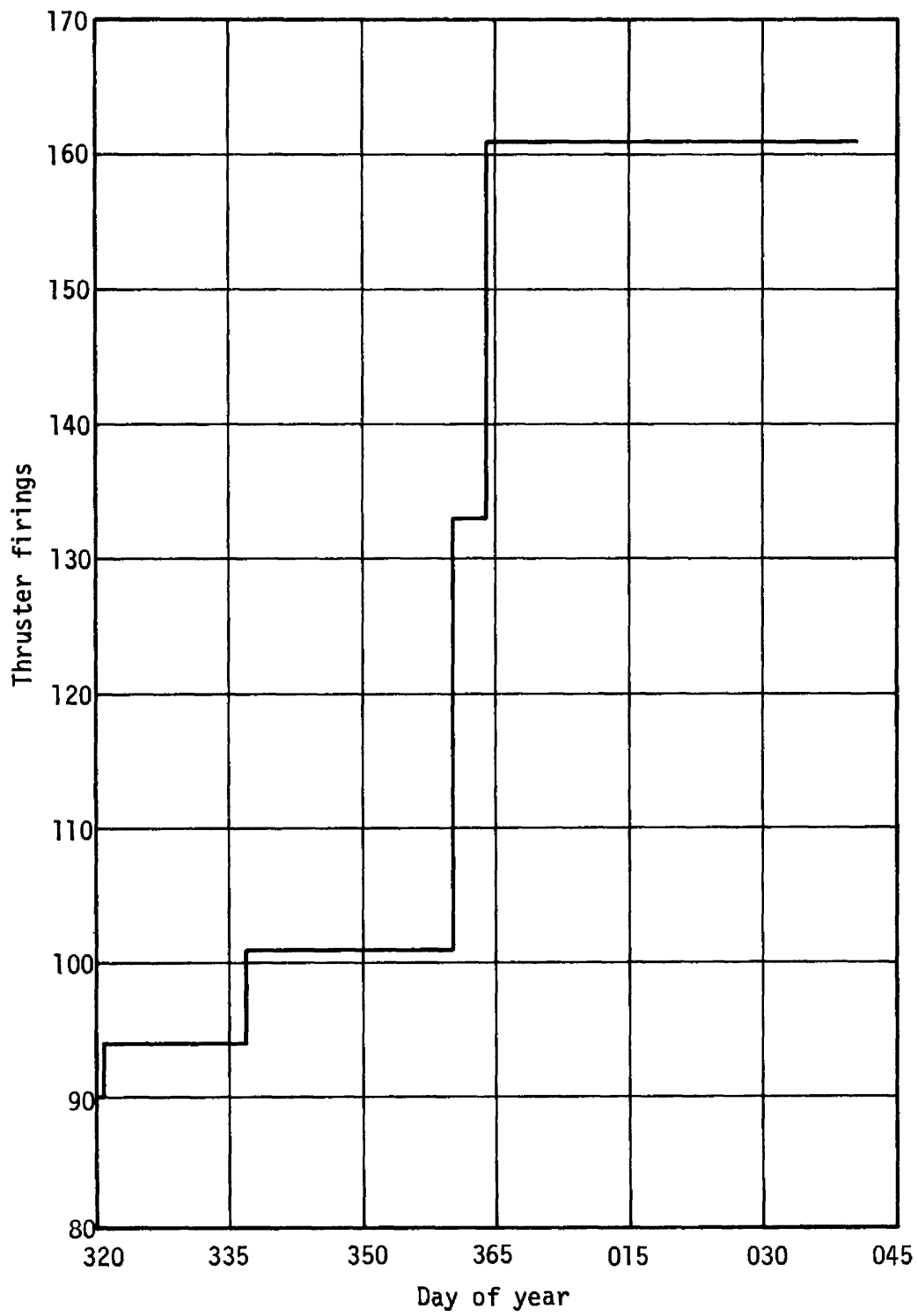


Figure 70.- Accumulated Full-On Firings, SL-4

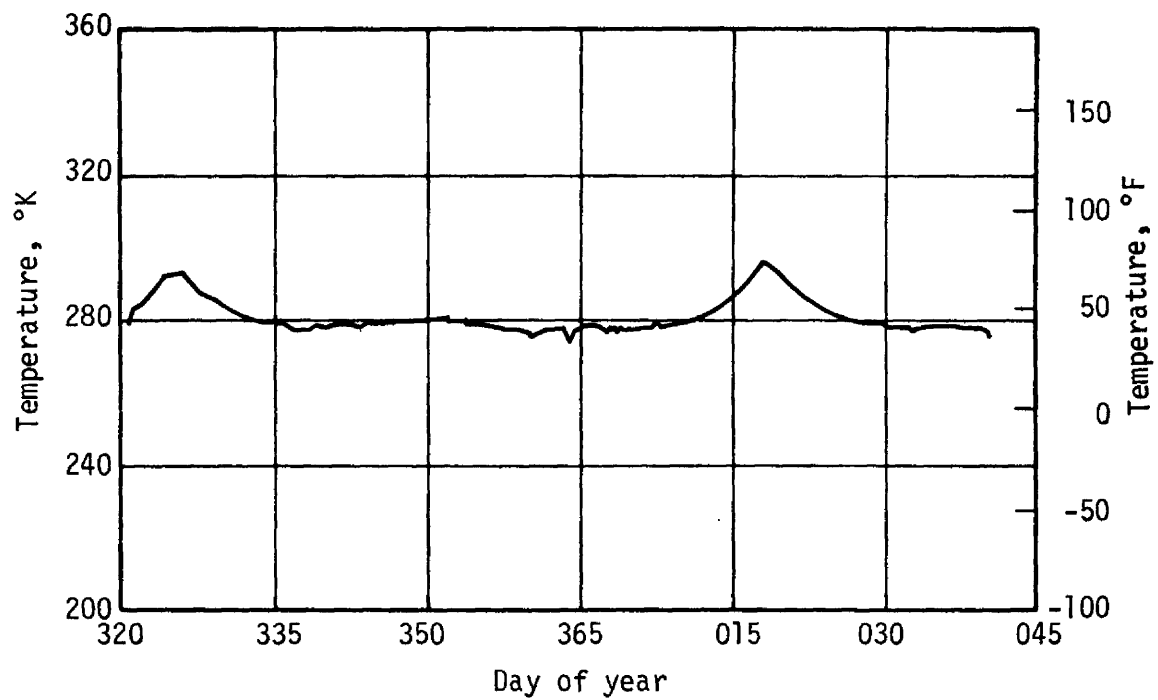


Figure 71.- Average GN₂ Bulk Gas Temperature, SL-4

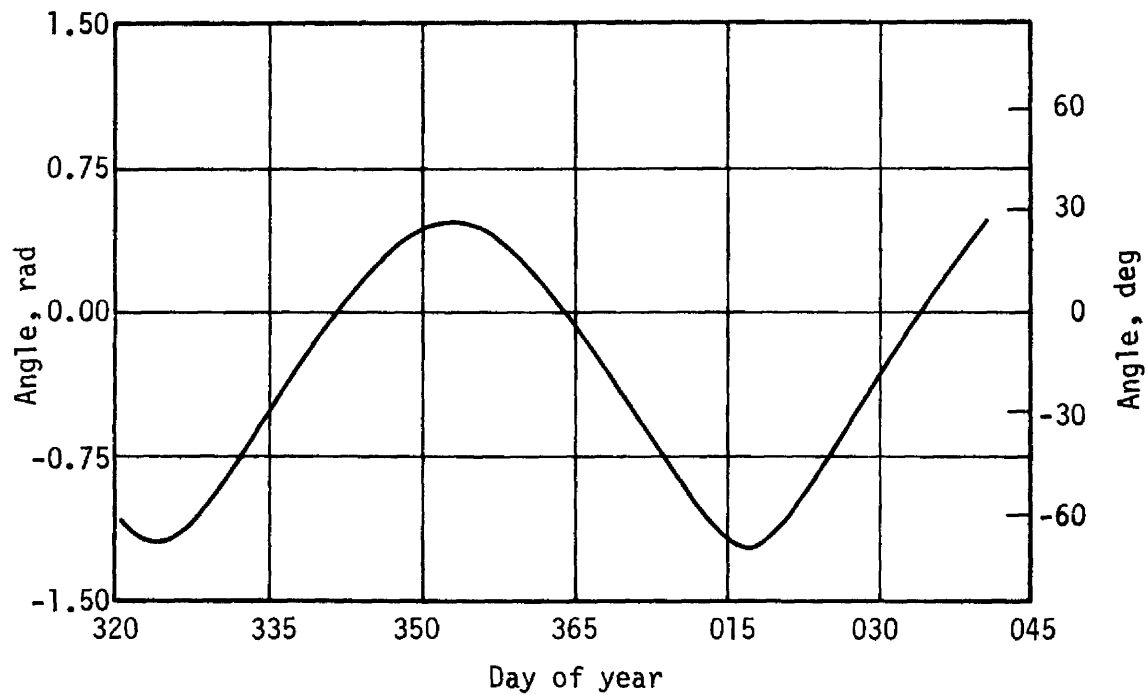


Figure 72.- Beta Angle, SL-4

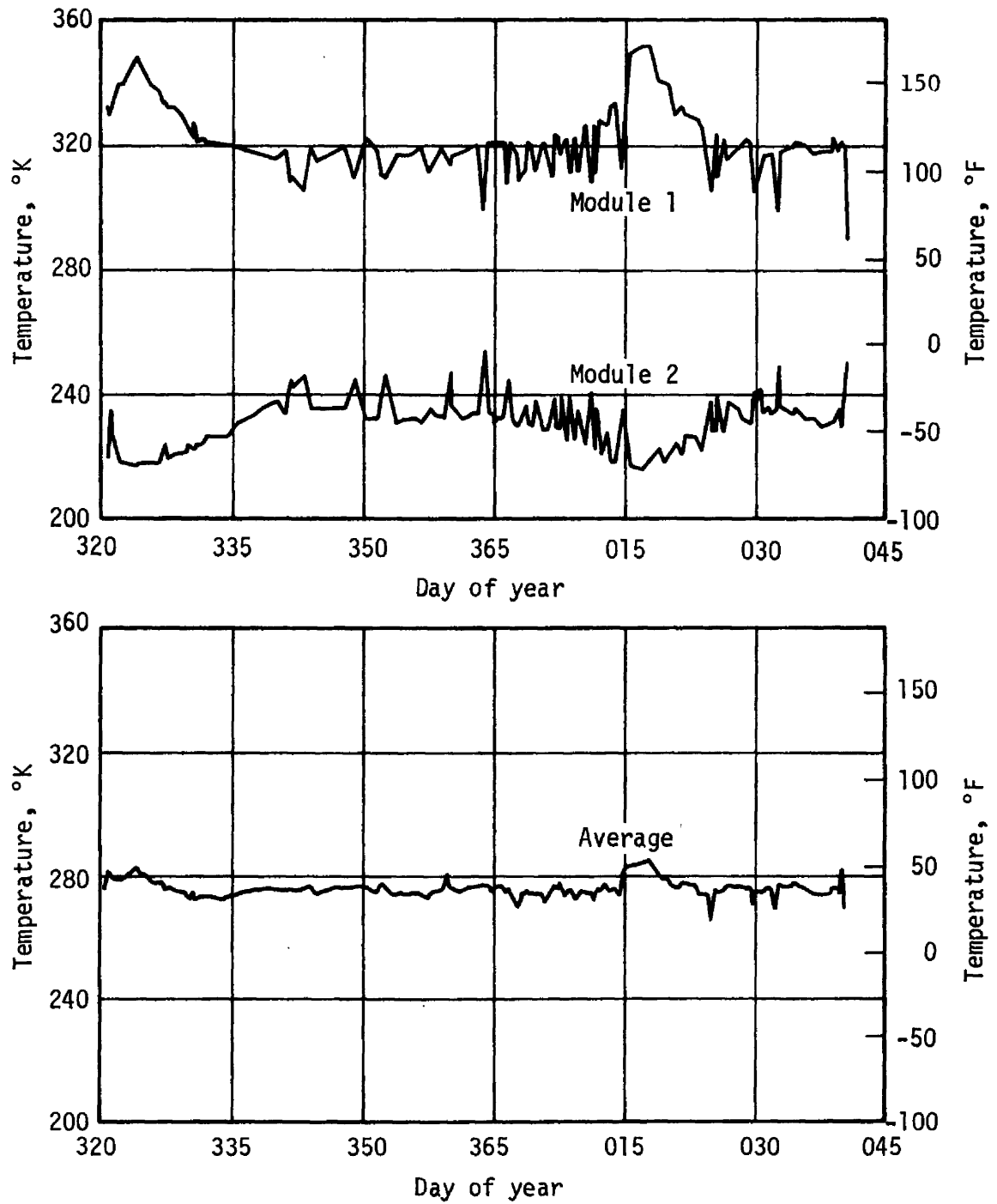


Figure 73.- Module Inlet Temperatures, SL-4

**APPENDIX A.
THRUSTER ATTITUDE CONTROL SYSTEM
COMPONENT OPERATING CHARACTERISTICS**

Component	SI	English Units
<u>Solenoid Control Valve</u>		
Operating Media:	GN ₂	
Temperature:	172 to 347 °K	-150 to 165 °F
Pressure:		
Operating	2.206×10^7 to 0 N/m ²	3200 to 0 psig
Proof	3.309×10^7 N/m ²	4800 psig
Burst	5.516×10^7 N/m ²	8000 psig
Leakage:		
External	1 scch	
Internal	Ambient downstream pressure--2 sccm ΔP of 10 to 12 percent--100 sccm	
Flow Rate and Pressure Drop:	0.68 kg/sec of GN ₂ at 294 °K and 2.068×10^7 N/m ² inlet pressure ΔP of 1.172×10^6 N/m ²	1.5 lb/sec of GN ₂ at 70 °F and 3000 psig inlet pressure. ΔP of 170 psi
Service Life:	35,000 cycles	
Filtration:	25 microns absolute	
Element Collapse Pressure:	1.379×10^6 N/m ²	200 psi
Electrical:		
Operating Voltage	24 to 30 Vdc	
Continuous Duty	24 to 30 Vdc for 12 hr at 347 °K	24 to 30 Vdc for 12 hr at 165 °F
Dropout Voltage	2 to 8 Vdc	
Pull-in Voltage	5 to 22 Vdc	
Current	3 A max.	
Response Time:		
Opening	42 msec max.	
Closing	35 msec max.	
Weight:	2.18 kg max.	4.8 lb max.

Component	SI	English Units
<u>Thruster Nozzle</u>		
Throat Area:	$1.36 \times 10^{-5} \text{ m}^2$	0.0211 in^2
Expansion ratio, ϵ :	50:1	
<u>Supply-Line Filters</u>		
Operating Media:	GN ₂	
Temperature:	172 to 347 °K	-150 to 165 °F
Filtration:	10 microns absolute	
Pressure:		
Operating	$2.206 \times 10^7 \text{ N/m}^2$ to 0 N/m^2	3200 to 0 psig
Proof	$3.309 \times 10^7 \text{ N/m}^2$	4800 psig
Burst	$5.516 \times 10^7 \text{ N/m}^2$ min.	8000 psig min.
Element Collapse	$1.103 \times 10^7 \text{ N/m}^2$ min.	1600 psid min.
Flow Rate and Pressure Drop:	1.36 kg/sec of GN ₂ at 2.206×10^7 and 294 °K. Max. ΔP of $5.17 \times 10^5 \text{ N/m}^2$ at rated flow.	3.0 lb/sec of GN ₂ at 3200 psig and 70 °F. Max. ΔP of 75 psid at rated flow.
Leakage (external):	1 scch max.	
Weight:	2.27 kg max.	5 lb max.
<u>GN₂ Storage Sphere</u>		
Operating Media:	GN ₂	
Temperature:	172 to 372 °K	-150 to 210 °F
Pressure:		
Operating	$2.206 \times 10^7 \text{ N/m}^2$ to 0 N/m^2	3200 to 0 psig
Proof	$3.309 \times 10^7 \text{ N/m}^2$	4800 psig
Burst	$5.516 \times 10^7 \text{ N/m}^2$ min.	8000 psig min.
Leakage (external):	1 scch	
Service Life:	500 pressure cycles (0 to 2.206×10^7 to 0 N/m^2)	500 pressure cycles (0 to 3200 to 0 psig)
Weight:	53 kg max.	117 lb max.

Component	SI	English Units
<u>Fill Disconnect</u>		
Operating Media:	GN ₂	
Temperature:	172 to 347 °K	-150 to 165 °F
Pressure:		
Operating	2.206×10^7 to 0 N/m ²	3200 to 0 psig
Proof	4.413×10^7 N/m ²	6400 psig
Burst	8.825×10^7 N/m ² min.	12,800 psig min.
Flow Rate:	0.386 kg/sec GN ₂	0.85 lb/sec GN ₂
Leakage (flight half only):		
External (cap installed)	9.832×10^{-2} sccm	
Internal	3.933 sccm	
Service Life:	400 cycles	
Weight:	0.118 kg max.	0.26 lb max.
<u>Bimetal Joint</u>		
Operating Media:	GN ₂	
Temperature:	214 to 350 °K	-75 to 170 °F
Pressure:		
Operating	2.206×10^7 to 0 N/m ²	3200 to 0 psig
Proof	4.413×10^7 N/m ²	6400 psig
Burst	8.825×10^7 N/m ²	12,800 psig
Leakage (external):	1×10^{-9} sccs	
Weight:	0.454 kg max.	1.0 lb max.
<u>Flexible Metal Tubing</u>		
Operating Media:	GN ₂	
Temperature:	172 to 347 °K	-150 to 165 °F

Component	SI	English Units
Pressure: Operating Proof Burst Leakage (external): Extension (axial): Offset (from center line): Angulation (from center line): Service Life: Weight:	2.206×10^7 to 0 N/m ² 4.413×10^7 N/m ² 8.825×10^7 N/m ² 1×10^{-5} sccs 2.38 mm max. 3.18 mm min. 0.0873 rad min. 500 cycles at 2.206×10^6 N/m ² and 347 °K 0.454 kg max.	3200 to 0 psig 6400 psig 12,800 psig 3/32 in. max. 1/8 in. min. 5° min. 500 cycles at 3200 psig and 165 °F 1.0 lb max.
<u>Pressure Transducer</u> Operating Media: Temperature: Pressure: Operating Proof Burst Leakage (external): Input Voltage: Output Voltage: Operating Life: Weight:	GN ₂ 172 to 347 °K 2.413×10^7 to 0 N/m ² 3.620×10^7 N/m ² 6.205×10^7 N/m ² 1×10^{-8} sccs 28 ±4 Vdc 0 to 5.0 V (proportional to pressure) 10,000 hr 0.454 kg max.	-150 to 165 °F 3200 to 0 psig 5250 psig 9000 psig 1.0 lb max.

Component	SI	English Units
<u>Temperature Transducer</u>		
Operating Media:	GN ₂	
Temperature:	116 to 478 °K	-250 to 400 °F
Pressure:		
Operating	2.413×10^7 to 0 N/m ²	3500 to 0 psig
Proof	4.826×10^7 N/m ²	7000 psig
Burst	9.653×10^7 N/m ²	14,000 psig
Leakage (external):	2.0×10^{-8} sccs	
Operating Life:	10,000 hr	
Weight:	0.227 kg	0.5 lb
<u>Pressure Switch</u>		
Operating Media:	GN ₂	
Temperature:	172 to 347 °K	-150 to 165 °F
Pressure:		
Operating	2.206×10^7 to 0 N/m ²	3200 to 0 psig
Proof	3.309×10^7 N/m ²	4800 psig
Burst	5.515×10^7 N/m ²	8000 psig
Leakage (external):	1×10^{-7} sccs	
Service Life:	6300 cycles	
Actuation Pressure:		
Pickup	8.274×10^5 N/m ² max.	120 psia max.
Dropout	4.826×10^5 N/m ² min.	70 psia min.
Actuation Time:	10 msec max.	
Weight:	0.454 Kg max.	1.0 lb max.

APPENDIX B.
THRUSTER ATTITUDE CONTROL SYSTEM IMPULSE USAGE

Time of TACS Usage		Usage			TMIB	TFOF	Reason for TACS Usage
From	To	MIB	FOF	N-sec	After Usage	After Usage	
134:17:30:00	134:17:39:52	0	0	0			Skylab boost phase, TACS inactive
134:17:39:52	134:22:20:05			36,716			IU control period
134:22:20:05					0	0	IU/ATMDC control transfer
134:22:30:03	135:11:48:31	916	10	29,808	916	10	APCS activation (incl thermal maneuvers)
135:11:48:31		0	0	0	916	10	CMG control re-enabled (nom wheel speed)
136:06:27:18	136:13:43:30	51	0	1,873	967	10	Three thermal maneuvers
136:15:25:00	136:20:52:06	248	11	10,200	1215	21	Maneuver to thermal attitude
137:07:06:00	137:07:10:03	47	0	1,157	1262	21	CMG reset
137:15:56:30	137:17:08:00	6	0	133	1268	21	Desat firings
137:17:15:30	137:17:16:30	56	0	1,246	1324	21	CMG reset
138:02:53:00	138:02:54:00	78	0	1,908	1402	21	CMG reset
138:14:55:00	138:14:55:30	1	0	27	1403	21	Desat firing
138:15:02:00	138:15:03:00	63	0	1,624	1466	21	CMG reset
139:04:06:30	139:04:07:30	41	0	1,001	1507	21	CMG reset
139:06:49:30	139:07:36:30	3	0	71	1510	21	Desat firings
139:07:38:00	139:07:38:30	44	0	1,068	1554	21	CMG reset
139:22:00:30	139:22:10:06	75	0	1,779	1629	21	CMG reset
140:08:10:00	140:08:20:00	55	0	1,290	1684	21	CMG reset
140:17:34:30	140:17:35:00	51	0	1,183	1735	21	CMG reset
141:00:59:00	141:01:00:30	65	0	1,481	1800	21	CMG reset
141:09:09:00	141:09:10:30	38	0	876	1838	21	CMG reset
141:12:47:30	141:13:19:00	3	0	67	1841	21	Desat firings
141:13:25:00	141:13:29:30	48	0	1,117	1889	21	CMG reset
141:15:33:30	141:17:16:00	10	0	227	1899	21	Desat firings
141:17:18:30	141:17:19:30	40	0	912	1939	21	CMG reset
141:20:52:30	141:21:33:30	7	0	156	1946	21	Desat firings
141:21:35:30	141:21:37:00	39	0	894	1985	21	CMG reset
142:01:36:00	142:01:36:30	36	0	818	2021	21	CMG reset
142:12:17:30	142:13:24:00	23	0	529	2044	21	Desat firings
142:13:28:00	142:13:28:40	86	0	1,962	2130	21	CMG reset
143:02:18:30	143:02:20:00	74	0	1,681	2204	21	CMG reset

Time of TACS Usage		Usage			TMIB	TFOF	Reason for TACS Usage
From	To	MIB	FOF	N-sec	After Usage	After Usage	
143:12:48:25	143:12:49:15	58	0	1,321	2262	21	CMG reset
143:20:09:40	143:20:10:30	30	0	681	2292	21	CMG reset
143:23:57:00	144:00:08:00	5	0	111	2297	21	Desat firings
144:00:10:00	144:00:10:48	69	0	1,544	2366	21	CMG reset
144:04:49:42	144:04:50:04	43	0	956	2409	21	CMG reset
144:11:21:09	144:11:21:51	58	0	1,281	2467	21	CMG reset
144:19:25:00	144:19:35:00	59	0	1,286	2526	21	CMG reset
144:23:44:30	144:23:45:30	44	0	961	2570	21	CMG reset
145:02:29:30	145:02:31:00	67	0	1,459	2637	21	CMG reset
145:06:16:00	145:06:22:00	6	0	133	2643	21	Desat firings
145:06:23:30	145:06:25:30	43	0	930	2686	21	CMG reset
145:08:08:30	145:08:09:00	1	0	22	2687	21	Desat firing
145:08:21:30	145:08:22:00	45	0	970	2732	21	CMG reset
145:13:48:00	145:13:49:30	36	0	890	2768	21	CMG reset
145:20:24:00	146:03:58:30	1796	17	48,566	4,564	38	Rendezvs & dckg first manned mission
146:04:18:30	146:05:17:30	15	0	311	4,579	38	Desat firings
146:05:44:30	146:05:45:00	18	0	378	4,597	38	CMG reset
146:10:47:00	146:10:48:00	50	0	1,081	4,647	38	CMG reset
146:16:35:00	146:16:36:30	57	0	1,237	4,704	38	CMG reset
146:18:25:00	146:18:30:00	97	20	5,978	4,801	58	Auto CMG reset
146:20:30:00	146:20:32:00	19	0	400	4,820	58	CMG reset
146:21:30:00	146:21:40:00	32	0	672	4,852	58	CMG reset
146:22:00:00	146:22:10:00	9	0	191	4,861	58	CMG reset
146:23:35:00	146:23:45:00	8	0	169	4,869	58	CMG reset
147:01:40:30	147:01:43:00	20	0	431	4,889	58	CMG reset
147:02:43:30	147:20:19:30	793	0	17,143	5,682	58	Maneuver to solar inertial, including post-maneuver momentum stabilization
149:00:59:30	149:01:10:36	127	0	2,580	5,809	58	CSM trim burn
150:20:59:00	150:21:49:00	12	0	249	5,821	58	EREP 1
152:01:01:43	152:01:01:44	2	0	40	5,823	58	Z-axis rate gyro anomaly
153:14:44:00	153:14:44:30	13	0	267	5,836	58	Rate gyro calibration
153:18:20:00	154:01:00:00	7	0	142	5,843	58	Desat firings (LBPN venting + IMD)

Time of TACS Usage		Usage			TMIB After Usage	TFOF After Usage	Reason for TACS Usage
From	To	MIB	FOF	N-sec			
153:20:00:00	154:01:00:00	16	0	329	5,859	58	EREP 2
154:01:00:00	154:05:46:00	2	0	40	5,861	58	Rate gyro Z-1 anomaly
154:19:17:00	154:19:35:00	1	0	22	5,862	58	EREP 3
157:20:23:50	157:20:24:30	3	0	62	5,865	58	Z-axis rate gyro anomaly
158:18:59:00	159:05:00:00	191	0	3,852	6,056	58	Maneuver to warm up SAS wing
160:15:00:00	160:15:15:00	1	0	18	6,057	58	EREP 6
160:16:37:00					6,057	58	Computer switchover
161:13:30:00	161:15:17:00	71	0	1,557	6,128	58	EREP 7 (crew error on maneuver time)
162:14:55:00	162:15:37:00	4	0	89	6,132	58	EREP 8
163:12:15:00	163:14:00:00	6	0	133	6,138	58	EREP 9
164:13:00:00	164:14:00:00	5	0	111	6,143	58	EREP 10
170:12:21:00	170:12:41:00	49	0	1,090	6,192	58	Auto CMG reset after EVA
173:06:30:00	173:09:30:00	134	0	3,074	6,326	58	Maneuver for refrigeration system (after undocking)
209:19:09:00	209:20:07:00	145	1	3,634	6,471	59	Second manned mission flyaround and docking
215:17:42:00	215:17:57:00	1	0	22	6,472	59	EREP 1
217:14:01:00	217:14:30:00	2	0	44	6,474	59	EREP 3
224:02:48:00	224:02:49:00	1	0	22	6,475	59	EREP 8
224:14:43:00	224:16:17:35	2	0	44	6,477	59	EREP 9
224:17:10:32	224:17:29:02	258	31	11,450	6,735	90	Bad momentum state--TACS only mode
225:14:13:52	225:20:51:53	13	0	285	6,748	90	Calibration maneuver (4) + LBNP venting (9)
236:17:13:00	236:21:20:00	157	0	3,719	6,905	90	Six-pack installation (EVA)
244:14:33:00	244:15:53:00	5	0	116	6,910	90	EREP 10
245:12:50:06	245:15:24:42	7	0	165	6,917	90	EREP 11
245:16:27:41	245:18:02:48	26	0	609	6,943	90	EREP 12 (crew error on maneuver time)
246:15:30:19	246:15:59:01	3	0	71	6,946	90	EREP 13
253:14:35:20	253:15:41:13	7	0	165	6,953	90	Desat firings (7) caused by LBNP vent
256:20:02:16	256:20:45:46	1	0	22	6,954	90	EREP 28
256:20:45:46	256:21:34:07	2	0	49	6,956	90	Desat firings (2)
258:16:35:16	258:16:46:18	1	0	24	6,957	90	EREP 31
258:18:18:29	258:18:22:58	1	0	24	6,958	90	EREP 32
259:15:48:46	259:16:06:32	1	0	22	6,959	90	EREP 33

Time of TACS Usage		Usage			TMIB	TFOF	Reason for TACS Usage
From	To	MIB	FOF	N-sec	After Usage	After Usage	
263:08:52:09	263:08:52:56	47	0	1,117	7,006	90	CMG reset (part of JOP 13)
264:00:10:00	264:01:46:00	5	0	120	7,011	90	Desat firings (bad NUz)
264:14:20:00	264:14:36:00	1	0	22	7,012	90	EREP 41
264:14:48:00	264:15:27:00	5	0	120	7,017	90	Desat firings (bad momentum state)
265:13:07:00	265:14:06:30	18	0	427	7,035	90	Desat firings during EVA 3
265:15:26:30	265:15:27:12	45	0	1,063	7,080	90	CMG reset
268:13:56:00	268:13:58:00	36	0	822	7,116	90	CMG reset (undocked gains)
268:18:03:00	268:18:04:00	43	0	1,007	7,159	90	CMG reset (undocked gains)
268:19:04:50	268:19:52:53	88	0	2,033	7,247	90	Attitude hold for undocking
320:21:16:00	320:22:05:00	165	4	4,608	7,412	94	Final manned mission docking
320:23:03:56	320:23:09:15	3	0	67	7,415	94	Desat firings (momentum peaks)
326:21:13:00	327:03:02:00	99	0	2,349	7,514	94	EVA No. 1
327:08:50:39		1	0	22	7,515	94	CMG 1 turnoff
327:13:46:00	327:13:55:00	1	0	22	7,516	94	Momentum peak (2 CMG operation)
327:14:36:50		1	0	22	7,517	94	Momentum peak (2 CMG operation)
327:15:22:00	327:15:23:00	3	0	71	7,520	94	Momentum peak (2 CMG operation)
327:16:57:47	327:16:57:57	2	0	49	7,522	94	Momentum peak (2 CMG operation)
328:00:44:00		1	0	22	7,523	94	Momentum peak (2 CMG operation)
329:02:22:00		1	0	22	7,524	94	CSM trim burn
329:16:21:00		1	0	22	7,525	94	Momentum peak (2 CMG operation)
329:17:08:00		1	0	22	7,526	94	Momentum peak (2 CMG operation)
330:14:52:30	330:14:53:00	1	0	22	7,527	94	Momentum peak (2 CMG operation)
330:15:38:00	330:15:40:30	2	0	44	7,529	94	Momentum peak (2 CMG operation)
330:16:24:30	330:16:27:30	3	0	67	7,532	94	Momentum peak (2 CMG operation)
331:00:13:00		1	0	22	7,533	94	Momentum peak (2 CMG operation)
331:01:00:00	331:02:00:00	1	0	22	7,534	94	Momentum peak (2 CMG operation)
331:02:31:27	331:02:33:55	2	0	44	7,536	94	Momentum peak (2 CMG operation)
331:03:18:37	331:03:18:46	2	0	44	7,538	94	Momentum peak (2 CMG operation)
331:03:22:26	331:03:22:33	1	0	22	7,539	94	Momentum peak (2 CMG operation)
331:14:53:08	331:14:53:36	3	0	67	7,542	94	S232 maneuver (desat firings)
331:15:38:59	331:15:39:43	2	0	44	7,544	94	S232 maneuver (desat firings)

Time of TACS Usage		Usage			TMIB After Usage	TFOF After Usage	Reason for TACS Usage
From	To	MIB	FOF	N-sec			
331:15:39:43	331:15:42:59	113	0	2,691	7,657	94	TACS only control (high rate in X)
331:16:04:00	331:16:07:00	5	0	111	7,662	94	Desat firings
331:17:18:10	331:17:19:09	2	0	44	7,664	94	Momentum peak (2 CMG operation)
333:23:43:00	333:23:43:30	2	0	44	7,666	94	Desat firings
334:00:19:29	334:00:20:29	9	0	200	7,675	94	Desat firings
334:00:29:59	334:00:30:29	1	0	22	7,676	94	Desat firings
334:01:16:00	334:01:16:30	2	0	44	7,678	94	Desat firings
334:03:39:00	334:03:40:00	1	0	22	7,679	94	Desat firings
334:16:12:00	334:16:56:00	40	0	881	7,719	94	EREP 4
335:05:23:00		1	0	22	7,720	94	Desat firings
335:17:10:00	335:17:48:30	39	0	845	7,759	94	EREP 5
336:16:26:00	336:17:02:00	137	7	4,221	7,896	101	EREP 6 (includes TACS only period)
336:17:16:00	336:18:25:30	61	0	1,254	7,957	101	EREP 7
336:18:45:30	336:19:47:00	11	0	236	7,968	101	Desat firings
337:15:38:00	337:16:22:00	77	0	1,624	8,045	101	EREP 8
337:16:22:00	337:17:51:00	91	0	1,922	8,136	101	EREP 9
338:16:05:30	338:19:51:30	34	0	703	8,170	101	EREP 10
339:16:21:30	339:16:49:30	8	0	191	8,178	101	EREP 11
341:02:06:00	341:02:40:00	2	0	49	8,180	101	Attitude hold for S183K
341:14:49:00	341:15:26:00	11	0	262	8,191	101	EREP 12
341:18:50:00	341:19:08:00	4	0	93	8,195	101	JOP 13
343:00:25:30	343:02:42:50	133	0	3,132	8,328	101	EREP 14
343:03:33:49	343:03:37:00	3	0	71	8,331	101	Desat firings
343:14:26:00	343:14:26:30	1	0	22	8,332	101	Desat firings
343:20:28:00	343:21:44:00	2	0	49	8,334	101	S063K maneuver
344:16:49:00	344:17:37:30	13	0	302	8,347	101	S063K maneuver
346:00:21:02	346:00:21:23	1	0	22	8,348	101	Desat firing (momentum peak)
347:14:52:30	347:14:53:00	3	0	71	8,351	101	S019 maneuver
347:21:36:00	347:22:09:00	1	0	22	8,352	101	Desat firing (momentum peak, IMD)
348:00:12:01	348:00:12:55	1	0	22	8,353	101	S183 maneuver
349:00:18:26	349:00:51:34	7	0	165	8,360	101	EREP 15

Time of TACS Usage		Usage			TMIB	TFOF	Reason for TACS Usage
From	To	MIB	FOF	N-sec	After Usage	After Usage	
352:02:15:38	352:02:45:47	3	0	71	8,363	101	EREP 16
352:02:56:20	352:03:24:19	5	0	116	8,368	101	EREP 16
352:11:47:00	352:11:59:50	4	0	93	8,372	101	EREP 17
353:16:24:05	353:16:27:14	3	0	71	8,375	101	JOP 18D
353:18:10:00	353:18:43:00	5	0	116	8,380	101	JOP 18D
353:19:11:59	353:19:19:59	20	0	467	8,400	101	CMG auto reset (JOP 18D)
355:02:20:00	355:12:00:30	2	0	47	8,402	101	Desat firings
355:16:15:30	355:16:19:00	2	0	47	8,404	101	JOP 18D
355:17:50:30	355:17:51:00	1	0	22	8,405	101	JOP 18D
355:18:13:30	355:18:14:00	1	0	22	8,406	101	JOP 18D
357:18:31:30	357:18:32:00	14	0	325	8,420	101	CMG reset
357:21:55:30	357:22:01:30	9	0	209	8,429	101	Desat firings
357:22:13:30	357:22:14:30	15	0	347	8,444	101	CMG reset
358:01:06:30	358:01:07:30	2	0	44	8,446	101	S019 maneuver
358:03:25:00	358:03:26:00	2	0	44	8,448	101	Desat firings
358:20:29:30	358:22:03:00	6	0	138	8,454	101	JOP 18
359:17:29:00	360:02:03:00	622	32	17,210	9,076	133	SL-4 EVA No. 2 (16 MIB, 21 FOF not fired)
363:17:21:30	363:21:00:00	522	28	16,022	9,598	161	SL-4 EVA No. 3
364:21:17:33	365:03:08:40	69	0	1,530	9,667	161	Desat firings (JOP 18D)
365:22:59:59	365:23:01:59	10	0	227	9,677	161	Firings associated with JOP 18D
365:23:25:59	365:23:29:59	3	0	67	9,680	161	Desat firings (JOP 18D)
001:00:01:59	001:00:03:32	8	0	182	9,688	161	Auto CMG reset (JOP 18D)
001:00:35:59	001:00:36:59	1	0	22	9,689	161	Desat firings (JOP 18D)
001:12:39:00	001:14:36:30	38	0	854	9,727	161	EREP 18
001:22:22:30	001:22:26:00	4	0	89	9,731	161	Desat firings (JOP 18D)
002:00:17:09	002:00:29:16	3	0	67	9,734	161	Desat firings (JOP 18D)
002:14:44:00	002:15:09:23	4	0	89	9,738	161	Desat firings (S063)
002:15:24:00	002:16:07:00	2	0	44	9,740	161	Desat firings (S063)
002:17:00:00	002:17:35:00	2	0	44	9,742	161	Desat firings (S063)
002:23:26:21	002:23:51:03	2	0	44	9,744	161	S201K maneuver
003:02:13:11	003:02:36:05	1	0	22	9,745	161	Desat firings

Time of TACS Usage		Usage			TMIB	TFOF	Reason for TACS Usage
From	To	MIB	FOF	N-sec	After Usage	After Usage	
003:10:28:58	003:11:47:29	3	0	67	9,748	161	EREP 19
003:12:12:00	003:12:48:00	6	0	138	9,754	161	EREP 19
003:16:19:00	003:16:52:00	4	0	89	9,758	161	S183K
003:23:44:00	003:23:50:01	21	0	476	9,779	161	JOP 18D
004:19:34:00	004:21:24:00	17	0	374	9,796	161	EREP 20
005:14:52:30	005:15:03:00	7	0	156	9,803	161	JOP 18D
005:16:27:30	005:16:30:00	2	0	44	9,805	161	Desat firings
005:19:57:30	006:02:04:00	6	0	133	9,811	161	Desat firings
006:18:18:57	006:18:19:30	2	0	44	9,813	161	EREP 21
006:18:24:30	006:18:25:00	2	0	44	9,815	161	EREP 21
006:19:07:30	006:19:41:30	10	0	218	9,825	161	EREP 21
006:23:30:30	006:23:39:30	8	0	173	9,833	161	JOP 18D
007:00:29:30	007:03:42:00	2	0	44	9,835	161	Desat firings
007:13:02:00	007:14:00:00	35	0	725	9,870	161	EREP cal
007:17:32:00	007:18:12:30	188	0	3,901	10,058	161	EREP 22
008:00:04:00	008:00:04:30	1	0	22	10,059	161	S019K
008:16:49:00	008:18:18:30	14	0	294	10,073	161	EREP 23
009:15:38:00	009:17:38:00	15	0	347	10,088	161	EREP 24
010:00:08:00	010:00:48:00	2	0	44	10,090	161	S183
010:00:58:00	010:01:01:43	2	0	44	10,092	161	S183
010:14:58:30	010:14:59:00	1	0	22	10,093	161	Desat firing (momentum dump inhibit)
011:01:16:24	011:02:19:37	20	0	472	10,113	161	EREP 25
011:02:20:00	011:03:54:00	8	0	187	10,121	161	EREP 25
011:14:19:00	011:14:19:30	1	0	22	10,122	161	Desat firing
011:17:49:30	011:19:19:30	18	0	423	10,140	161	EREP 26
011:23:36:00	011:23:40:00	3	0	67	10,143	161	Desat firings
012:17:06:45	012:17:14:42	9	0	205	10,152	161	EREP 27
012:17:55:27	012:17:55:34	1	0	22	10,153	161	EREP 27
012:17:57:43	012:18:12:40	3	0	67	10,156	161	EREP 27
012:18:37:52	012:18:39:44	3	0	67	10,159	161	EREP 27
013:12:59:00	013:12:59:30	1	0	22	10,160	161	Desat firing (momentum dump inhibit)

Time of TACS Usage		Usage			TMIB After Usage	TFOF After Usage	Reason for TACS Usage
From	To	MIB	FOF	N-sec			
013:22:17:30	013:22:18:30	2	0	44	10,162	161	S063
014:00:17:00	014:01:55:00	1	0	22	10,163	161	Desat firing
014:15:40:43	014:15:47:15	4	0	93	10,167	161	EREP 28
014:16:53:22	014:17:19:11	7	0	160	10,174	161	EREP 29
014:19:58:00	014:19:58:30	1	0	22	10,175	161	Desat firing
014:21:08:30	014:21:10:15	2	0	44	10,177	161	S019K
017:17:41:30	017:17:42:00	1	0	22	10,178	161	Crew motion
017:23:25:00	017:23:26:00	24	0	596	10,202	161	CMG reset
018:20:50:50	018:20:51:08	5	0	120	10,207	161	EREP 30
018:21:41:00	018:21:43:30	2	0	49	10,209	161	EREP 30
018:22:31:30	018:22:32:00	1	0	22	10,210	161	EREP 30
019:13:38:30	019:13:43:00	6	0	142	10,216	161	Desat firings (-Z SAL venting)
019:16:44:30	019:16:44:38	2	0	49	10,218	161	Desat firings (-Z SAL venting)
019:17:10:12	019:17:13:30	3	0	71	10,221	161	Desat firings
019:17:58:30	019:17:59:41	1	0	22	10,222	161	Desat firings
019:18:32:00	019:18:49:00	1	0	22	10,223	161	Desat firings
019:21:09:00		1	0	22	10,224	161	Desat firings
020:17:42:30	020:17:43:00	2	0	49	10,226	161	Desat firings (momentum dump inhibit)
020:19:02:30	020:19:21:30	12	0	289	10,238	161	EREP 32
020:22:00:00	020:22:00:30	2	0	49	10,240	161	Desat firings
021:21:19:30	021:21:36:54	40	0	943	10,280	161	EREP 35
022:19:48:30	022:19:53:30	4	0	93	10,284	161	EREP 37
023:13:23:00	023:13:23:30	2	0	44	10,286	161	Desat firings (momentum dump inhibit)
023:18:47:30	023:18:49:30	1	0	22	10,287	161	Desat firing
023:21:56:00	023:21:56:30	1	0	22	10,288	161	Desat firing
024:18:09:30	024:18:10:00	2	0	44	10,290	161	EREP 40
025:01:52:00		1	0	22	10,291	161	Desat firings
025:14:20:00	025:14:20:30	1	0	22	10,292	161	Desat firings
025:17:17:00	025:17:33:00	7	0	156	10,299	161	EREP 41
026:20:08:00	026:20:09:09	7	0	156	10,306	161	EREP 42
026:20:54:30	026:21:01:30	8	0	178	10,314	161	EREP 42